Ore Geology Reviews 92 (2018) 205–239

Contents lists available at ScienceDirect

Ore Geology Reviews

journal homepage: www.elsevier.com/locate/oregeorev

Geology and chemistry of Variscan-type pegmatite systems (SE Germany) – With special reference to structural and chemical pattern recognition of felsic mobile components in the crust

H.G. Dill

Gottfried Wilhelm Leibniz University, Welfengarten 1, D-30167 Hannover, Germany

ARTICLE INFO

Keywords:
Pegmatite
Lithology
Structural geology
Chemistry
Variscan-type

ABSTRACT

The geology of pegmatite systems encompasses lithology, shape, and structure while the chemistry of major and trace elements is indicative of the ore composition; both are the "pillars" of the CMS classification scheme (**C**hemical composition-**M**ineral assemblage-**S**tructural geology) for barren and rare-metal pegmatites, including their granitic affiliates. The term Variscan-type has been coined to describe a style of formation linked to the ensialic orogens and a timebound mineralization sandwiched between the Caledonides and the Alpides. The primary formation covers the time from the Neoproterozoic through the Permian and ends with a hydrothermal phase waning eventually in the supergene alteration and is subdivided into three stages: (1) from diatectic to metatectic gneisses, (2) from metapegmatites, metamorphic pegmatoids to thrusting, (3) from the crust to the mantle and from barren to rare metal pegmatites. This evolution is characterized by a retrograde metamorphism from HP/MP to LP regimes. The tabular and stock-like pegmatitic, aplitic and granitic rocks in autochthonous and allochthonous units are grouped into 8 types (A–H) based on the above qualifiers of the CMS scheme. On a large scale, felsic mobilizates are accumulated by mimetic (facsimile) crystallization in anticlines with the most effective traps encountered where the directions of great circle plunges cut each other at almost right angle (stereonet analysis). The term "mobilizates" is used to describe felsic mobile components in the crust which migrated to a different extent from the site of their formation. On a small scale, where southward-dipping planar architectural elements are cut across by deep-seated lineaments the "temperature depression" of the retrograde system occurs and rare-metal pegmatites are located. This subhorizontal plane is correlated with a gently dipping Moho and vertical lineamentary fault zones with bulges of the Moho (chemical contour map analysis). Spider diagrams whose element contents are normalized to a reference paragneiss are categorized into 4 chemical patterns: (1) circular patterns (= metamorphic mobilizates, magmatic mobilizates), (2) necking-down patterns (= different degrees of fractionation), (3) lens-shaped patterns (= wall rock alteration), (4) stellate pattern (= different degrees of fractionation and mixing of fluids). The marker assemblages among the major elements are: Si-Fe-P: metamorphic to magmatic (sub)crustal mobilizates, K-Na-Al: metamorphic mobilizates, Ti-Mg: restites of metamorphic and magmatic mobilizates, Ca: remnant in the exocontact of pegmatitic systems, Mn: marker of depth-pressure The marker assemblages among the minor elements are: As-Bi: HT hydrothermal-metamorphic fluids, Cu-Ni-Mo: hydrothermal-deep-seated + (ultra)basic sources, U-Zn: hydrothermal-deep-seated sources, Pb: LT hydrothermal, Nb-Ba-Rb: pegmatitic fractionation-Ba (early)-Rb (late), Zr: restites of metamorphic mobilization + fractionation, REE: metamorphic mobilizates. The marker to discriminate hypogene and supergene kaolinization are: (1) hypogene (Ca- Mg out, Zn-Cu-Bi-Rb-Nb in), (2) supergene (Zr-Ti in).

1. Introduction

Based on their mineralogical composition and economic use, pegmatitic rocks and their fine-grained brethren, called aplites, are subdivided into "barren pegmatites" with a simple mineralogical association of quartz, alkaline feldspar and mica and into "rare-element pegmatites" which in addition to this granite-like mineral assemblage are abundant in incompatible elements, such as Nb, Ta, Be, Li and Cs (Ackerman et al., 2007; Dill, 2015a). Only less than 1% of these felsic intrusive rocks warrant the use of the term "rare-element pegmatites". Taking a glimpse at the wealth of publications on pegmatites, however, may give the reader a total different picture as to the significance of pegmatites as a source of ceramic raw materials (barren pegmatites) and strategic metallic deposits (rare element pegmatites). More than

E-mail address: haralddill@web.de.

https://doi.org/10.1016/j.oregeorev.2017.11.016
Received 15 August 2017; Received in revised form 7 November 2017; Accepted 17 November 2017
Available online 22 November 2017

90% of publications, mainly in the field of mineralogy, deal with minerals and their formation in rare-metal pegmatites. To get an impression of the predominance of mineralogy in the study of pegmatites the reader is recommended to browse the special volume of ELEMENTS in 2012, where only one contribution is devoted to industrial minerals, and by the way touching the geology of barren pegmatites (Glover et al., 2012) whereas the overview by London (2008) may act as an intro to the mineralogical and genetic papers, e.g., Linnen et al. (2012), Simmons et al. (2012) and Černý et al. (2012). Since the first study of Jahns (1955) on pegmatites the view on the emplacement of these rocks was narrowed down to the mineralogical angle. One of the most comprehensive studies by Schneiderhöhn (1961) began outlining the morphology and geology of pegmatites on a world-wide basis. But written in German, this book gained only limited access by foreign researchers. Detailed studies of the geology of pegmatites are either found in company reports inaccessible to an international audience or in open-file reports issued by geological surveys whereas such studies on pegmatites involving extensive field work are rarely conducted in the course of projects at universities (Bauberger,1957; Norton, 1964; Derré et al., 1986; Bettenay et al., 1988; Bassot and Morio,1989; Lahti, 1989; Baljinnyam et al., 1993; Aryal, 2001; Kremer and Lin, 2006; Bynoe, 2014; Konzett et al., 2015; Silva et al., 2015). A holistic approach has been taken and linking geology to the mineralogy of pegmatitic and aplitic rocks in combination with the whole-rock chemistry of these intrusive rocks became the key element of the CMS classification scheme (**C**hemical composition-**M**ineral assemblage-**S**tructural geology). It is to mitigate the existing disproportion between mineralogy and geology and also constitutes the centerpiece of the current study (Table 1) (Dill, 2015a, 2016a). None of the existing classification schemes of pegmatites allows for a combination of geology, including geophysical data, whole-rock geochemistry and mineralogy because all of them are mineralogically-minded and thereby undermine what a classification scheme is all about to cover as much as possible of the realm it is designed for (Simmons, 2005). The descriptive CMS classification is a binary system, addressing the ore body as well as the ore composition and also enables the user to cross the lithological border between pegmatitic rocks and affiliated lithologies such as those of the granitic clan, the calcsilicate rocks and skarn deposits often associated in space and time with pegmatites and aplites (Tables 1, 2a, 2b). Offering these opportunities, the CMS system directly translates into genetic statements and unaddressed genetic ideas. The scope of this current reference study of the shallow Variscan-type pegmatite system is as follows:

- To describe the outward lithological appearance of pegmatitic and its affiliated rocks according to the CMS system so as to be applicable for field work as some sort of a manual.
- To statistically manage chemical data in a D-2 manner and compare them with structural geology and in the field (contour maps vs. stereonet diagrams) in order to recognize the thermal hot spots and chemical trends for a source analysis of elements
- To discuss the pegmatitic rocks in view of adjacent non-pegmatitic mineral deposits
- To figure out to what extent the geodynamic processes in allochthonous and autochthonous units played a part during the emplacement of pegmatites

The pegmatite province in the NE Bavarian Basement has been selected for its good coverage with large-scale geological and geophysical data and because of its numerous sites well studied as to the mineralogy but also still undernourished with regard to geological and chemical field work (Fig. 1) (Dill, 2015b – see further literature cited there).

2. Methodology and terminology

2.1. Samples and methods

The number of samples investigated during the current study amounts to 352 from a total of 117sites (Fig. 1b). They have been supplemented with data from literature: 6 data sets of the Flossenbürg and Bärnau Granites (Wendt et al., 1994), 5 of aplitic gneisses (Richter and Stettner, 1986), 18 from older granites south of the Luhe Line listed in unpublished exploration reports of former Saarberg-Interplan Uran Company (1982) and 68 from an unpublished KTB report (Steiner, 1986).

It is the hand specimens which in the classical way are subjected to visual examination. To obtain the petrographic data for the 1st and 2nd order terms listed in the CMS classification scheme, mineralogically uncertain cases were tackled by supplementary XRD, SEM-EDX and the examination of thin sections. The measuring conditions have been described in Dill et al. (2012, 2013). All chemical data were subjected to a statistical treatment. Different interpolation methods can be used such as directional weighing, linear interpolation, polynomial trend analysis, inverse distance, kriging and minimum curvature. The latter method has proved most meaningful for the data management and regional mapping of the element abundances as contour maps (Section 4.2). Moreover a statistical treatment of planar structural elements associated with the pegmatitic rocks has been conducted to better understand the tectonic impact on the emplacement and alteration of pegmatites. The structural elements are plotted into a stereonet diagram (Schmidt Net equal area presentation onto the lower hemisphere) to show the great circles and density contour intervals of the various features (Section 4.3). To ease a visual comparison of the chemical data for each lithotype from A to H, spider diagrams were constructed, one showing the major element pattern (SiO_2, TiO_2, Al_2O_3, Fe_2O_3, MnO, MgO, CaO, Na_2O, K_2O, P_2O_5) and another the trace elements relevant for the emplacement of the pegmatitic rocks (As, Ba, Bi, Cu, Mo, Nb, Ni, Pb, Rb, U, Zn, Zr and REE_{tot}) (Section 4.1). The major elements were normalized to reference biotite-cordierite-sillimanite gneisses most typical of the region and their maximum and mean values plotted on a logarithmic scale in the spider diagrams. The common x–y plots were used to discriminate hypogene and supergene argillitization (Section 4.4).

2.2. Terminology of rocks and processes

The current study describes a lithological transition from well-structured metamorphic rocks displaying planar features (cleavage) which have been deformed to different degrees and laid into folds of varying types through felsic intrusive rocks lacking any preferred orientation of their rock-forming minerals and emplaced as zoned or unzoned rock bodies (Passchier and Trouw, 2005). The latter encompass the felsic rocks categorized as granitic, pegmatitic or aplitic. They are felsic mobile components within the crust which migrated to a different degree from the site of formation and called for reasons of presentation in the current study as “mobilizates”. The term mobilizate is in accordance with the “Glossary of Geology “and has been translated from the German word “Mobilisat” introduced to refer to the mobile phase of any consistency that existed during migmatization (Bates and Jackson, 1987). Apart from this general technical term which was used in context with the formation of migmatites (“mixed rocks”), there are some other terms used to specify the lithogenic processes leading eventually to the series of felsic rocks under study (Mehnert, 1968). They are defined in the succeeding paragraphs following the recommendation of the IUGS Subcommission on the Systematics of Metamorphic Rocks (migmatites and related rocks) (Wimmenauer and Bryhni, 2007).

Migmatite: A composite silicate metamorphic rock, pervasively heterogeneous on a meso- to megascopic scale. It typically consists of

Table 1
The CMS classification scheme (**C**hemical composition-**M**ineral assemblage-**S**tructural geology) of pegmatitic and aplitic rocks for applied and genetic economic geology. All items are self-explanatory and listed in the classification scheme, proper.

ORE BODY						
Host rock lithology	**Metamorphic rocks**			**Metamorphic and magmatic rocks**	**Magmatic rocks**	**Remarks**
1 st order term **Type of pegmatitic/ aplitic rock**	**Pseudopegmatite/ pseudoaplite**	**Metapegmatite/ metaaplite**	**Pegmatoid/ aploid**	**Pegmatite/ aplite**	**Plutonic pegmatite/ aplite**	**Mandatory**
	Aplitic: grain size << host rock and homogeneous Pegmatitic : grain size >> host rock and heterogeneous **Fixed terminology**				Aplitic: grain size << host rock Pegmatitic : grain size >> host rock host rock and heterogeneous	
Specific type of host rock	*Gneiss, amphibolite , eclogite* *e.g., cordierite-sillimanite-gneiss-hosted pegmatoid*				*Granite, syenite, granodiorite* *e.g. syenite pegmatite*	*Optional*
Determination	Mapping in the field the ore-host rock relation and measuring the grain size by visual examination					
2 nd order term **Shape and structure**	**Tabular, schlieren, stock-like, pockets, vein-type, pipes, chimneys, floors** e.g. tabular Sc-Nb aplite, schlieren quartz-albite pegmatoid **Open terminology**				**Miarolitic, pod-like, pockets, vein-type, schlieren** e.g. miarolitic granite pegmatite	**Mandatory**
Internal structure	Unzoned - rimmed-complex/ ungraded-complex/ graded (e.g. UST) **Open terminology**					
Size (thickness)	*cm-sized, dm-sized , meter-sized*					*Optional*
Determination	Mapping in the field the shape by visual examination and measuring the morphological increments and size with a yardstick					
3 rd order term **Chemical qualifier**	**Sn, W, Ta, Nb, Sc, Be, Li, Cs, Rb, REE ,Y, U, Th, B, F, P, Zr** **e.g. Nb-Li pegmatite, (Sc-U)-Nb-P aploid** **Open terminology**					**Mandatory** Can be linked to the "Chessboard classification scheme of mineral deposits", using alpha-numerical codes
Determination	By visual inspection of rock-forming minerals, including hand lens for accessory minerals (put in brackets) Rock-forming and accessory minerals ⇒ chemical symbols (e.g. beryl, euclase ⇒ Be, Li mica ⇒ Li, allanite ⇒ REE, if necessary LREE)					
4 th order term **Mineralogical qualifier**	**quartz, feldspar, foid, garnet, zeolite, mica, corundum, graphite** **e.g. (andalusite)-quartz-feldspar metapegmatite, graphite- feldspar-quartz pegmatite** **Open terminology**					**Mandatory** Can be linked to the "Chessboard classification scheme of mineral deposits", using alpha-numerical codes
Specific type of minerals for gemstone-bearing pegmatites , fine-tuning and genetic interpretation	*e.g. Al pegmatite (ruby), F-Sn-W granite pegmatite (topaz>fluorite), Li-Nb-P pegmatite (triphylite), Li-Nb-P pegmatite (amblygonite)* **Open terminology**					*Optional - Composite of level 3 and 4*
Determination	See 3 nd order term for determination an					
ORE COMPOSITION						

darker and lighter parts. The darker parts usually exhibit features of metamorphic rocks whereas the lighter parts are of igneous-looking appearance.

Neosome: The newly formed parts of a migmatite (metatects and restites).

Restite: Remnant of a metamorphic rock from which a substantial amount of the more mobile components has been extracted without being replaced.

Metatexite: A variety of migmatite with discrete leucosomes, mesosomes, andmelanosomes (cf. leucosome, mesosome, melanosome).

Leucosome: The lightest-colored parts of a migmatite which may end up in a barren aplitic or pegmatitic rock.

Melanosome: The darkest parts of a migmatite, usually with prevailing dark minerals. It occurs between two leucosomes or represents the more or less unmodified parent rock if still present. As far as the pegmatites are concerned they are representative of the felsic intrusive rocks containing accessory minerals such as cordierite, andalusite or sillimanite.

Diatexite: A type of migmatite where the darker and the lighter parts form schlieren and nebulitic structures which merge into one another.

3. Geological and geodynamic setting

For geoscientists who are interested in pegmatites in Northern America as well as Western Europe, it is inevitable to have a closer look at the western prolongation of the European Variscides and tie up the Variscan pegmatite provinces on both sides of the Atlantic Ocean (Fig. 1a) (Alderton, 1993; Alfonso and Melgarejo, 2000; Martins et al., 2011; Neiva et al., 2012; Alves and Mills, 2013; Barros et al., 2015; Bradley et al. 2015; Garate-Olave et al. 2015; Roda-Robles et al., 2015). By analogy with the Variscan/Hercynian orogeny in Europe, the Alleghanian or Appalachian orogeny was in full swing during the Late Paleozoic creating the Appalachian and Allegheny Mountains along the Eastern coast of Northern America (Bartholomew and Whitaker, 2010) (Fig. 1a). It is imperative to keep a keen eye on this period of time when the plates eventually collided and the granites, pegmatites and aplites

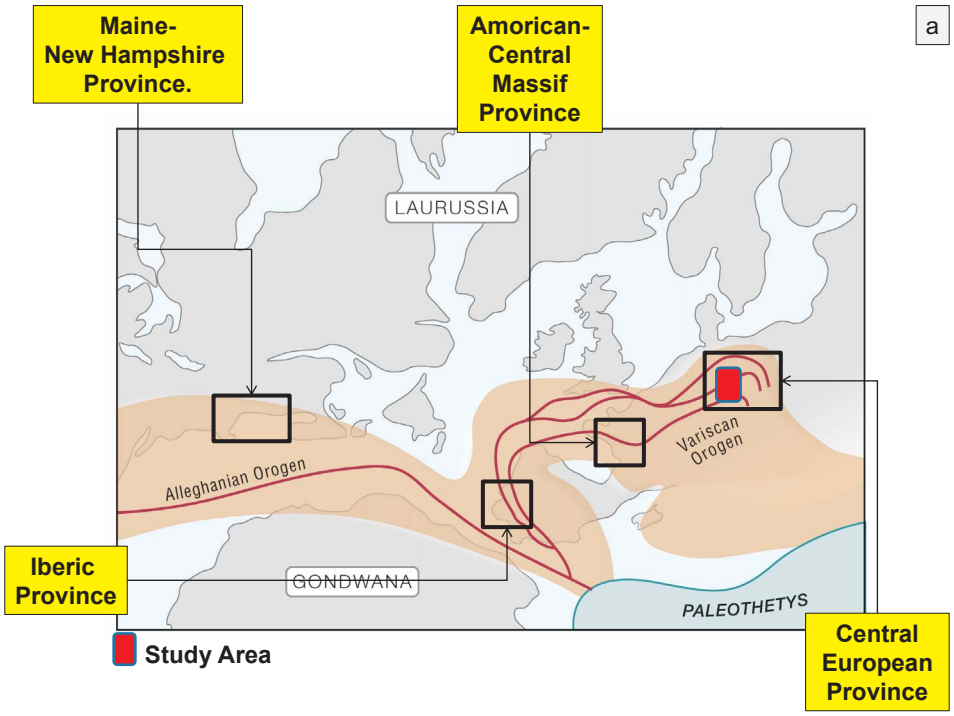

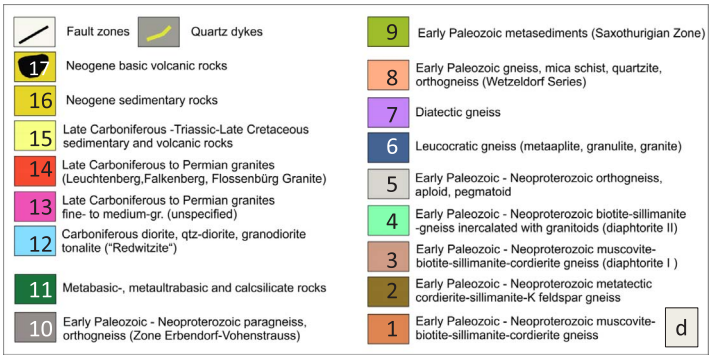

Fig. 1. Sampling sites and geological setting of the Variscan-type pegmatites in the NE-Bavarian Basement, Germany. a) Reconstruction of the mountain belt produced in the course of the Alleghanian/Appalachian and Variscan/Hercynian orogenies during the Late Paleozoic on both sides of the present-day Atlantic Ocean, amalgamating Laurussia and Gondwana and giving host to four pegmatite provinces. b) Sites and sampling density in the study area of Fig. 1c. Rectangle denotes position of the chemical maps of Fig. 7. c) The geological setting of the NE-Bavarian Pegmatite Province. The geological map has been modified from the map "Geological map of the Upper Palatinate Forest" 1:150,000 issued by the Bavarian Environment Agency (2009). To ease correlation with lithostratigraphic units referred to into the text and avoid a permanent repetition of age and lithology the various shades given in boxes are supplemented with Arabic numerals. Towns are given for reference: TIR = Tirschenreuth, BAR = Bärnau, WIN = Windischeschenbach, FLO = Flossenbürg, WEN = Weiden, VOH = Vohenstrauß, WAI = Waidhaus, PFR = Pfreimd, ESL = Eslarn. *FLO*: Flossenbürg Granite, *FAL:* Falkenberg Granite, *LEU*: Leuchtenberg Granite, *BAR*: Bärnau Granite: A-A′: Luhe Line Lineamentary Fault Zone, B-B′: Franconian Line Lineamentary Fault Zone, C-C′: Boundary fault between the Moldanubian and Saxothuringian Zones. d) Legend of the geological map in Fig. 1c.

came into existence in the Central European Variscides. An overview of the geodynamics of this crustal section has been given by Matte (2001), von Raumer et al. (2003) and Linnemann et al. (2007).

The lithology of the Central European Variscan basement is rather complex and only treated as far as it is essential to understand the emplacement of these intrusive rocks. For those who want to get a full-blown picture during the Neoproterozoic and Paleozoic, the reader is recommended to consult the book of Dallmeyer et al. (1995). For the current investigation, the geological setting has slightly been modified from the official map issued by the Bavarian Environment Agency

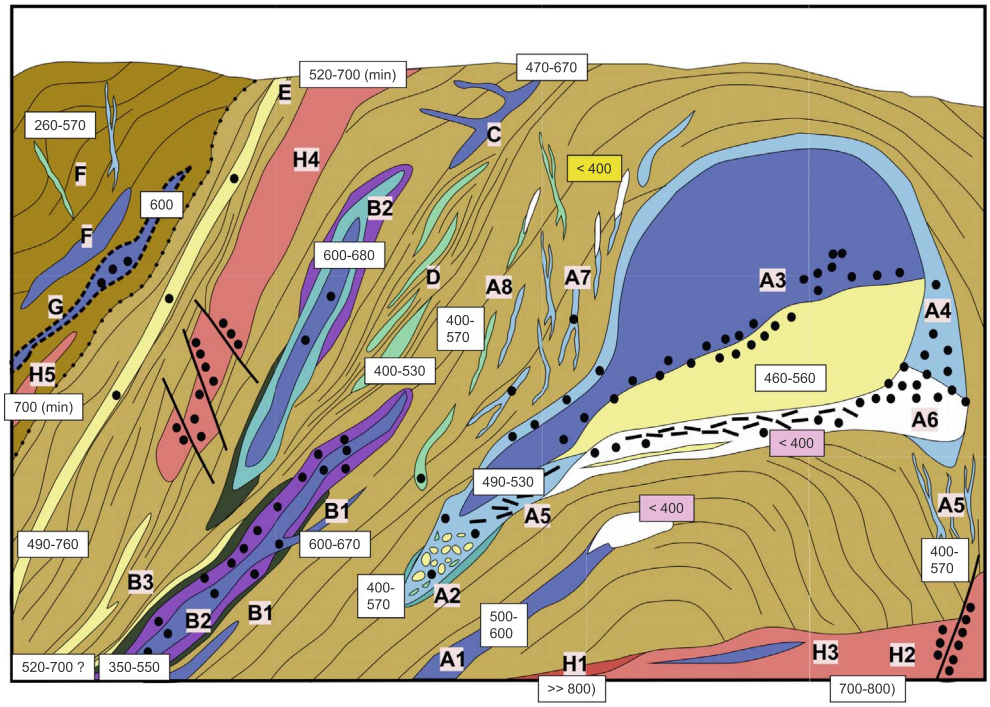

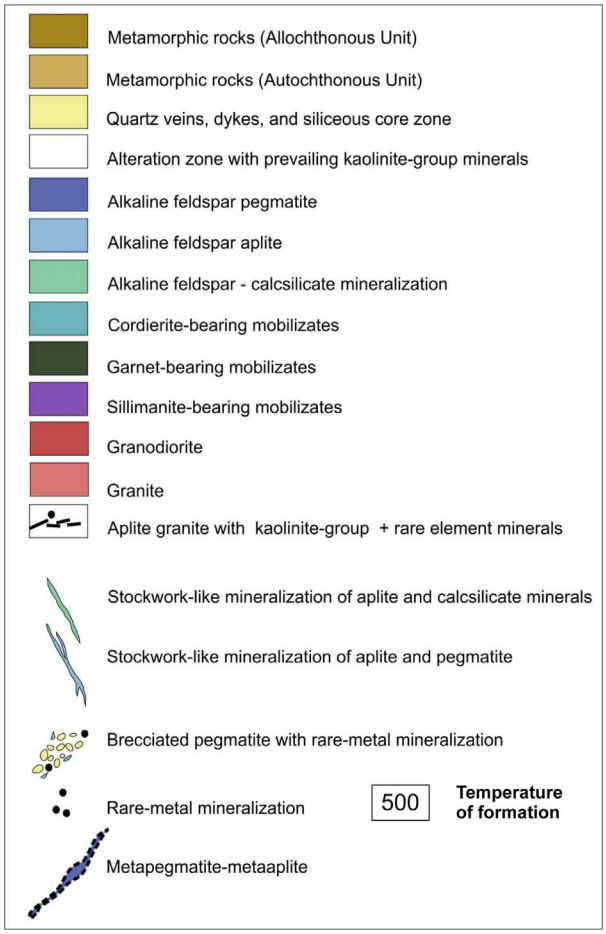

Fig. 2. Idealized cross section through the crystalline basement made up of allochthonous and autochthonous units hosting the Variscan-type pegmatitic, aplitic and granitic rocks (not to scale). The position of the granitic suite (H1–H3) relative to the pegmatitic and aplitic rocks is for reasons of space in the cartoon and has no genetic connotation as to the granite-pegmatite relation. a) Morphology and composition of pegmatitic, aplitic and granitic rocks. For more details of the various types (e.g. A) and sub-types (e.g. A2) see Tables 2a, 2b. The temperature of formation during emplacement are given in white boxes the temperature of argillic alteration in purple boxes (pH ≤ 7) and yellow boxes (pH ≥ 7). b) Legend of Fig. 2a. (For interpretation of the references to color in this figure legend, the reader is referred to the web version of this article.)

(2009) (Fig. 1c, d). To ease correlation with lithostratigraphic units and avoid repetitions of age data and lithologies the legend is supplemented with Arabic numerals (Fig. 1d).

The NE Bavarian Basement has been exposed by a strong uplift covering the Mesozoic and Cenozoic eras. At its western rim it is encroached upon by Triassic and Cretaceous sediments and in parts covered by volcaniclastic and volcanic rocks of Late Paleozoic age (Fig. 1c, d – 15) – (Dill and Klosa, 2011 – further literature cited

Table 2a
Geology and lithochemistry of Variscan-type pegmatitic, aplitic and granitic rocks. Application of the CMS classification scheme to the transect barren pegmatic rocks- rare-element pegmatites-granitic lithologies. The codes in the first column refer to the numbering in the text and in the cartoon of Fig. 2a. The structural, mineralogical and chemical descriptions in column 2 through 5 follow the guidelines given in the CMS classification scheme in Table 1.

Code	Type of pegmatite (CMS 1)	Shape and structure (CMS 2)	Chemical qualifier (CMS 3)	Mineralogical qualifier (CMS 4)	Geodynamic setting	Structural type	Interpretation of processes	Economic relevance	Pysical-chemical regime	Chemical pattern (major)	Chemical pattern (minor)
A1	pegmatoid	tabular	(P-As)	(garnet) feldspar-mica-quartz	autochthonous unit	anticlinal hinge to limb	Metamorphic felsic mobilizate affected by late-stage hydrothermal kaolinization Mixing of fluids metamorphic-hydrothermal	feldspar, kaolinite	P: 500°C-600°C, Eh < 0 S: < 400°C, pH < 7	Circular Shift: Na, K, P	Stellate: As, Rb, Pb
A2	pegmatite (pegmatoid)-aplite	tabular-wedge-shaped	(Ba)	(amphibole-diopside-epidote-andalusite) feldspar-mica-quartz	autochthonous unit	anticlinal hinge to limb	Metamorphic felsic mobilizate Incipient stage of fractionation	feldspar	P: 400°C-570°C, Eh oscillating around 0	Circular Shift: Na, K, P, Ca	Lens-shaped Ba, Pb, Rb
A3	pegmatite-(aplite)	stock-like/zoned	As-Bi-Cu-Sn-U-Zn-Be-Ta-Nb-Li-P	feldspar-mica-quartz	autochthonous unit	anticlinal hinge	Self-intrusive and strongly fractionated molten felsic body piled up in the topmost part of an anticline Mixing of processes with fluids derived from HT pegmatitic fractionation and deep-seated fluid sources	feldspar, quartz, rare elements	P: 460°C-560°C	Necking-down Na, K, P, Al, Fe, Mn, Ca	Stellate: Bi, Nb, Cu, Zn, As, Rb
A4	aplite-(pegmatite)	stock-like/zoned, veinlets-dyke-layer (special facies with "nigrine")	As-Bi- Li-P (Ti-Nb)	(tourmaline)-feldspar-mica-quartz	autochthonous unit	anticlinal hinge	Metamorphic felsic mobilizate - marginal part of a fractionated molten felsic body with relics Mixing of processes with fluids derived from HT pegmatitic fractionation and deep-seated fluid sources (the latter dominates in faultbound felsic bodies)	feldspar, quartz, rare elements		Circular Shift: Na, K, P, Ti	Stellate: As, Bi, Nb, Rb
A5	aplite granite	tabular/ graphic/ porphyritic fading out in stockwork-	(Ta)-Nb-P	(mica)-feldspar-quartz	autochthonous unit	anticlinal hinge to limb	Metamorphic felsic mobilizate unaffected by late-stage hydrothermal kaolinization Mixing of processes with fluids derived from HT pegmatitic	feldspar	P: 490 C - 530°C S: > 400°C, pH ≥ 7	Circular Shift: Na, K, P	Stellate: Rb, Nb, As
		like veinlets (≈ A8)					fractionation and deep-seated fluid sources				
A6	aplite granite-aplite	tabular-stock-like	(P)-Bi-Ta-Nb	(mica-feldspar)-kaolinite - quartz	autochthonous unit	anticlinal hinge (to limb)	Metamorphic felsic mobilizate moderately fractionated - strongly affected by late-stage hydrothermal kaolinization Mixing of processes with fluids derived from HT pegmatitic fractionation and deep-seated fluid sources	kaolinite	P: 490 C - 530°C S: < 400°C, pH ≤ 7	Necking-down Na, Mn, P	Stellate: Nb, Rb, Bi, As
A7	aplite	vein-layer / stockwork-like	(Mo-Nb-Mn)-P	(smectite-kaolinite-vermiculite-chlorite) mica-feldspar-quartz	autochthonous unit	anticlinal hinge (to limb)	Hanging wall metamorphic rock (exocontact zone) proximal alteration zone Mixing of processes with fluids derived from HT pegmatitic fractionation and deep-seated fluid sources	no economic significance / ore guide	S: < 400°C, pH < 7 to pH ≥ 7	Lens-shaped Mn, P, Fe	Lens-shaped Zn, Mo, Rb, Nb
A8	aplite	vein-layer / stockwork-like	(Sr-P)-Ca	(diopside, clinozoisite, grossularite, dolomite) feldspar-mica-quartz	autochthonous unit	anticlinal limb (to hinge)	Hanging wall metamorphic rock (exocontact zone) distal alteration zone Typomorphic mineralization	no economic significance / ore guide	P: 400°C-570°C, pH ≥ 7	Circular Shift: P Ca, Mn	Circular U
B1	aplite-aploid	tabular (with porphyritic reaction zone abundant in biotite)	(Pb-Zn-As)	(chlorite-talc) feldspar-mica-quartz	autochthonous unit	limb	Marginal facies of some B-type rocks with wall rock alteration and incorporation of metamorphic parent material HT and LT hydrothermal processes with little pegmatitic fractionation	no economic significance / ore guide	P: 600°C-670°C	Circular ±Ca, ±Ti, ±Fe	Lens-shaped (to stellate): Pb, As, Bi, ±Rb, ±Nb
B2	aploid-pegmatoid-aplitic gneiss	tabular-layer/ zoned	(Bi-Pb-Zn-F-Cu-Sc-Nb-U) - Mn-As-P (Au?)	(cordierite-sillimanite)-garnet- mica-feldspar-quartz	autochthonous unit	limb	Metamorphic felsic mobilizate resultant from retrograde processes with moderate wall rock reaction HT and LT hydrothermal processes with pegmatitic	Feldspar+ rare metal (e.g. Sc)/ ore guide gold?	P: 350°C-550°C	Lens-shaped Mn, P, ±Fe, ±Ca, ±Na	Stellate: Rb, As, Zn, Cu, Nb

(*continued on next page*)

Table 2a (*continued*)

							fractionation				
B3	aploid to aplogranitoid	tabular (boudinage) zonal arrangement with aploids and pegmatoids (central or marginal)	Zr	(sillimanite-cordierite) mica-feldspar-quartz	autochthonous unit	limb	Relict facies of metamorphic mobilizates with mainly Si provoked by retrograde regional metamorphism (diaphtorites) of paragneisses. Strong fractionation/ depletion	no economic significance	P: 520°C - 700°C?	Circular Si, Ti, ± Ca	Circular (to necking down) Zr
C	pegmatite/ pegmatoid - aplite	tabular-layer/graphic -vein	(As-U-Ba-Mn)-P	(tourmaline-dumortierite-andalusite) feldspar-mica-quartz	autochthonous unit	limb and structure zones	Metamorphic felsic mobilizate resultant from retrograde processes with moderate wall rock reaction Moderate fractionation	no economic significance (gemstone?)	P: 470°C to 670°C	Lens-shaped P, Mn	Lens-shaped to stellate As, Ba, Pb, Rb, U
D	aplite	Shear veins-breccia	(Sr)-Ca	epidote-mica-feldspar-quartz	autochthonous unit	tectonized structure zones	Felsic mobilizate derived from the metamorphic rocks along shear zones. Moderate pegmatitic fractionation.	no economic significance (relation to A8)	P: 400°C-530°C	Circular (with necking-down) Ca, K, P	Circular (trend to stellate) Strong depletion Ni, Cu, As, Zn
E	pegmatite	Vein, dykes	(Nb-Ta-Co-Cu-Mo-Pb-Zn) P-Mn-Fe	Fe-Mn oxide feldspar-quartz	autochthonous unit	lineamentary structure zones	Felsic mobilizate retrograde metamorphic processes and deep-seated crustal source Mixing of fluids derived from pegmatitic fractionation and deeply circulating fluids	no economic significance (relation to A8)	P : 490°C - 760°C	Lens-shaped Mn, Fe, P with necking-down)	Lens-shaped (with necking down) Cu, Mo, Zn, Rb, Nb
F	pegmatoid-aploid-aplite	layer-lens-vein/ stockwork-like	(REE)-Cu-Pb-As-Zn-S (in Muglhof Mn-P)	(amphibole, clinopyroxene, zeolite-chlorite) feldspar-mica-quartz	allochthonous unit	limb-, thrust- and fault-bound	Felsic mobilizate derived from retrograde metamorphic processes HT and LT hydrothermal mineralization and postmagmatic alteration linked to deep-seated crustal source	no economic significance (in places detrimental to the quality of aggregates and dimension stones	P : 260°C - 570°C	Circular pattern Na, K, ±Ca, ±Fe	Lens-shaped (to stellate): As, Pb ±Bi, ±Mo, ±Zn, ±REE
G	meta-pegmatite	tabular	As-Pb-Zn (Püllersreuth Nb-Be)	feldspar-mica-quartz	allochthonous unit	anticlinal hinge to limb	Pegmatite overprinted and recrystallized LT hydrothermal mineralization >> HT mineralization and pegmatitic mineralization	feldspar	P: ≈ 600°C	Circular pattern Shift: Na, K	Stellate: Zn, Pb, As, Bi
H1	granodiorite (to diorite)	stock-like to sheet-like		(amphibole) mica-quartz-feldspar	autochthonous and allochthonous unit	deep-seated structure zones	Postorogenic magmatic mobilization from a subcrustal source (?) and fractionation leaving behind a restites ("cumulate")	aggregates and dimension stones	>> 800°C	Circular pattern Na, K, Ca, P	Circular pattern ±Pb, ±Ba
H2	granite	stock-like to sheet-like	U	mica-quartz-feldspar	autochthonous unit (H2a) + allochthonous unit (H2a/b)	deep-seated structure zones	Postorogenic magmatic mobilization ("Older Granites" S of the Luhe Line H2a / ("Younger Granites" N of the Luhe Line H2b).	aggregates and dimension stones, relevance for faultbound mineralization only	< 800°C	Circular pattern Na, K, P	Circular pattern With necking down (H2a)
H3	pegmatite granitic	schlieren		(tourmaline) mica-quartz-feldspar	allochthonous unit	endo-contact zone	Intragranitic mobilization and fractionation from H2b ⇒ H3	no economic significance	unknown	Necking-down Na, K, P,	Necking-down (stellate) Rb, Pb, Nb, Bi
H4	granitoid-metagranite-orthogneiss / granitic gneiss	tabular, layer, schlieren	U faultbound (Fig. 8a)	(cordierite-sillimanite+ garnet)-mica-feldspar-quartz	autochthonous unit (H4a) + allochthonous unit (H4a/b)	anticlinal hinge to limb	Pre-synorogenic mobilization from paragneiss. Cor-Sill-Gar-metagranites S of the Luhe Line H4a, muscovite-bearing Cor-Sill-Gar granitoid N of the Luhe Line H4b Early Granitoids H4 are more strongly fractionated than the Late Paleozoic granites (H2). Metamorphic differentiation is much stronger than magmatic.	no economic significance in its pristine stage, relevance for faultbound mineralization only	P: 520°C - 700 °C (min)	Circular pattern Shift: P, Na, K (necking down)	Circular pattern (stellate) Pb, Rb , As
H5	granitoid	tabular, layer, schlieren		(cordierite-sillimanite+ garnet)-mica-feldspar-quartz	allochthonous unit	anticlinal hinge to limb	Syn- to postorogenic mobilization from paragneiss, strongly fractionated	no economic significance	P: 700 °C (min)	Circular pattern P, Na, K	Stellate pattern: As, ±Pb, ±Rb

therein). Neogene sediments and volcanites (Fig. 1c, d – 16 to 17) resulted from the subsidence of the ENE-WSW striking Eger Graben (Ulrych et al., 1999) and a pervasive chemical weathering of basement rocks under tropical conditions (Dill, 2017a,b). Only the chemical weathering impacted on the evolution of the pegmatitic rocks and is resumed later in the study (Section 4.4).

The crystalline rocks of the NE Bavarian Basement pertain to two geodynamic zones, the Saxothuringian Zone, represented by Ordovician and Cambrian rocks at the northern margin of the study area (Fig. 1c, d – 9) and the Moldanubian zone which encompasses a great variety of rocks and hosts the pegmatitic and aplitic rocks (Fig. 1c, d – 1 to 8, 10 to 15). The Moldanubian Zone is made up of an autochthonous unit (Fig. 1c, d – 1 to 8) called the Moldanubicum *sensu stricto* and an allochthonous one (Fig. 1c, d – 10 to 11) named the Teplá-Barrandian zone or in Bavaria as Zone of Erbendorf-Vohenstrauß "ZEV" (Malkovský, 1979; Weber and Behr, 1983; Stettner, 1992; Franke et al., 1995). Their rocks are of Neoproterozoic through Early Paleozoic age. First records of detrital material in paragneisses on zircons showed an event around 2600–2400 Ma, followed by signs referring to a medium-pressure metamorphic event (MP) at about 380 Ma and strong low-pressure- high-temperature metamorphic event (LP) at 320 Ma (Hansen et al., 1989). The granitic rocks resemble the pegmatites with regard to their basic chemical and mineralogical compositions but on the other hand are very much distinct in their age of formation, structure and last-but-not least geodynamic setting (Fig. 1c, d – in parts 4, 5 to 7, 12 to 14) (Voll, 1960; Forster, 1965; Forster and Kummer, 1974; Steiner, 1986). The granitic lithologies in the map of Fig. 1c are subdivided into four groups.

(1) The metamorphic rocks south (No. 2) of the Luhe Line and along its eastern extension (No. 1) are rife with leucocratic and diatectic gneisses revealing a general W-E trend (Figs. 1c-6 and 7).
(2) Between Eslarn and the area East of Tirschenreuth garnet-cordierite-sillimanite gneisses underwent retrograde regional metamorphism getting less intensive from the S towards the N (diaphtorite I ⇒ diaphtorite II). They are interbedded with granitoids, pegmatoids and aploids, only the larger lenses are plotted in the map (Fig. 1c – 5).
(3) In the nappe of the ZEV, granitoids are intercalated into the paragneisses (Fig. 1c – 10).
(4) The last suite of granitic rocks in the study area shows a tripartite subdivision. It is a series of irregularly-shaped fine-to medium-grained granites (no 13) confined in their occurrence to the cordierite-sillimanite gneisses (no 1, 2). North of the Luhe Line (Fig. 1c – A-A′) large complexes of S-type granites crop out in a NNW-SSE trending zone and are arranged in order of their intrusion (Fig. 1c – 14): Leuchtenberg (LEU), Falkenberg (FAL) Flossenbürg Granites (FLO) with its eastern outlier at Bärnau (BAR). The origin of some more basic enclaves of intrusive rocks of granodioritic through gabbroic composition called "Redwitzites" is still enigmatic (No. 12) (Stettner, 1992). The lithological results of the late-stage thermal events in the Moldanubian Zone of the Variscides sparked several chronological studies yielding ages in the range 330–310 Ma (Köhler et al., 1974; Wendt et al., 1986, 1992, 1994; Kalt et al., 2000; Gerdes et al., 2006; Siebel et al., 2008).

4. Results

4.1. Lithotypes and lithochemistry – a basis for classification

The pegmatitic s.l. and granitic rocks in the study area are subdivided according to the CMS classification scheme into 8 lithotypes (A–H) based on their structural and compositional features and geodynamic settings (Tables 1, 2a, 2b, Fig. 2a, b). The analysis of the structural geology and metamorphic processes affecting the pegmatites is conducted according to the basics published by Fry (1991), Davis and Reynolds (1996), Best (2002), Van der Pluijm and Marshak (2004), Fossen (2010) and Lisle et al. (2011). To be applicable also for field work as some sort of a manual, the outward lithological appearance of pegmatites *sensu lato* and their affiliated rocks as well as the geological and chemical results are treated in the text of Section 4.1 (Tables 2a, 2b, Figs. 2–5).

4.1.1. A-type anticlinal pegmatitic and aplitic lithotypes

Geological results: A-type rocks are located in the hinge zones (A3, A4) of anticlines and also found in their limbs (A1, A2, A5–A8) (Fig. 2a, Table 2a). Forster (1965) published a line drawing from north of Pleystein, characteristic of the tectonic setting in the study area (Fig. 3a). It shows the size of the pegmatitic body to achieve a maximum in the hinge zone, whereas towards the limbs it gradually pinches out. You might find these features often in hand specimens from the study area as well as abroad, e.g., Mendoza Pegmatite Province, Argentina (Fig. 3b, c). These stock-like concentrations are common trapping features of pegmatitic rocks, however, sometimes difficult to detect as being refolded and exposed as an isoclinal fold which may pretend a simple tabular felsic body. It is well represented in the study area by the zoned Hagendorf-South, Hagendorf-North and Pleystein pegmatites, where the feldspar rim has, however, been eaten away by pervasive argillitization (Fig. 2a, 6b, 4a, b). The interlimb angle describes these anticlinal structures as open folds (Figs. 2, 4a, b). The pegmatites of A3 and A4 tend to wedge out in pegmatoids of A2 as they approximate the limbs. The latter rock types are very much different with regard to their mineral assemblage (e.g. amphibole, diopside, epidote, andalusite, biotite) which are moderately aligned (Tables 2a, 2b, Fig. 5a). In the present case history, A2-type pegmatoids only develop along the western flanks of the fold structures attesting to an asymmetrical host anticline (Figs. 2, 3, 4b). The structural types A5 and A6 significantly differ from each other with respect to the intensity of kaolinization which is widespread underneath the pegmatite in A6 and decreases towards the pegmatite in A5 in favor of a muscovitization (Fig. 5b). A5-type aplite veinlets are also common to the eastern footwall rocks of the Kreuzberg Pegmatite (Fig. 2a). Together with A1 pegmatoids they make up the footwall facies of the A-type pegmatites (Fig. 2a). Unlike, other tabular pegmatoids or aploids (see e.g., B-type), A1 is also affected by kaolinization. The hanging wall facies of the A-type pegmatites is made up of two different types of stockwork-like veinlets and layers of aplites. A7 is representative of the proximal facies, abundant in clay minerals mainly kaolinite-group minerals, whereas A8 is representative of the distal facies and rife with calcsilicate minerals and dolomite (Tables 2a, 2b, Fig. 5d, f).

Chemical results: Major elements and diagnostic minor or accessory elements are presented in spider diagrams to allow for a genetic comparison among the lithological types (Fig. 6a, b) (Dill et al., 2014a,b; Paxton et al., 2016). The major elements of the lithological types A1, A2, A4, A5, and A 8 display a circular pattern more or less shifted towards the Na_2O-K_2O-P_2O_5 circle segment. Some have a small, peak such as A1 towards Al_2O_3, or type A8 towards CaO and to a minor degree also towards MnO. The most striking pattern is the necking-down pattern most conspicuously represented by A3 which is strongly enriched in CaO, Na_2O, K_2O, P_2O_5, Al_2O_3, Fe_2O_3, and MnO but impoverished in MgO and TiO_2 (Fig. 6). Less well expressed, you might find this chemical pattern in type A6, too. The lens-shaped pattern is only encountered in type A 7 which shows a conspicuous trend P_2O_5 – MnO (Fig. 6b). The minor elements, rather called accessory elements due to its build-up of ore zones in the pegmatite only rarely come close to a circular pattern as in A8 (Tables 2a, 2b, Figs. 2a, 6). A typical lens-shaped pattern can be seen in A2, less well expressed in A7. The first type A2 has a considerable Ba anomaly, the second one Zn, Mo, Rb, and Nb peaks. The majority of spider diagrams may be denominated as a stellate pattern.

Table 2b
Mean chemical composition of pegmatitic, aplitic and granitic rocks normalized to a reference LP paragneiss (sillimanite-cordierite-biotite gneiss) from the study area. H2a-S means south and H2b-N north of the Luhe-Line Fault Zone, respectively (see Fig. 1c).

Type	SiO_2	TiO_2	Al_2O_3	Fe_2O_3	MnO	MgO	CaO	Na_2O	K_2O	P_2O_5	As	Ba	Bi	Cu	Mo	Nb	Ni	Pb	Rb	U	Zn	Zr	REE
A1	1.11	0.07	1.03	0.12	0.08	0.12	0.33	1.83	1.67	1.19	2.83	0.15	0.90	0.17	0.91	0.50	0.10	1.60	1.58	0.89	0.36	0.06	0.85
A2	1.11	0.27	0.84	0.21	0.27	0.31	1.48	1.69	2.28	1.92	0.62	4.31	1.00	0.30	0.93	0.50	0.15	1.83	1.67	0.94	0.42	0.51	1.05
A3	1.10	0.02	0.83	0.31	0.65	0.01	0.49	1.59	1.83	5.67	54.06	0.07	465.42	120.57	0.83	215.01	0.08	2.59	10.21	39.59	58.72	0.23	0.63
A4	1.34	0.50	0.48	0.20	0.35	0.17	0.29	0.87	0.71	2.13	59.86	0.25	10.11	0.49	0.57	1.94	0.83	1.13	1.18	0.61	0.39	0.25	0.52
A5	1.22	0.21	0.74	0.16	0.34	0.11	0.48	2.22	1.06	2.42	1.12	0.28	1.18	0.20	0.94	2.27	0.14	0.89	4.28	1.02	0.34	0.76	0.94
A6	1.14	0.05	0.96	0.20	0.83	0.07	0.14	0.82	1.02	0.98	1.56	0.15	3.08	0.45	0.74	7.15	0.16	1.26	5.04	0.75	0.92	0.23	0.70
A7	1.09	0.37	0.86	0.66	7.62	0.26	0.17	0.56	1.19	1.84	0.91	0.90	0.92	0.88	2.11	1.72	0.54	0.82	3.08	1.22	1.77	0.60	1.08
A8	1.11	0.47	0.88	0.29	1.22	0.10	4.86	0.78	0.72	1.66	0.69	0.63	0.46	0.47	0.39	0.84	0.25	1.05	0.76	0.97	0.31	0.84	0.64
B1	1.14	0.37	0.78	0.37	0.28	0.45	1.51	1.38	1.81	1.38	1.87	0.77	0.92	0.16	0.86	0.88	0.44	2.44	1.20	0.83	0.54	0.09	0.78
B2	1.14	0.14	0.80	0.40	2.60	0.16	0.74	1.87	1.16	4.94	42.27	0.29	0.76	0.73	0.68	1.14	0.25	1.25	8.64	0.95	0.57	0.30	0.64
B3	1.29	0.65	0.51	0.41	0.47	0.39	0.81	0.81	0.58	0.69	1.20	0.74	0.17	0.25	0.37	0.59	0.35	0.79	0.58	0.98	0.37	1.85	0.86
C	1.16	0.09	0.87	0.21	1.50	0.17	0.54	1.46	1.61	2.16	2.11	0.86	0.91	0.24	0.84	0.62	0.16	2.01	1.38	1.12	0.37	0.14	0.76
D	1.05	0.62	0.84	0.47	0.24	0.02	4.96	0.93	2.32	1.08	0.46	1.15	1.00	0.16	1.11	0.75	0.12	0.37	1.85	0.97	0.35	1.16	0.92
E	0.23	0.28	0.56	8.05	46.37	0.04	0.16	0.13	0.77	7.76	2.62	1.43	1.67	13.01	9.36	4.68	0.52	0.57	4.96	3.22	8.52	0.12	2.39
F	1.04	0.25	0.70	1.07	0.23	0.45	1.85	2.21	0.86	0.74	23.10	0.51	1.50	1.12	1.20	0.62	0.31	2.78	0.95	1.11	1.43	1.04	1.79
G	1.09	1.01	0.83	0.42	0.48	0.42	0.75	1.69	1.69	0.91	6.05	1.07	2.17	0.37	0.38	0.95	0.44	8.27	0.72	0.63	23.97	1.66	0.48
H1	1.03	0.77	0.88	0.51	0.51	0.65	3.01	1.59	1.88	2.08	0.46	1.46	1.00	0.30	1.00	0.86	0.28	1.93	1.19	0.94	0.44	0.81	0.98
H2a-S	1.18	0.49	0.75	0.44	0.26	0.18	0.65	1.46	1.77	0.38	0.69	0.49	0.71	0.31	0.68	0.91	0.11	2.46	2.58	1.40	0.50	0.69	0.90
H2b-N	1.19	0.17	0.76	0.17	0.29	0.10	0.59	1.91	1.56	1.96	1.18	0.25	0.83	0.27	0.76	1.00	0.22	2.19	3.08	1.11	0.47	0.37	0.90
H3	1.20	0.05	0.78	0.08	0.17	0.04	0.32	1.65	1.92	1.79	0.46	0.84	1.42	0.40	0.93	1.39	0.10	1.74	2.93	1.22	0.34	0.08	0.86
H4a-S	1.17	0.22	0.79	0.22	0.31	0.17	0.63	2.06	1.42	3.32	1.60	0.26	0.39	0.17	0.52	0.45	0.12	1.44	1.41	0.82	0.39	0.36	0.86
H4b-N	1.19	0.08	0.79	0.10	0.27	0.05	0.33	2.15	1.52	2.92	1.23	0.25	0.69	0.13	0.52	0.46	0.07	1.74	1.45	0.72	0.22	0.25	0.86

4.1.2. B-type limb-hosted pegmatitic and aplitic lithotypes

Geological results: Tabular type-B pegmatitic and aplitic rocks occur outside the main anticlines along the limbs; they may be folded but they never pile up and get accumulated in a way like A-type lithologies. Their marginal facies is often characterized by mega crystals of biotite (Fig. 5e). In the majority of cases pegmatitic and aplitic rocks of this type belong to the (cordierite-sillimanite)-garnet- mica-feldspar-quartz pegmatoids and aploids (Fig. 5g, Table 2a). B-3 rocks have already been recorded by Forster (1965) as "Graywacke-Quartzite Gneiss". They form lenses as much as 2 km long and less than 100 m wide with a general strike around NNE-SSW. Some of them display boudinage and occur in a zonal arrangement with aploids and pegmatoids of B 1 and B 2 either forming a rim around them or the core zone or genetically bound to the diaphtorites (Fig. 1c). Based on their mineral assemblage and their high silica content the above metasedimentary connotation is discarded and using the term (sillimanite-cordierite) mica-feldspar-quartz aploid – aplogranitoid assigned to the felsic mobilizates (Table 2a).

Chemical results: The chemical signature of B1- and B3 lithotypes is conspicuously characterized by circular patterns devoid of any shift, being almost identical with the bulk composition of the host paragneisses (Fig. 6b). The majority of aploids and pegmatoids gradually fade out in aplitic gneisses and chemically have to be classified as lens-shaped (Tables 2a, 2b, Fig. 6b). The simplest trace element pattern categorized as circular with a slight tendency of necking down, is observed in B3 where a strong positive Zr anomaly is accompanied by negative anomalies of Bi, Cu, Ni, Zn, Mo, and Rb (Fig. 6b). The chemical pattern of B1 gradually converts from a lens-shaped/stellate into a true stellate pattern.

4.1.3. C-type limb- and structure-bound pegmatitic and aplitic lithotypes

Geological results: C-type pegmatitic rocks are denominated as (tourmaline-dumortierite-andalusite) feldspar-mica-quartz pegmatite/pegmatoid-aplite (Fig. 5h). They exhibit the stratiform structure of limb-hosted B-type lithologies as well as the features of structure bound mineralizations cross-cutting through the metamorphic S planes (Figs. 2a, 3a, b).

Chemical results: It is a lens-shaped chemical pattern as far as the major elements are concerned with a pronounced Mn-P trend and transitional from lens-shaped into stellate patterns with regard to the trace element variation (Fig. 6c).

4.1.4. D-type shear-zoned hosted aplitic lithotypes

Geological results: D-type saccharoidal aplite is penetrated by shear veins mineralized with Fe-enriched epidote (Fig. 5i). It is a facies type mostly found at the edge of pegmatite systems.

Chemical results: The chemical pattern is dominated by calcsilicates and lack of Mg-bearing silicates: This lead to the coiled shape of a circular pattern with necking-down features (Fig. 6c). The trace elements are similar to that of the metamorphic country rocks which while depleted in Ni, Cu, As, and Zn eventually yield a circular pattern (trend to stellate pattern).

4.1.5. E-type aplitic and pegmatitic lithotypes bound to lineamentary structure zones

Geological results: The CMS classification scheme has been designed to integrate different rocks of a pegmatitic system even those which do not strictly fulfill the tripartite granitic mineral assemblage of feldspar, quartz and mica. It is mainly NW-SE striking dykes and veins of felsic and basic composition which are common to pegmatite provinces and whose role for the emplacement of pegmatitic and aplitic rocks is still hotly debated (Kramer and Seifert, 1994; Baumann et al., 2000; Seifert, 2008; Dill, 2015b). While there is plenty of literature dealing with lamprophyres and basic dykes, classification schemes applicable to the full spectrum from the granite and pegmatite clans through to the quartz and mineral veins is scanty (Streckeisen, 1980; Cox et al., 1979; Le Bas et al., 1986; Pivec et al., 2002; Vasyukova et al., 2011). In the current study, it is the gap between deep-seated quartz dykes extending over a distance of more than 1 km and quartz veins less than 1 km in length and 1 m in thickness which are mineralized, in places, with Fe

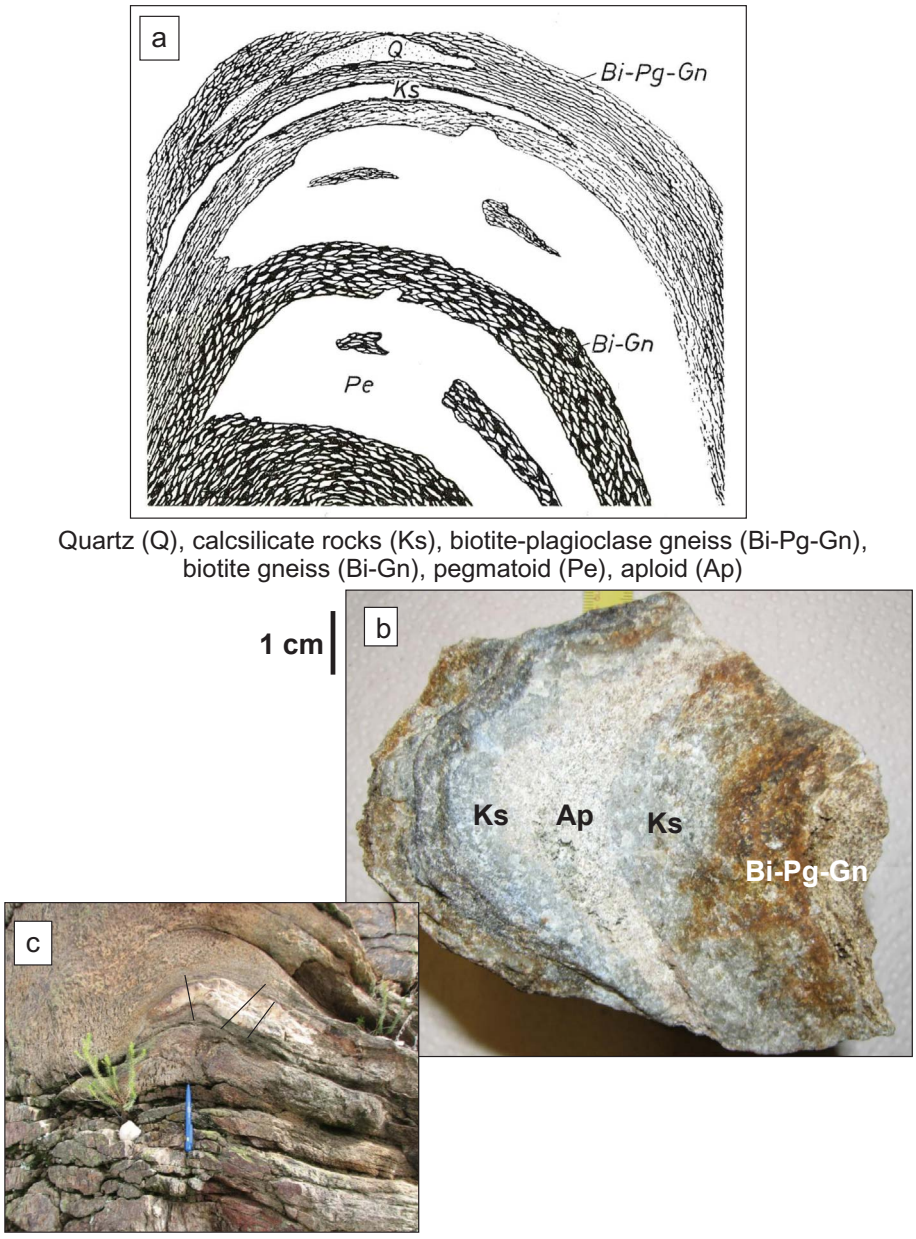

Fig. 3. Limb- and hinge-zone hosted anticlinal pegmatitic and aplitic rocks. a) Line drawing published by Forster (1965) showing the pegmatites concentrated in the hinge zone of folds which gradually pinch out along the limbs (see also Fig. 2A3). Lenses of pegmatites controlled by the schistosity may be traced over 50 m. Locality: Peugenhammer Quarry north of Pleystein. b) Hand specimen from the Kupferholz (mica)-feldspar quartz pegmatoid. c) Pegmatoid at outcrop in the Mendoza Pegmatite Province, NW Argentina, for comparison. The fractures fanning out in the hinge zone are marked with black lines.

and rare elements, on one side and the pegmatitic, aplitic and granitic rocks on the other that has to be bridged by the CMS classification. Such an association of quartz dykes and pegmatitic rocks is not uncommon to pegmatite fields (Dill, 2010; Neiva et al., 2008; BurIánek et al., 2011). E-type structures range from (kaolinite) – goethite-mica quartz veins through magnetite-hematite-feldspar-quartz veins. Iron oxides occur as mushketovite (magnetite pseudomorphic after hematite) or specularite (Fig. 5j). Quartz veins with this glittering vein hematite are known from Merritt, Canada (Laznicka, 1985) and from N of the study area at Gleissinger Fels, in granites of the Fichtelgebirge Mts. (Dill et al., 2008b).

Chemical results: The spider diagram of the major element of E-type veins is lens-shaped (Mn-Fe-P). Its chemical pattern comes close to what has been observed in B2 pegmatoids which show a strong depletion in MgO (Fig. 6c). The minor elements, however, give a vaguely expressed lens-shaped pattern with a pronounced necking-down for Zr.

4.1.6. F-type limb- and faultbound aplitic and pegmatitic lithotypes in allochthonous units

Geological results: The F-type rocks are exclusive to metabasic rocks of allochthonous tectonic units. This is underscored by the presence of minerals such as amphibole, clinopyroxene, zeolite and chlorite in the quartz-feldspar matrix of the Na-enriched pegmatoids and aploids (Fig. 5k).

Chemical results: The major elements make up a typical circular pattern whereas the minor elements point to a lens-shaped pattern with As and Pb with a stellate trend (Fig. 6c)

4.1.7. G-type limb- and hinge-related metapegmatitic lithotypes in allochthonous units

Geological results: G-type rocks stand out from the afore-mentioned ones owing to their dynamo- and regional metamorphic overprinting in the allochthonous units of the ZEV which lead to two generations of white mica very much different in size, with mega-crystals measuring 4 × 4 × 0.5 cm (Figs. 1c, 5l). The metapegmatites went through different metamorphic processes, with youngest of which taking place under MP and HT conditions (Dill, 2015b). They are quite similar to the garnet-bearing barren pegmatoids from the autochthonous units. Only one metapegmatite at Püllersreuth is exceptional for its occurrence of beryl and columbite (Linhardt, 2000).

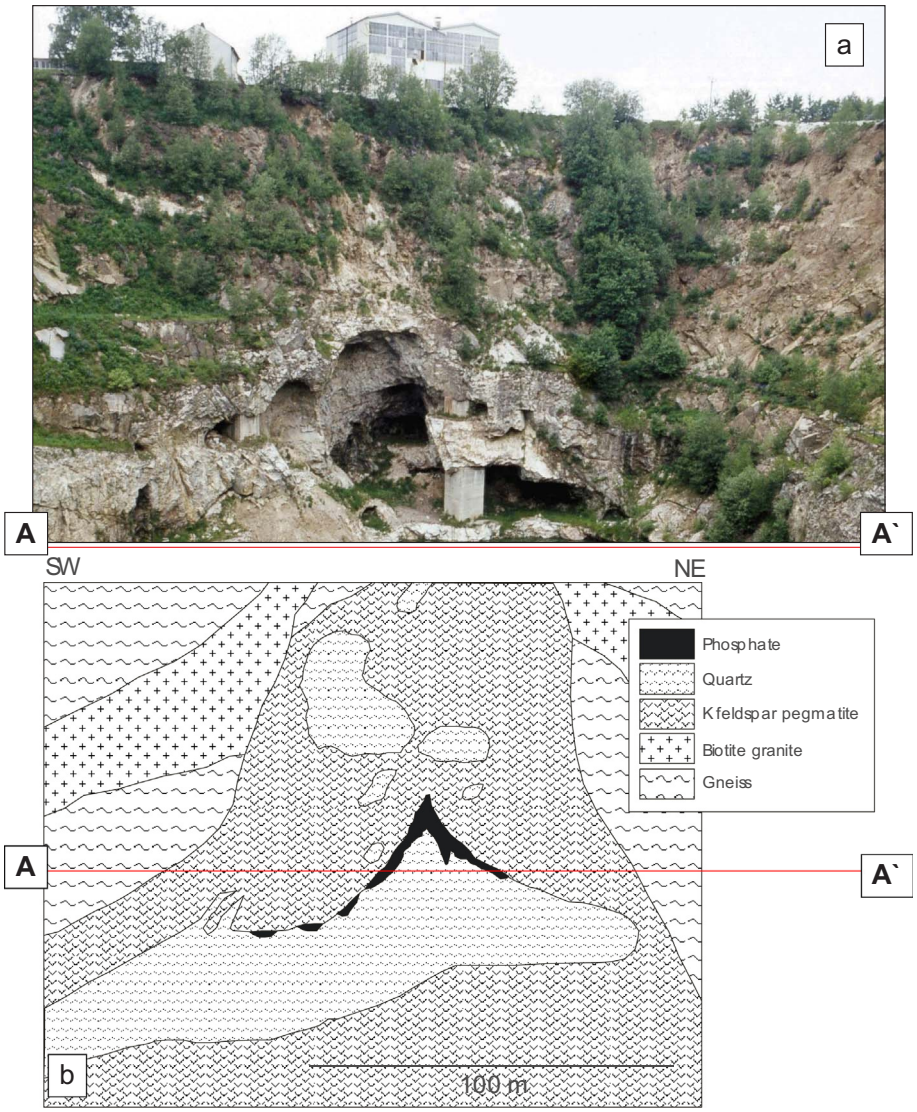

Fig. 4. The zoned stocklike As-Bi-Cu-Sn-U-Zn-Be-Ta-Nb-Li-P (aplite)-pegmatite Hagendorf-South. a) The uppermost part (A3 + A4) at outcrop in the open pit above the 67-m level (photograph: Rank 1984). b) Cross section unraveling the geology of the Hagendorf-South Pegmatite. The horizontal red lines are drawn for correlation of the cross section and the photograph. (For interpretation of the references to color in this figure legend, the reader is referred to the web version of this article.)

Chemical results: The circular chemical pattern is common to many sampling sites under study with a shift either to Na or K (Fig. 6c). Unlike their major elements, the trace elements exhibit a stellate pattern dominated by Zn, Pb, Bi and As.

4.1.8. H-type granitoids and granitic pegmatites straddling the Luhe-Line fault zone

Geological results: H-type lithologies are subdivided into 5 subtypes, only one of which can be named granitic pegmatite *sensu stricto* (Tables 2a, 2b, Fig. 6c – H3). In contrast to the lithotypes mentioned in Sections 4.1.1–4.1.7, which do not attain a size to qualify them for being plotted on the map of Fig. 2c, H-lithotypes do so, excluding the granitic pegmatites H3 and H5 in the allochthonous unit which resemble metapegmatites of lithotypes G (Table 2a). H1 lithotypes are scattered complexes of Early Carboniferous age (Fig. 1c-12). They are the basic predecessors to the large Late Carboniferous to Permian granite intrusions (Fig. 1d – 15, 14, Tables 2a, 2b – H2a, H2b) exposed on both sides of the Luhe-Line (Fig. 1c – A-A′). H-1 lithotypes mainly show a granodioritic to dioritic composition in terms of Streckeisen's diagrams (1976) (Dill, 2016a,b). The post-orogenic monzo- to syenogranitic intrusions of H2a and H2b are attributed to the category 3 of Finger et al. (1997) which were emplaced between 340 and 310 Ma in Central Europe, particularly along the western rim of the Bohemian Massif and described as S-type and high-K I-type granites (Richter and Stettner, 1986).

The lithotypes H 4 are straddling the Luhe-Line and represented by the lithologies 7, 6, 5, and 4 in the geological map (Fig. 1c – A-A′, d). In general, they can be denominated as (cordierite-sillimanite-garnet)-mica-feldspar-quartz granitoids and metagranites in the current study and described as to their lithological evolution according to Dill (1983) and Steiner (1986). The metagranites and orthogneisses south of the Luhe Line (lithotypes H4a) reveal a blastocataclastic texture and underwent two metamorphic processes, the first one during Ordovician to Silurian/Devonian times at a depth of 15 km and 690 ± 50 °C (amphibolite facies) and the second one leading to a homogenization of the matrix, post-late Devonian in age (Fig. 5m). The latter is characterized by strong albitisation, muscovitization, chloritisation all of which are common to greenschist facies conditions. H4b lithotypes N of the Luhe-Line are strongly affected by muscovitization and accompanied in their host rocks by a striking petrological change reflected by a retrograde metamorphism from diaphtorite II to diaphtorite I (Fig. 1c). The northernmost H4b lithotypes (Fig. 1d) E of Tirschenreuth no longer qualify as metagranites but true mobilizates and need to be termed granitoids which are intercalated into the Neoproterozoic to early Paleozoic biotite-sillimanite gneisses of diaphtorite II.

Chemical results: Not unexpectedly, the H1 granodiorites to diorites show an enrichment in Ca and P and a moderate shift towards Na and K (Fig. 6c). The minor element variation is a mirror image of the major

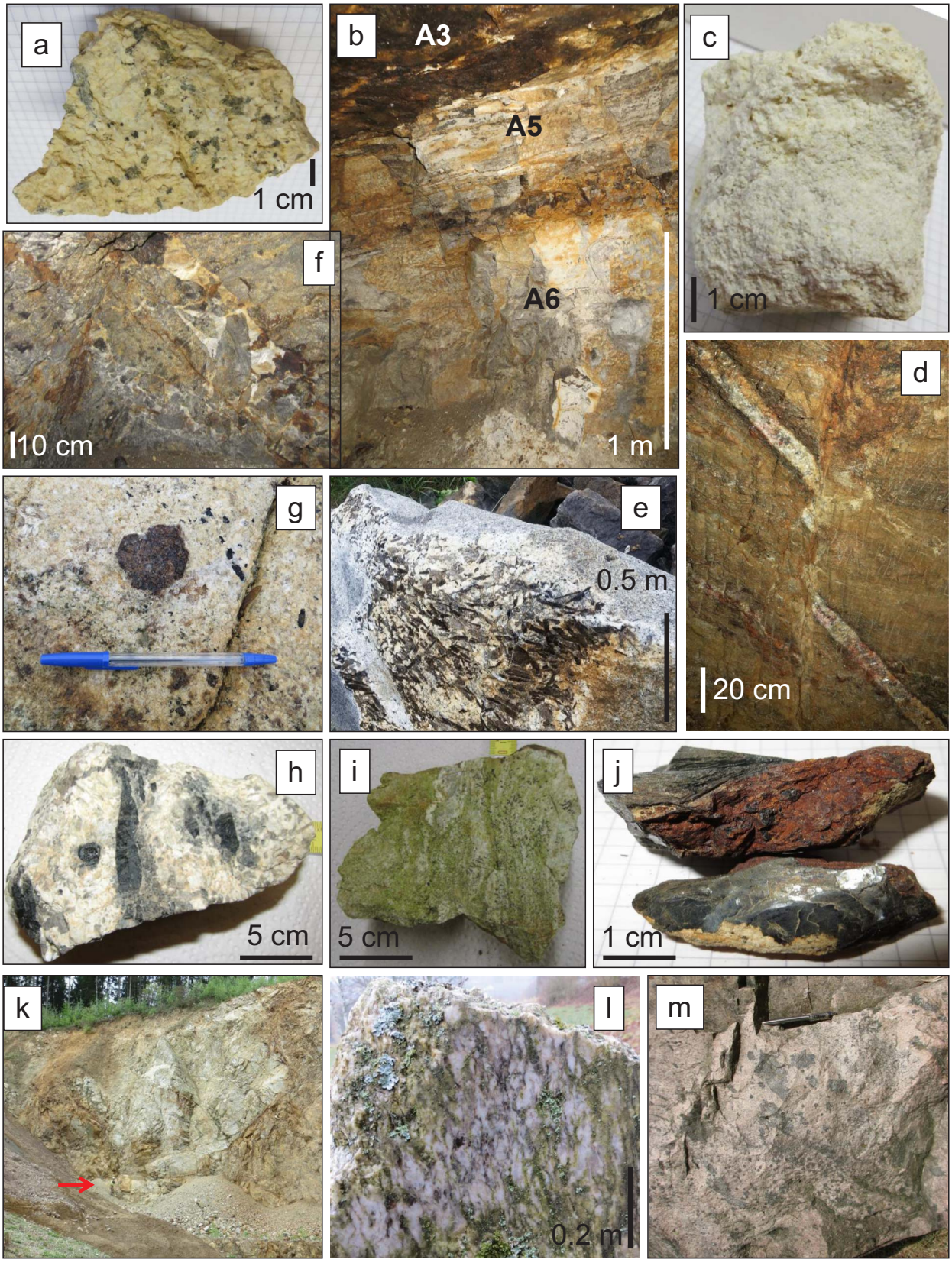

(caption on next page)

elements and reflects a primitive or initial stage of evolution with little deviation from the paragneiss standard. The major elements of lithotypes H2a and H2b, both belonging to the granitoid clan and similar in their felsic state (silica) are categorized as circular pattern with a shift towards, Na, K and P. H2b reveals some necking down for Ti and Mg. There are characteristic chemical changes depending on where the granitoids formed. The chemical pattern of the minor elements of H2a and H2b strongly differ from each. In the S, it is a circular pattern with

Fig. 5. Structural types in hand specimen. a) Zoned tabular amphibole-feldspar pegmatoid A2, W of the Kreuzberg Pegmatite at Galgenberg. b) Cross section through the proximal footwall facies from A6 (strongly kaolinized) through A5 (strongly muscovitized), underneath the Kreuzberg Pegmatite at Pleystein. c) Kaolinized tabular pegmatoid A1 from the Weiss Pit near Pleystein. d) Different generations of aplite veins (A7) intersecting biotite gneiss in the proximal hanging wall facies of the A-type pegmatites, underground storage system in the town of Pleystein. e) Marginal facies enriched in biotite mega crystals of an aploid type B1 at Schafbruck. f) A-7 rotational breccia with fragments of biotite gneiss floating in a saccharoidal aplitic matrix (hydraulic breccia). Pleystein underground storage room. g) B-2 pegmatoid-aploid with spessartine-enriched garnet mega crystals and schorl crystals aligned parallel to the contact of the mobilizates at Miesbrunn. h) C-type pegmatoid with mega crystals in a graphic matrix at Gsteinach. i) D-type sheared sacharoidal aplite with abundant green epidote. W of Pleystein pegmatite. j) E-type Fe ore minerals magnetite and tiny plates of hematite are altered to goethite W of Pleystein. k) F-type Na-enriched pegmatoids and aplite veins in metabasic rocks of the ZEV allochthonous unit at Remmelberg open pit. Red arrowhead denotes person for scale. l) Metapegmatite (G lithotype) at Neustadt a.d. W. in the allochthonous unit. m) Patchy aploid (H4a) characterized by porphyroblasts of cordierite, south of the Luhe-Line near Böhmisch Bruck. See biro for scale. (For interpretation of the references to color in this figure legend, the reader is referred to the web version of this article.)

necking-down for Ni, whereas in the N it is a lens-shaped one with a relative enrichment of Rb, Pb and As. H3 lithotype is representative of a pegmatitic mineralization in druses and schlieren in the Leuchtenberg Granit (H2b lithotype) and its necking-down chemical pattern a logic consequence in the evolution from the host granite to the granitic pegmatite (Fig. 6c). The same holds true for the chemical pattern from lens-shaped (H2b) to a necking-down pattern with a strong depletion in Ni and Zr and a moderate increase in Rb, Nb, Pb and Bi. The couple H4a and H4b representative of granitoids, metagranites, and orthogneiss closely resemble the couple H2a-H2b in their chemical patterns despite

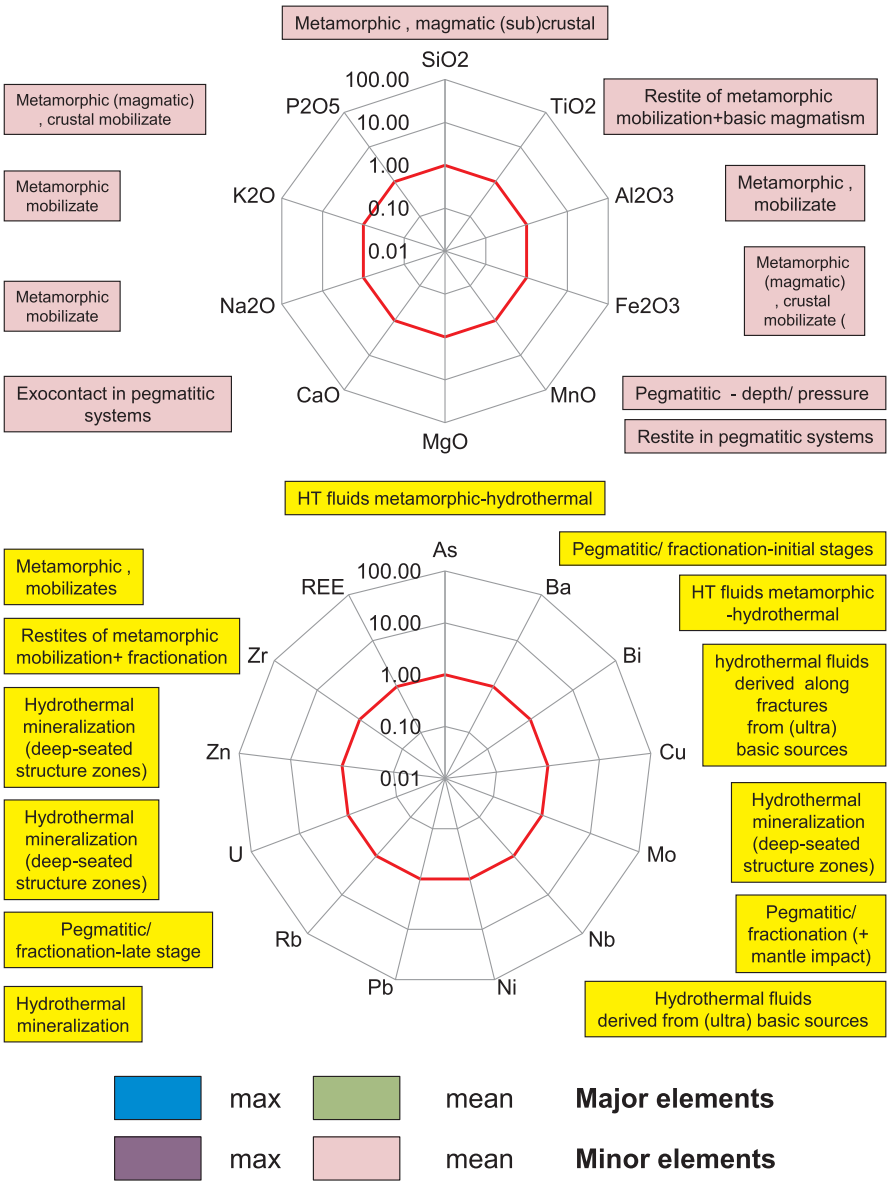

Fig. 6. Chemical patterns ("spider diagrams") revealing the increase of major and minor elements of pegmatitic, aplitic and granitic rocks relative to a paragneiss standard of the study area in the NE Bavarian Basement. The data are plotted on a logarithmic scale with the "red ring" denoting the reference line 1. Below 1 means depletion and above enrichment of elements. Excluding A3 minor elements (max. 1000.00), all other diagrams display the same range 0.01–100.00 of depletion and enrichment, respectively. Rock types discussed in the text and shown in Fig. 6b and c are plotted at a lower magnification than in Fig. 6a. side-by-side with each other so as to allow for a quick-look visual comparison. For individual elements see Fig. 6a and for numerical data (mean value) Table 2b. a) Key for the spider diagrams. b) Major and minor element spider diagrams of A- and B-type pegmatitic and aplitic rocks. c) Major and minor element spider diagrams of C-, D-, E-, F-, G- and H-type pegmatitic, aplitic and granitic rocks. (For interpretation of the references to color in this figure legend, the reader is referred to the web version of this article.)

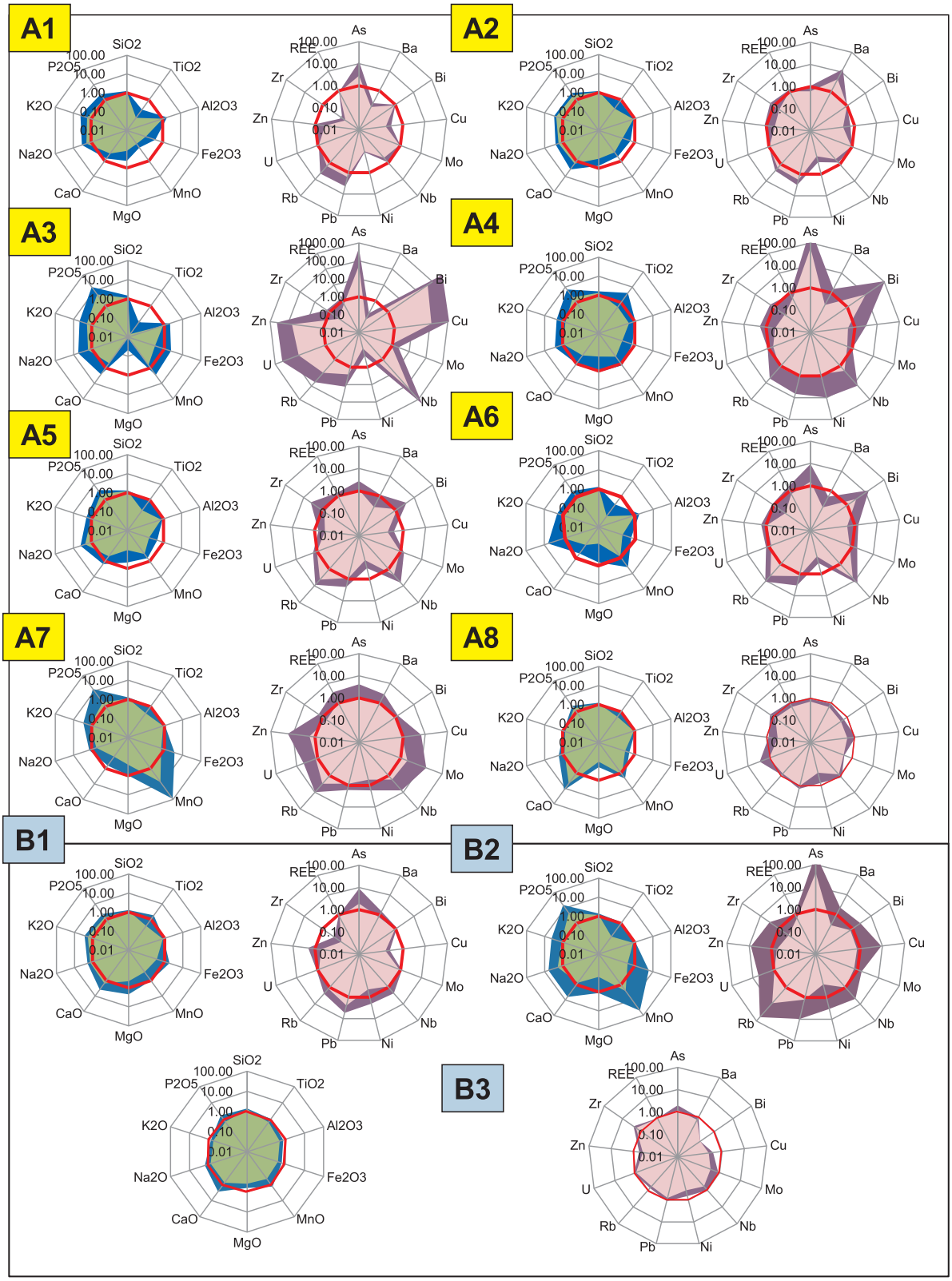

Fig. 6. (*continued*)

their different evolutions indicated by the petrographic, structural and chronological differences. A comparison of the necking-down factor of the circular patterns $(CaO_{norm} + SiO_{2norm})/(MgO_{norm} + TiO_{2norm})_{major\ elements}$ reveals that this factor is more pronounced in the pre-to syn-metamorphic granitoids (H4) than in the younger post-metamorphic granites (H2) (Tables 2a, 2b).

4.2. 2D-geochemical mapping and element variation

To correlate the major and trace elements relevant for the genesis of

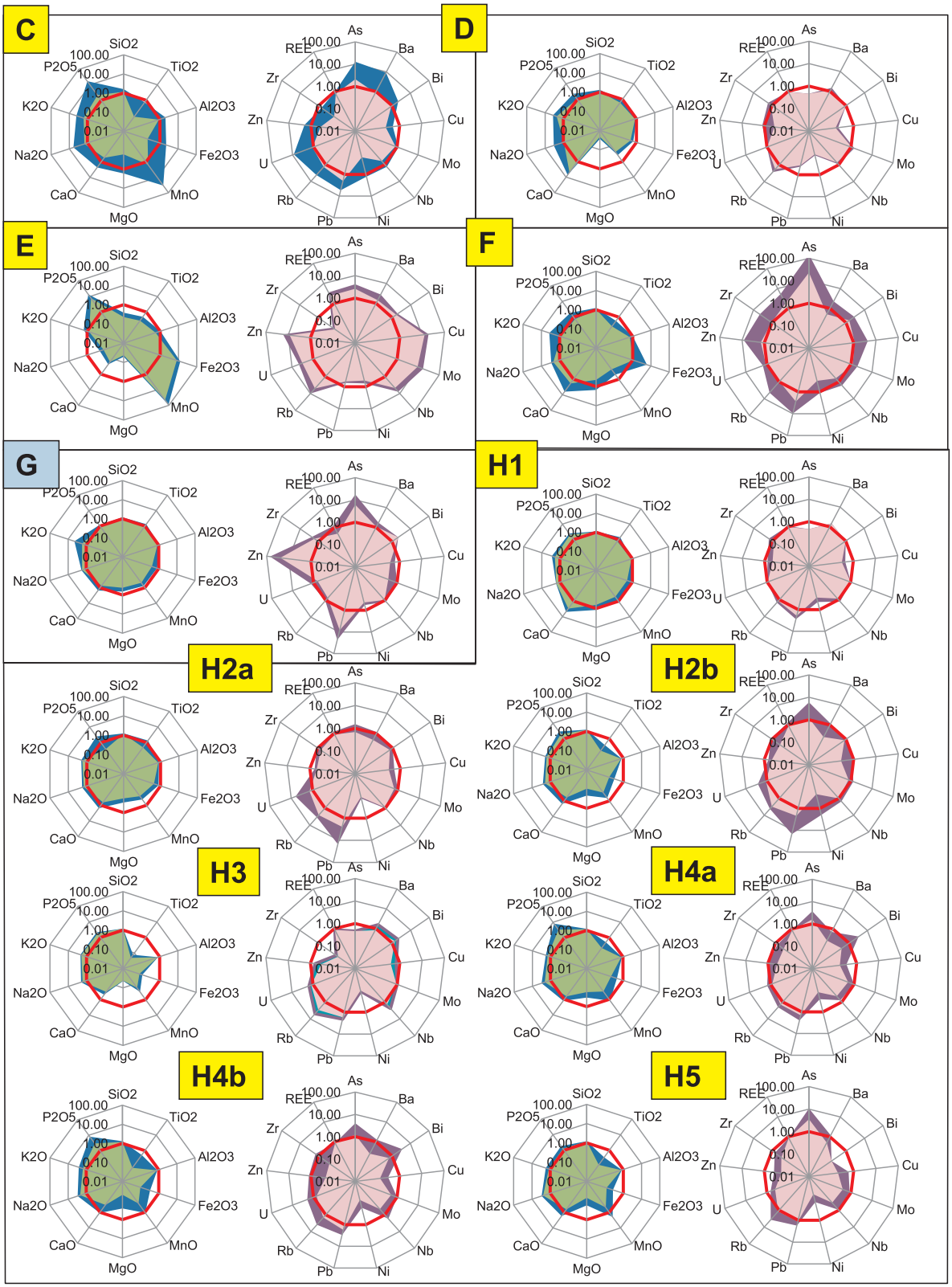

Fig. 6. (*continued*)

pegmatitic and granitic systems different approaches have been taken and suggested in studies mainly conducted by geological surveys (De Vos et al., 2005; Reimann et al., 2014) and applied in mineral exploration (Saffarini and Lahawani, 1992; Moon et al., 2006; Paz-Ferreiro et al., 2010). In the current study, the area hosting the majority of granitic rocks, pegmatites and aplites, among others the Hagendorf-Pleystein Pegmatite Province, was selected to design the contour maps (Figs. 1b, 7a, b). The trends and clusters are correlated with the geological map of Fig. 1c. The chemical patterns on display in Fig. 7a and b are subdivided into two types, coherent belts and trends, including

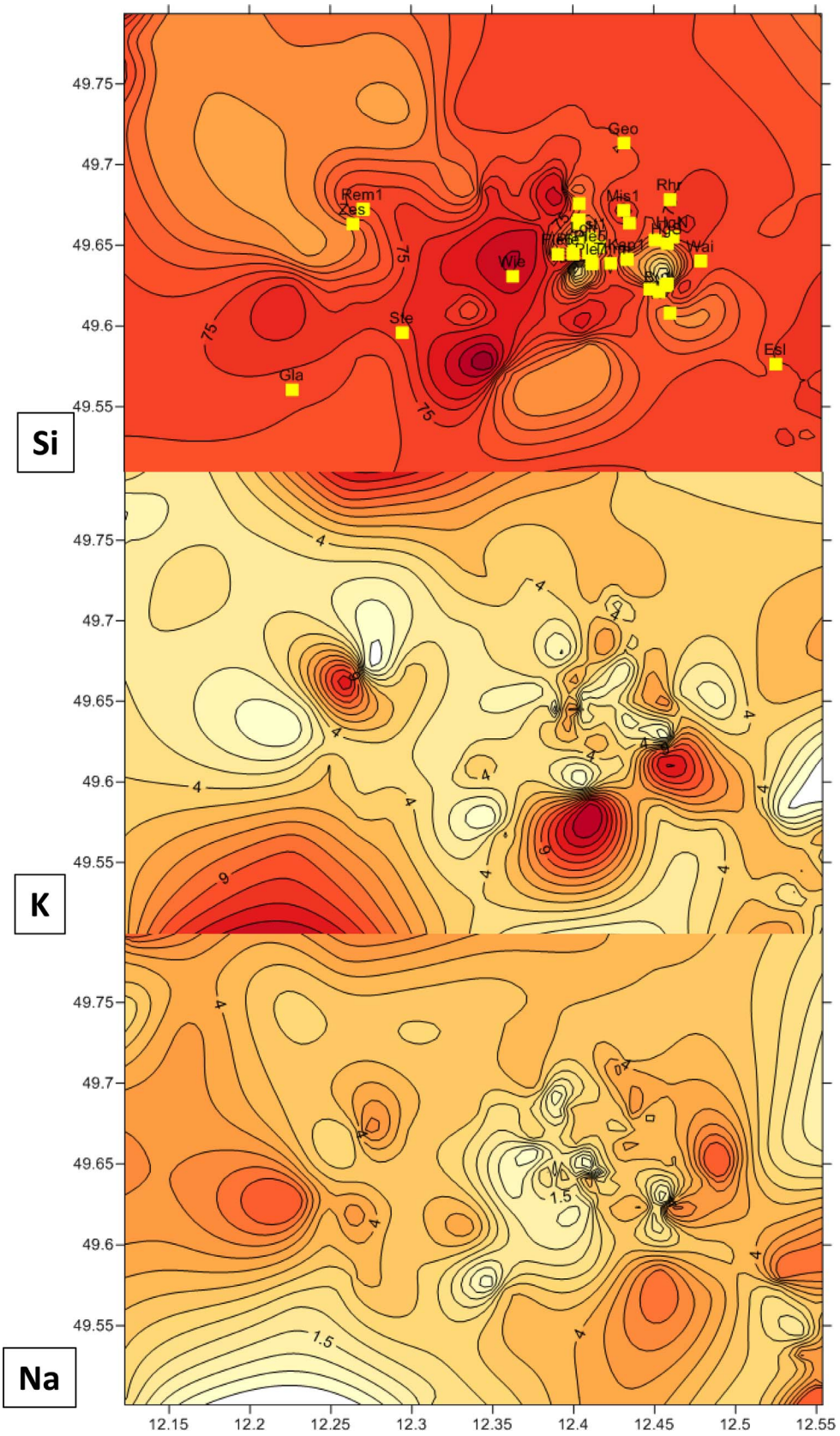

Fig. 7. Chemical maps and element trends. For precise positioning of the chemical maps see Fig. 1b. a) Aerial distribution of Si, K, and N in pegmatitic, aplitic and granitic rocks; these chemical maps are reproduced on a larger scale than those of Fig. 7b to show some relevant pegmatite and aplites deposits and occurrences for positioning (see also Fig. 1b and c). The abbreviation refer to the name of mining and sampling sites: BU1: Burkhardsrieth, ESL: Eslarn, GEO: Georgenberg, GST1: Gsteinach, HGN: Hagendorf-North, HGS: Hagendorf-South, KAP1: Kaplansteig, LOH: Lohmar, MIS1: Miesbrunn, PLE1: Pleystein town, PLE5: Kreuzberg, PLE6: Kühbühl, PLE7: Weiss Mine, GLA: Glaubendorf, STE: Steinach, REM1: Remmelberg, ZES: Zessmannsrieth, WIE: Weiβenstein, RHR: Reinhardsrieth, THM: Trutzhofmühle, WAI: Silbergrube Mine. b) Aerial distribution of Ba, As, Mo, Ti, Mn, Rb, P, and Nb in pegmatitic, aplitic and granitic rocks. These plots of element variation are reproduced on a smaller scale for the assessment of chemical trends only.

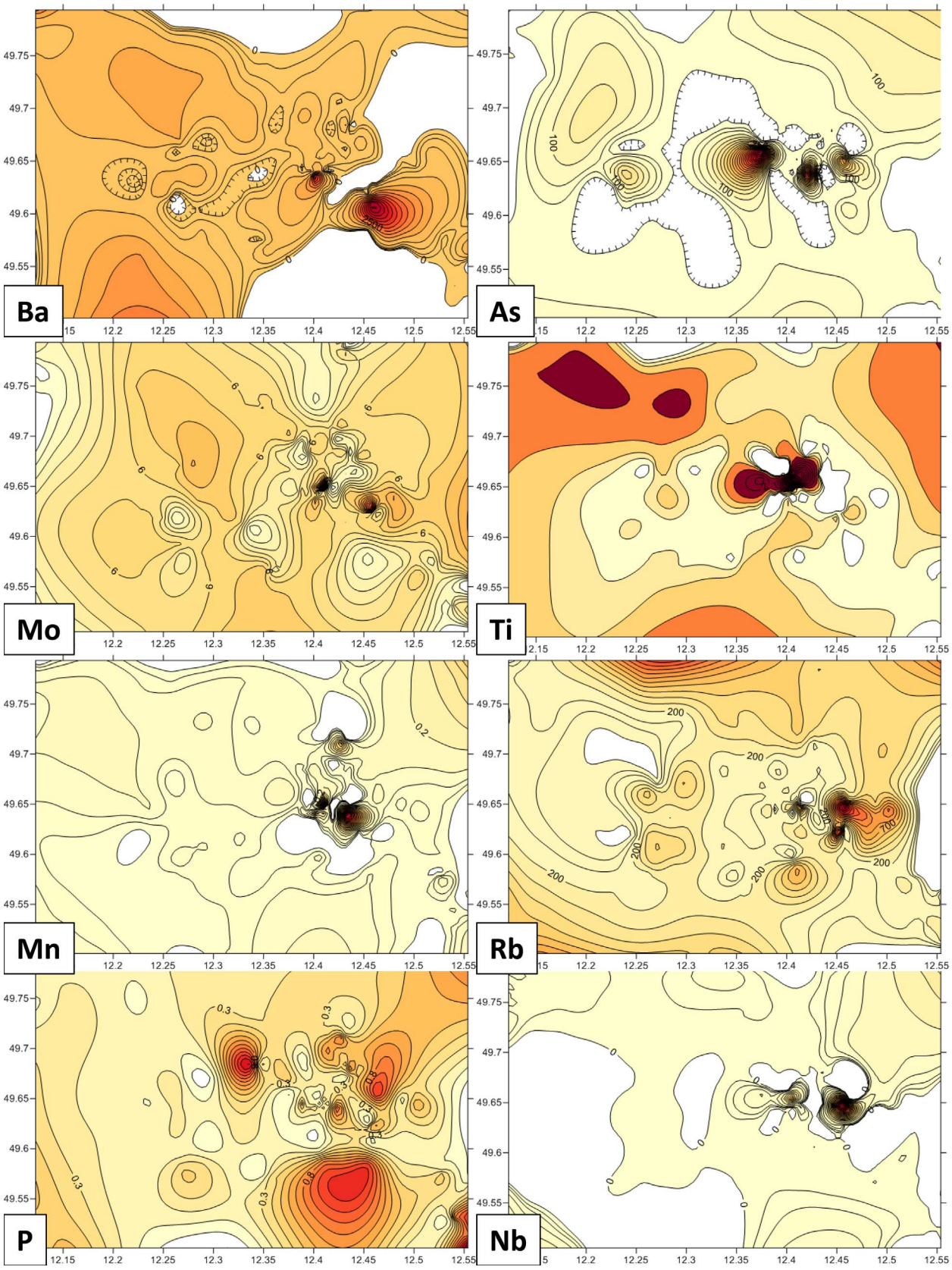

Fig. 7. (*continued*)

Table 3
Aerial distribution of major and minor elements expressed as belts, trends and clusters.

Element	Trends	Geodynamic control
Si	Belt: W-ENE-NNE	Belt coincides with lithologies 6,7,13 south of the Luhe. Pegmatite cluster in the turning point where W ⇒ NNE-ENE. Hot spot lies in the intersection of the NW-SE quartz veins with this belt.
Al	Belt: W-ENE-NNE	
K	Belt: W-ENE	
REE	Belt: W-NNE-ENE	
Na	Trend: SW-NE	Trend coincides with lithologies 6,7,13 east of the Luhe. Hot spot lies in the intersection with this trend lines
Fe	Trend: SW-NE	
P	Trend E: SW-NE	
As	Trend: W-E	Early Variscan Luhe Line is the controlling lineamentary fault zone
Fe	Trend: W-E	
Ni	Trend: W-E	
Ti	Trend: W-E	
Nb	Trend : W-E	
Bi	Trend: W-E	
Cu	Trend: W-E	
K	Trend: NW-SE	Late Variscan embryonic Franconian Line is the controlling lineamentary fault zone Late Variscan Lineament of Bad Elster-Bad Brambach Marienbad-Taus is the controlling lineamentary fault zone (Teuscher and Weinelt , 1972)
Ba	Trend: NW-SE	
Mo	Trend: NW-SE	
Mn	Trend: NW-SE	
Zn	Trend: NW-SE	
Ti	Trend NW-SE (2^{nd} order)	
Rb	Trend: NW-SE (1^{st} order)	
Pb	Trend: NW-SE	
Zr	Trend: NW-SE (1^{st} order) Trend: N-S (2^{nd} order)	
Mg	Trend: NW-SE (1^{st} order) Trend: N-S (2^{nd} order)	
Ca	Trend: NW-SE (1^{st} order) Trend: N-S (2^{nd} order)	
P	Trend W: NW-SE	
U		Unspecific structural event

clusters and described as to their orientation in Table 3. In the study area there is one belt shown by the Si, Al, REE and K distribution which stretches W-E, turns towards the NE and coincides with the lithologies 6, 7 and 13 (Fig. 1c, d). The pegmatites cluster in the turning point of the directions (Fig. 7a). Sodium, iron and phosphorus reveal trends in NE-SW direction. Another set of elements, As, Ni, Ti, Nb, Bi, Cu and Fe display a marked E-W extension of their anomalies. The SW-NE and E-W trends are controlled by swarms of fault zones, the latter by the Early Variscan lineamentary fault zone of the Luhe Line (Fig. 1c). The NW-SE trend line is characterized by concentrations of K, Ba, Mo, Mn, Zn, Ti, Rb, Pb, Zr, Mg, Ca, and P. It runs parallel to the Late Variscan embryonic Franconian Line terminating today the basement towards the W and controlled by a spate of quartz dykes intersecting the basement rocks. At the turning point of direction in the chemical belt NW-SE trending quartz dykes cut through and last-but-not least mark the zone where the pegmatites cluster. The N-S trend is a trend of subordinate order only vaguely expressed in the chemical plots and spanned by the REE, Zr, Ca and Mg distribution. It may be correlated with the Late Variscan Lineament of Bad Elster-Bad Brambach-Marienbad/Mariánské Lázně-Taus/Domažlice (Teuscher and Weinelt, 1972).

4.3. 1D-geochemical profiling and structural geology

The 1-D chemical mapping or vertical profiling follows the same rules and methods applied to the chemical mapping in plan view (Section 4.2) (Table 3). The fine-tuning of the chemical variation of those elements relevant to the emplacement of pegmatitic rocks is achieved by the current chemical approach (Section 4.3) which is corroborated by a structural analysis based on field surveys and interpreted by means of equal area presentations in the lower hemisphere of stereonet diagrams. The profiling has been performed by capturing digital data in the field or underground (Fig. 8a) or collecting samples from drill holes along a transect (Fig. 8b) (Dill et al., 2014a,b, 2017).

4.3.1. Chemical profiling

The cross section of Fig. 8a covers the transition zone from biotite gneisses into granitoids – type H4 at the 120 m-level of the Poppenreuth U deposit (Fig. 2a). The rock series pertains to the Neo-Proterozoic to Early Paleozoic biotite-sillimanite gneisses (Fig. 1c, d- unit 4). The intensity of the gamma radiation along the wall can be deduced from the colored contour map based on a survey with a hand-held scintillometer (Fig. 8a). The ore mineralization consists of chalcopyrite-pyrite veinlets bound to vertical joints and U oxides with brannerite in a matrix of impsonite cross-cutting the contact of gneiss towards H-4 granitoids (Table 2a). The U mineralization is mainly bound to subvertical joints extending from the granitoid into its gneissic footwall rocks. The granitoids H-4 (G_2) are bounded by sub parallel faults (U_2) mineralized with U minerals (Figs. 8a, 9a). The cross cutting U-bearing faults (U_1) control the position of the U which took place only near the intersection of the granitoids and faults (Fig. 8a- inset).

The second case-history is centered on the F pegmatoids in metabasic rocks (Figs. 2a, 8b, Tables 2a, 2b). The pegmatoids strike WNW-ESE and dip towards the N (Fig. 9b). A couple of reverse and normal faults in the hanging wall rocks similar in strike but different in the dip directions accompany these pegmatoids (Fig. 9c). Seven drill holes sunken along a transect into the metabasic rocks and the F-type pegmatoids formed the basis for the profile of Fig. 8b. The major elements

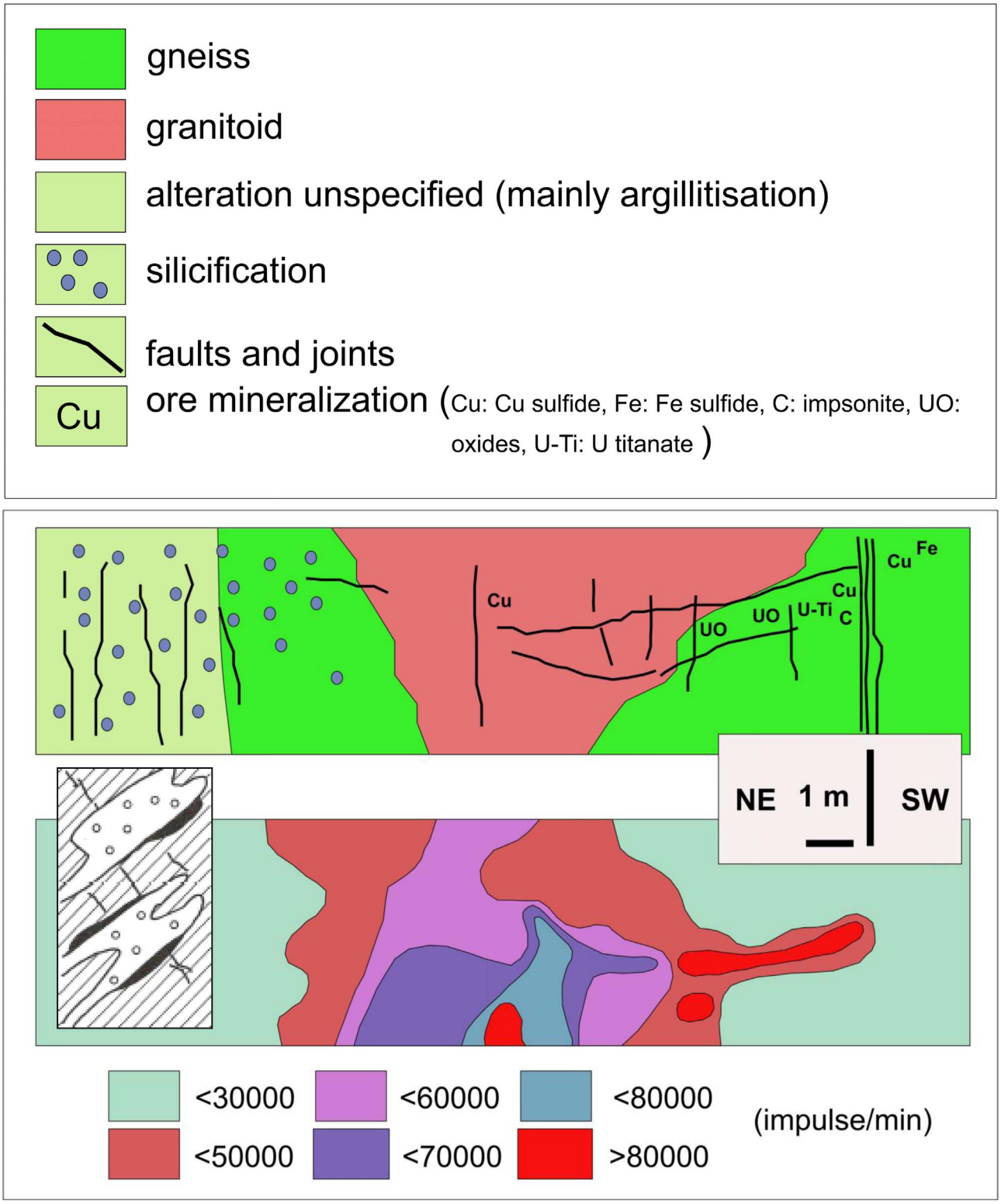

Fig. 8. Chemical profiling by means of capturing digital data at outcrop or subcrop and collecting samples for laboratory-based analysis. a) Cross section along the wall of a cross-cut of the 120 m – level of the Poppenreuth uranium deposit, showing the distribution of U ore mineralization within the exocontact of granitoid H4. The gamma-radiation was determined using a hand-held scintillometer. b) 7 drill holes were sunken along a transect through the F-type pegmatoid and its metabasic wall rocks. The pegmatoid rocks are characterized by the marker elements Si and Na, whereas the elements bound to the marginal faults Pb, As, Cu, and Zn are indicative of the rare-element introduction (see also the spider diagram Fig. 6c).

Si and Na and the minor elements Pb, As, Cu, and Zn which are indicative of the rare-element introduction into the pegmatites have been selected to depict the lithology and chemical variation of the F-type pegmatite system (Fig. 6c). A strong Na anomaly denotes the presence of pegmatoids, whereas the base metals and As are strongly enriched along fractures intersecting the metamorphic rocks in the profile from 60 m to 140 m (Fig. 8b). The rare elements above are bound to subvertical faults and faults dipping at an angle around 45°, well in accordance with the dip angle deduced from the stereonet diagrams (Fig. 9c). The rare element contents in the fracture zones are some

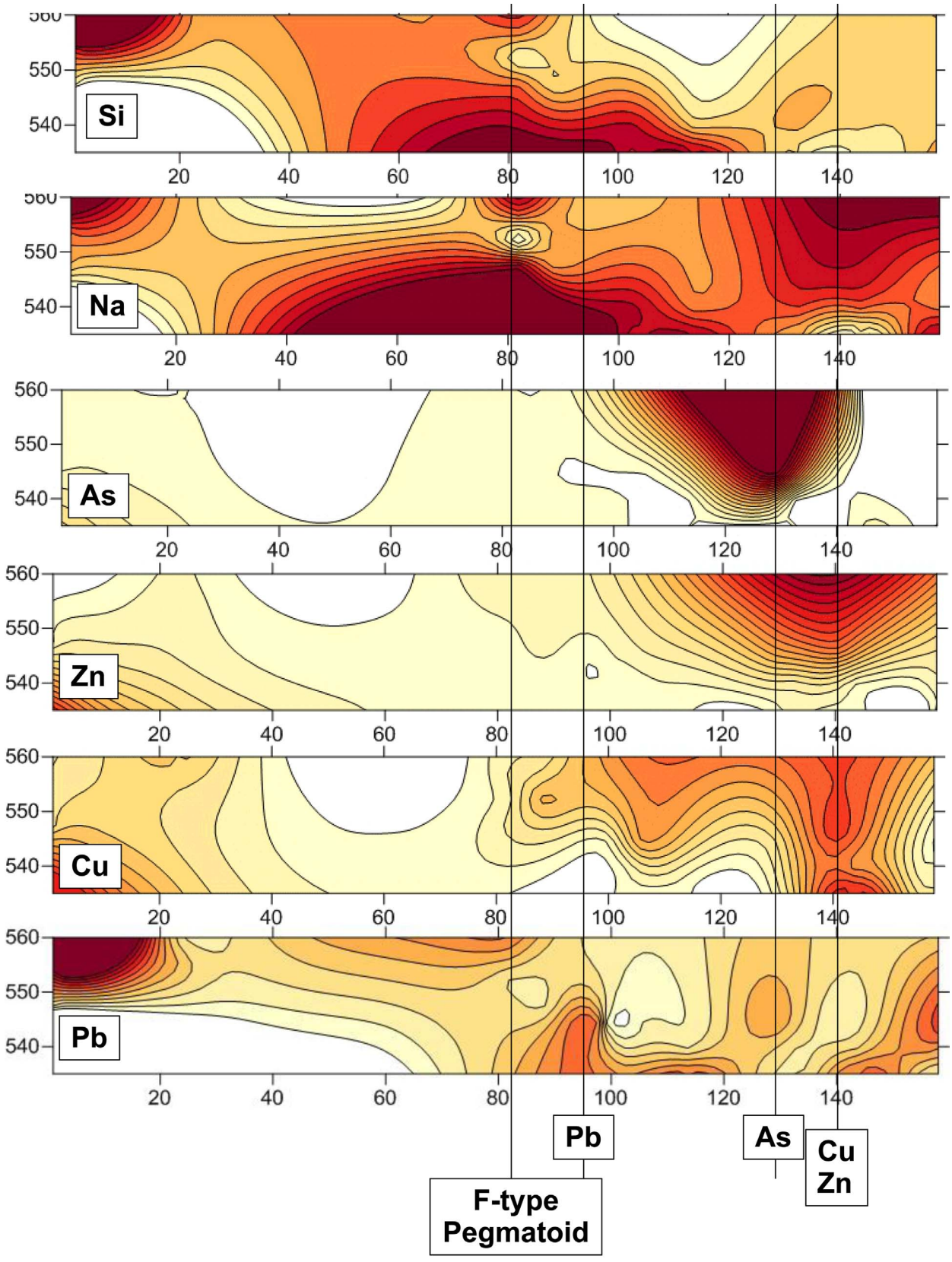

Fig. 8. (*continued*)

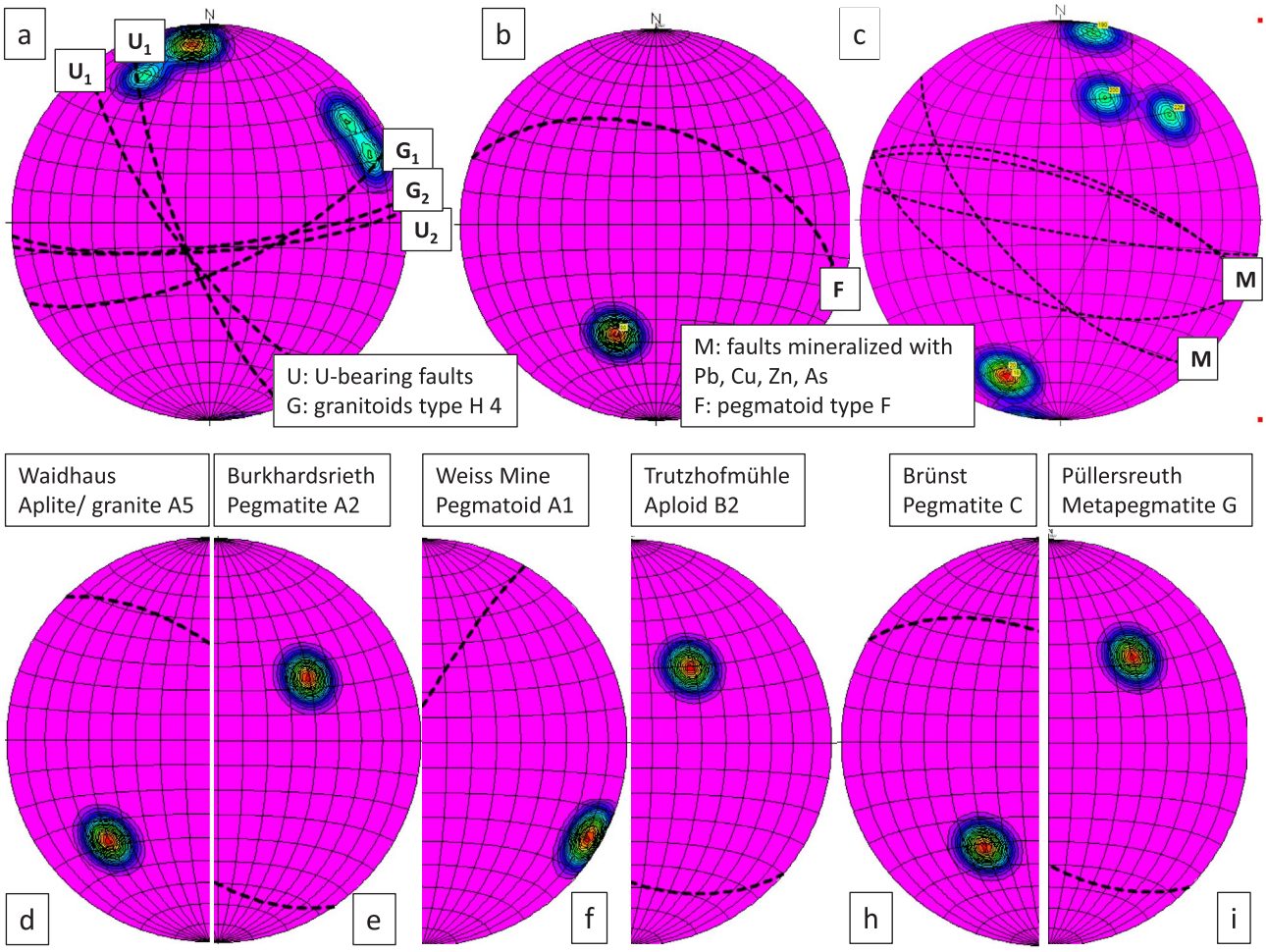

Fig. 9. Stereonet diagrams projected onto the lower hemisphere of tabular, layer-shaped and sheet-like pegmatitic and granitic rocks; for categorization see Fig. 2a and Tables 2a, 2b. a) H-4 granitoid (G) with U-bearing faults sub parallel to and cross-cutting the granitoids of autochthonous unit 4 in Fig. 2a. Poppenreuth U deposit E of Tirschenreuth (Fig. 1c, d). The inset illustrates the accumulation of U ore minerals at the edge of the granitoids where they are cut by NW-SE-trending faults. b) F pegmatoid W of Vohenstrauss at outcrop in the allochthonous units. c) Marginal faults in the hanging wall rocks of F-type pegmatoids of Fig. 9b. d) Type-A5 aplite/aplite granite at Silbergrube Mine near Waidhaus (dip direction 45°/dip angle 60°). e) Type-A2 pegmatite at Burkhardsrieth Haunerberg Mine (dip direction 235°/dip angle 45°). f) Type-A1 pegmatoid of Weiss Mine S of Pleystein (dip direction 300°/dip angle 83°). g) Type-B2 aploid at Trutzhofmühle (dip direction 220°/dip angle 45°). h) Type-C pegmatite at Brünst Mine (dip direction 30°/dip angle 50°). i) Type-G metapegmatite at Püllersreuth Mine (dip direction 225°/dip angle 50°).

orders of magnitude higher than those obtained from the whole-rock analysis of the pegmatites used for the calculation of the spider diagram in Fig. 6c. Faultbound element concentration in the border zone of pegmatitic, aplitic or granitic rocks has not been considered for the lithochemical assessments in Fig. 6.

4.3.2. Structural analysis

Irrespective of the host lithologies of the various pegmatitic and granitic rocks in allochthonous (F-type) or autochthonous units (H-type) and their structure, the position may be defined by the general dip direction and dip angles projected onto the lower hemisphere of stereonet diagrams (Fig. 9a, b, d–f, h, i). The structural analysis refers to pegmatitic and aplitic bodies unless stated otherwise. The anticlinal A-types, some of which are renowned for their rare element contents show rather complex structural patterns which can be grouped as to their facies (Fig. 2a), their great circle azimuth as well as great circle plunge (Fig. 10). The orientation of these anticlinal types have been determined by measuring the planar elements of this structural type using data derived from underground mining plans. Hagendorf-North and Hagendorf-South show steeply dipping great circle plunges; Hagendorf-South represents a horizontal upright fold, its neighbor Hagendorf-North a horizontal inclined fold with its steeper limb facing eastward. A similar scenario cannot be determined for the Kreuzberg quartz pegmatite whose feldspar rim was completely destroyed as a result of argillitization (Fig. 2a, Tables 2a, 2b, A3–A4). Its present-day quartz reef is highlighted by the colored contour lines and its strike by the great circle azimuth (Fig. 10c). The well preserved A5-A6-type footwall aplite granite underneath the Kreuzberg quartz pegmatite shows a great circle azimuth of 319° and a great circle plunge of 77° (Fig. 10c). It is on open fold whose axis gently dips approx. 10°/230°. The same hold true for the aplite veinlets, towards the east of the footwall aplite granite which form a plunging inclined fold (Fig. 10d). The stockwork aplite veins of the proximal and distal facies in the hanging wall rocks do not differ from each other with regard to their structural signature but contrast with the overall patterns as they have great circle data oriented almost perpendicular to the principal pegmatite bodies and their footwall facies (Fig. 10e, f). A8-types fade out in the S-planes of the metamorphic country rocks. There is a negative correlation between the plunge of the great circle and the accumulation of pegmatites in the hinge zones of the folds (Fig. 10).

4.4. Chemical signature of hypogene and supergene argillitization

Kaolin (kaolinite, dickite, nacrite with different degrees of Si/Al disorder and halloysite) is a common argillic alteration encountered in a wide range of parent rocks, predominantly on felsic rocks such as

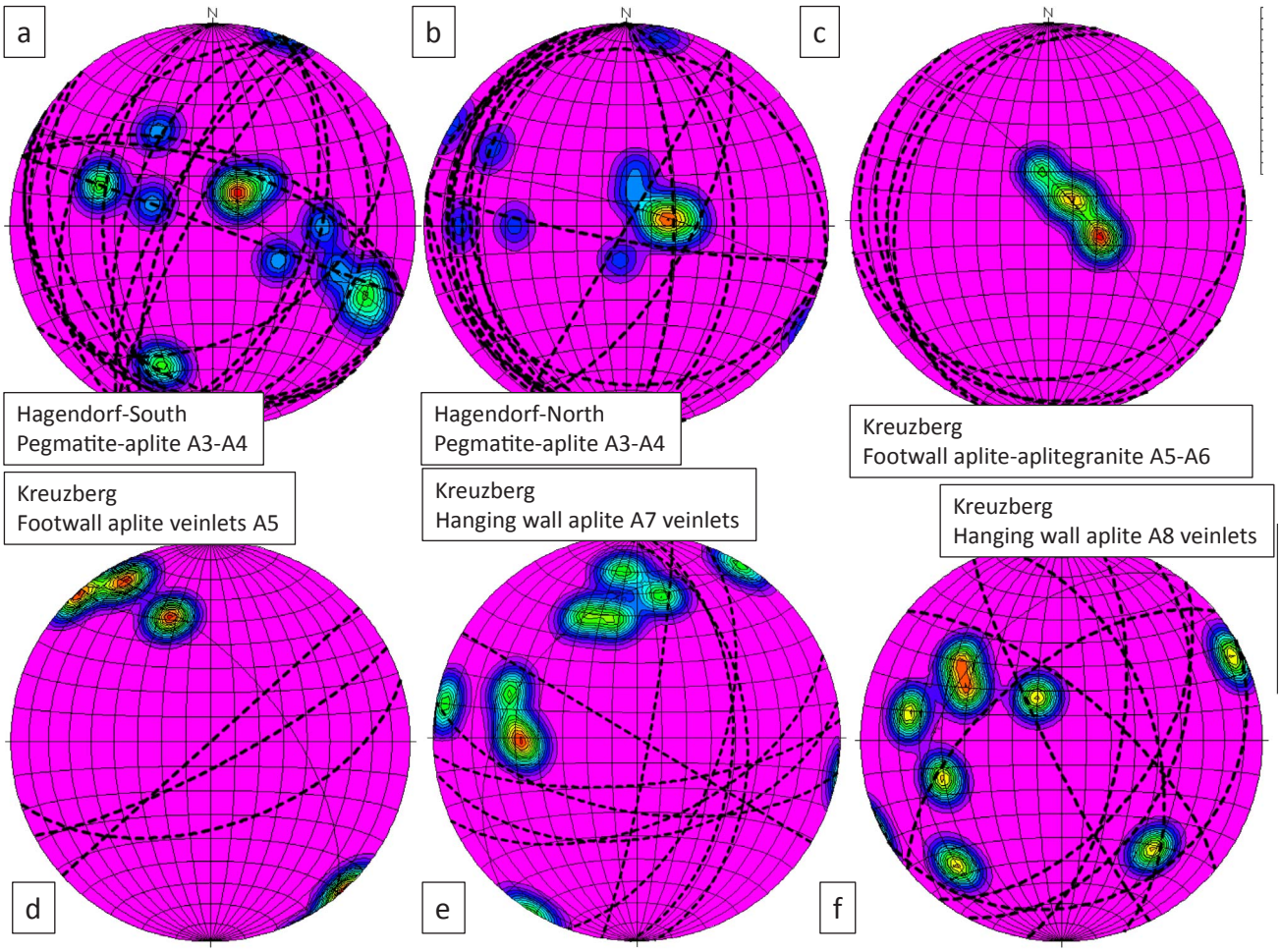

Fig. 10. Stereonet diagrams projected onto the lower hemisphere of vein-type, stockwork and stock-like, anticlinal pegmatitic and aplitic rocks in the hinge zone; for categorization see Fig. 2a and Tables 2a, 2b. a) A3-A4-type anticlinal stock-like pegmatite Hagendorf-South (great circle azimuth 203°/great circle plunge 87°). b) A3-A4-type anticlinal stock-like pegmatite Hagendorf-North (great circle azimuth 286°/great circle plunge 82°). c) A5-A6-type footwall aplite layer and aplite granite of the Kreuzberg quartz pegmatite ("pegmatite ruin") in the city of Pleystein (great circle azimuth 319°/great circle plunge 77°). d) A5-type aplite veinlets in the footwall rock of the Kreuzberg quartz pegmatites near Finkenhammer-Pleystein (great circle azimuth 320°/great circle plunge 60°). e) A7-type stockwork aplite veinlets in the hanging wall rocks of the Kreuzberg quartz pegmatites (proximal facies) western part of the city of Pleystein (great circle azimuth 222°/great circle plunge 38°). f) A8-type stockwork aplites veinlets in the hanging wall rocks of the Kreuzberg quartz pegmatites (distal facies) westernmost part of the city of Pleystein (great circle azimuth 233°/great circle plunge 43°).

those of the granite- and pegmatite-aplite suites (Dudoignon et al., 1988; Kitagawa and Köster, 1991; Bristow and Exley, 1994; Psyrillos et al., 1998; Beurlen et al., 2001, 2009; LeBoutillier, 2002; Scott and Bristow, 2002; Dill et al., 2014b, 2015, Dill, 2016b). Tirschenreuth kaolin is still mined in a large granite-hosted supergene kaolin deposits, whereas in the Hagendorf-Pleystein kaolin is present in relic patches left over as the feldspar rim was eaten away by this hypogene alteration (Fig. 11). The major elements reveal significant differences in the Mn and P contents which are accumulated in the hypogene kaolinization relative to the supergene one (Fig. 11a). Among the minor elements Ba, Bi, Cu, Mo, Nb, Sr, Ta, and Zn are enriched by some orders of magnitude relative to the supergene kaolin, whereas Ni, Pb, U, V and Zr show a reverse trend.

5. Discussion

5.1. Types and physical-chemical regimes of pegmatitic and granitic rocks

Like in many pegmatite provinces elsewhere in the world, barren pegmatites prevail over rare metal pegmatites also in this region. Logically, a holistic approach has been taken covering the entire spectrum of feldspar-quartz-mica mobilizates when it comes to constrain the physical-chemical regime. The physical-chemical regimes of the different types of rocks is determined based on marker minerals, marker reactions as well as the quartz thermometry making use of trace elements. The Ti-in-quartz geothermometer of Wark and Watson (2006) provides a tool to determine the quartz crystallization temperature based on the temperature dependence of the $Ti^{4+} - Si^{4+}$ substitution in quartz and given the presence of rutile or, in its absence, an estimate of the TiO_2 activity of the system. This geothermometer is frequently used for magmatic and metamorphic processes and can be applied to temperatures up to as much as 1000 °C (Storm and Spear, 2007; Breiter and Müller, 2009). In this region is has been used for the first time by Dill et al. (2012) for pegmatites.

5.1.1. A-type pegmatoids, aplites, aplite granites and pegmatites

The A-type rocks show a tripartite facies zonation (Fig. 2a): Footwall facies (A1, A2, A5, A6), central facies (A3, A4), hanging wall facies (A7, A8).

Footwall facies: The felsic mobilizates of type A1 originated from paragneisses as a consequence of metamorphic mobilization and the temperature regime can be deduced from the presence of almandine-enriched garnet s.s.s. Its formation facilitates by reducing environments and its temperature of formation decreases when the partial water pressure and total pressure diminish. The silicate marks medium-grade conditions in a T interval of 500–600 °C (Thomas, 2005; Bucher and

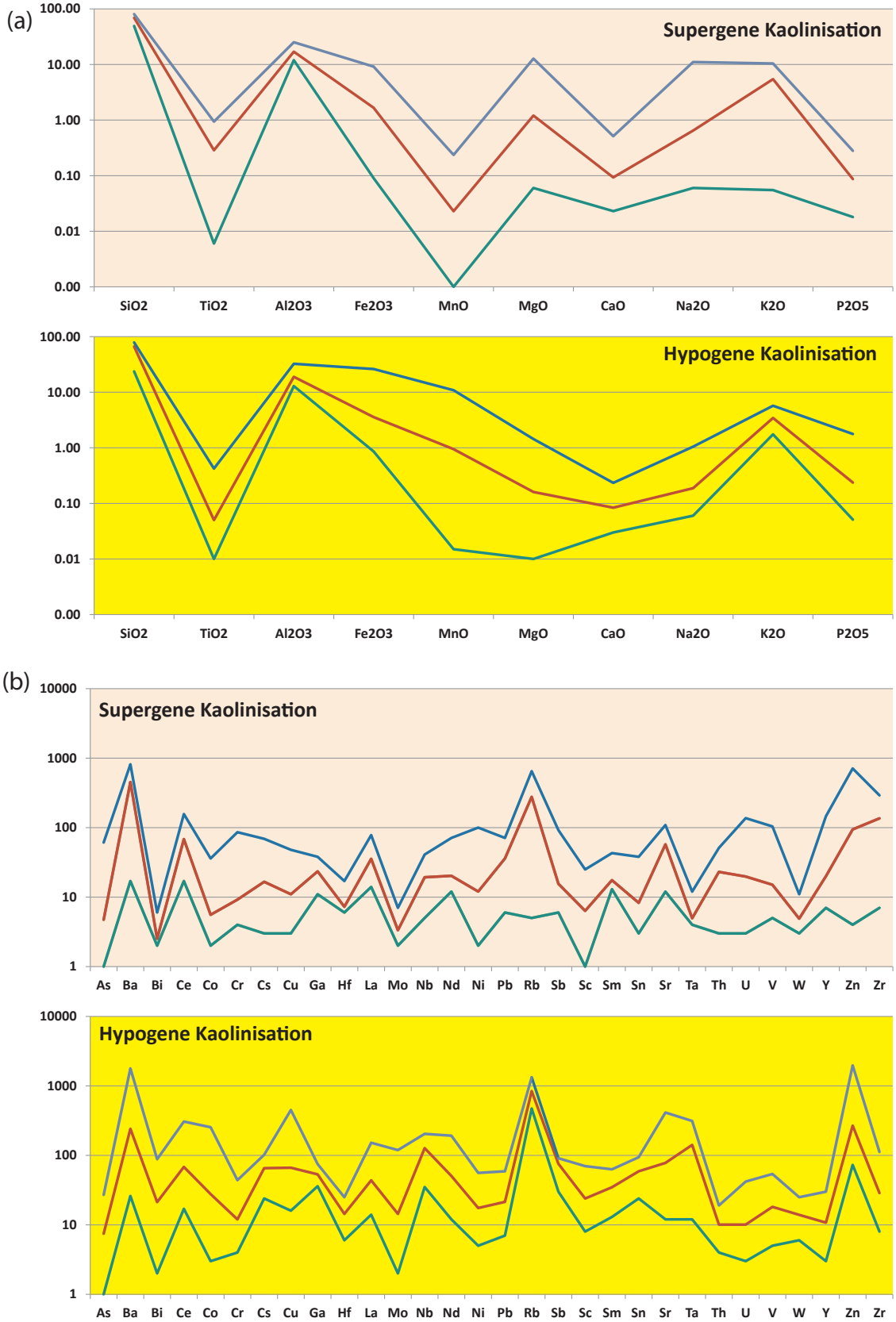

Fig. 11. Hypogene and supergene kaolinization given in a logarithmic scale. a) Minimum (green), mean (red) and maximum contents of major elements in hypogene and supergene kaolinization of pegmatitic and granitic rocks in the study area. b) Minimum (green), mean (red) and maximum contents of minor elements in hypogene and supergene kaolinization of pegmatitic and granitic rocks in the study area. (For interpretation of the references to color in this figure legend, the reader is referred to the web version of this article.)

Grapes, 2011). The A1 pegmatoids also lie within the reaches of the hypogene kaolinization (Fig. 2a). There is only one well-defined reaction cited in many textbooks (Winkler, 1976) that gives the upper stability limits of kaolinite: 1 kaolinite + 2 quartz ⇔ 1 pyrophyllite + $1H_2O$ (390 ± 10 °C 2 kbar). There was no conduit by fissures between A1 pegmatoids and the remaining A-type pegmatitic rocks during the primary emplacement of the A1 pegmatoids. By contrast, during latter stages such conduits existed and provoked the kaolinization of part of the pegmatoids. A2-type rocks resemble the aforementioned A1-types but opposed to them, A-2 types are also connected in space and time with the overall pegmatite body (Fig. 2a). A2 pegmatitic rocks contain several silicates typical of contact and regional metamorphic processes indicative of a certain level of temperature of formation: epidote-clinozoisite s.s.s.: 400–530 °C, diopside s.s.s: 430–570 °C. A5 and A6 only differ from each other by the degree of argillitization. A5 shows strong muscovitization at temperatures > 400 °C and a pH ≥ 7, whereas the kaolinized type A6 developed at lower temperatures and a pH below 7. The A5 stockwork formed under a T regime similar to A2 between 530 °C and 490 °C (Fig. 2a – right side).

Central facies: The highly differentiate quartz-feldspar pegmatites A3 and A4 developed between 460 °C and 560 °C based on the quartz thermometry.

Hanging wall facies: The facies type A7 is a mirror image of the footwall facies A 6 with regard to the marker minerals and the T of formation. With regard to the pH, however, there is a difference owing to the presence of phyllosilicates of the smectite group attesting to a more alkaline fluid regime than below the main pegmatite ore body (Tables 2a, 2b, Fig. 2a). A8 is a mirror image of the A5 stockwork facies of the footwall facies with respect to the mineral association and consequently with respect to the temperature too.

The temperature gradient is “centripetal” with little variation during the primary emplacement and the fractionation into the various subtypes. The outer rim of calcsilicate minerals is not only meaningful as to the temperature variation but also reflects some sort of a restite during fractionation. A conspicuous vertical differentiation is observed during the secondary argillic alteration process which reveals an upward change from an acidic to an alkaline fluid regime.

5.1.2. B-type pegmatoids, aploids and aplitic gneisses

The B-type rocks show a steeper temperature gradient than the afore-mentioned A types from the barren B1 through to the mineralized B2 types. B3 which was investigated by Forster (1965) misses diagnostic minerals such as cordierite and sillimanite so that its upper T limit has to be given with a question mark (Fig. 2a).

5.1.3. C-, D and E type pegmatoid, pegmatites and aplites

The C- and D-type rocks are similar as to their structural setting and reflect a temperature drop from 670 °C down to 400 °C. Epidote is the marker mineral to fix the lower T limit. The E veins fall into the range 490–760 °C judging by the quartz thermometry. Schmidt and Dandar (1995) studied fluid inclusions in feldspar formed during the early stages of such pegmatoids. They found an average temperature of homogenization of as much as 675 °C and determined the pressure to be 350 Mpa. Physico-chemical investigations centered on these pegmatitic mobilizates carried out by Okrusch et al. (1991) in the NE-Bavarian Basement, Germany yielded a maximum temperature of 620 ± 30 °C. None of these case histories saw granites close by being involved as a heat source.

5.1.4. F type pegmatoid, aploid and aplites

The physical-chemical regime of the pegmatoid-aploid-aplite assemblage of type F is constrained by the Fe-poor diopside towards higher temperatures and on the opposite side by the Ca-bearing zeolite laumontite (Tables 2a, 2b, Fig. 2a). With regard to laumontite, the equivalent data are 230 to 260 °C (3 kbar) (Bucher and Grapes, 2011). These zeolites are absent in the presence of fluids containing appreciable amounts of CO_2.

5.1.5. G type metapegmatites

The metapegmatites in the study area underwent the same P-T conditions as their metamorphic host rocks during the Devonian high-temperature regional metamorphism with its temperature increasing to as much as 600 °C (Dill, 2015b).

5.1.6. H type granitic and pegmatitic rocks

The H-type rocks of the granitoid clan are ordered in a sequence as follows based on the host rock magma interaction: H4 ⇒ H5 ⇒ H1 ⇒ H2 ⇒ H3. The (cordierite-sillimanite-garnet)-mica-feldspar-quartz granitoids of type H4 and H5 plot onto the ternary melt minimum at approximately 700 °C. According to Steiner (1986) H5 granitoids are representative of a syn- to postmetamorphic mobilization, whereas H4 granitoids are the product of (pre)-synmetamorphic mobilization from paragneisses with two different retrograde metamorphic events starting off from amphibolite-facies conditions and fading out under greenschist facies conditions as muscovite-bearing granites north of the Luhe Line (Fig. 2a). The retrograde metamorphism and creation of felsic mobilizates is also mirrored in the map of Fig. 1c by the lithological units 1 through 7 from S of the Luhe Line through to the boundary between the Moldanubian and Saxothuringian Zone in the North (Fig. 1c-C-C′).

Concluding from the petrology of the H1-type granodioritic to dioritic rocks (Fig. 1c, d- No 12) a temperature of > 800 °C may be assumed, whereas the larger granite complexes of the Leuchtenberg-, Falkenstein- and Flossenbürg Massifs formed at a lower temperature typical of a granitic magma between 700 °C and 800 °C. Their contact aureole is narrow with some diopside and only known from the southern border of the Leuchtenberg Granite (Fig. 1c) (Voll, 1960). The pegmatitic H5 schlieren escape any determination of the temperature of formation due to the lack of critical minerals and non-fulfillment of the requirements for the application of the quartz geothermometer (Wark and Watson, 2006).

The contour lines displaying the isotherms (maximum temperature of formation based on silicate minerals (e.g. wollastonite, diopside, epidote, andalusite…….) and quartz thermometry) in the Hagendorf-Pleystein Pegmatite Province and its surroundings denote a temperature high striking NNW-SSE and mark a cluster belt extending from the W-WNW towards E-ESE (Fig. 12). The marker mineral wollastonite cannot be created by any of the type-H2 granites. The zone of maximum kaolinization forms an anomaly also running in NNW-SSE direction sub parallel to the “high-T zone” as a consequence of a non-granitic heat source either.

5.2. Structural patterns and the emplacement of pegmatites

Felsic mobilizates evolving in the wake of the LP-HT metamorphism have to be called pegmatites or pegmatoids based on their structural features which entails a postkinematic to late synkinematic origin (Table 4). The type-A and B planar architectural elements shown in a composite stereonet diagram yield a great circle azimuth of 54° and a plunge of 89° which lies in a “temperature depression” of the NW-striking high-T anomaly attaining a value of as much as 800 °C (Figs. 10d, 12 – blue double arrowhead marking the 1 st generation structural phase). The horizontal anticline inclined towards the SW and hosting the major pegmatites – blue pattern in Fig. 12 – has an amplitude of several kilometers and is correlated with the F4 folding recognized by Stein (1988). Considering the stereonet data, the F4 folding structures were also crucial for the emplacement of the A7 (222°/38°) and A8 (215°/41°) stockwork mineralization in the hanging wall of the hinge-and-anticline bodies of type A3 and A4 (Figs. 2a, 10e, f, 13). Their great circle azimuth is almost identical with that of the main host anticline, whereas the plunge is steeper and in line with the temperature gradient (Fig. 12).

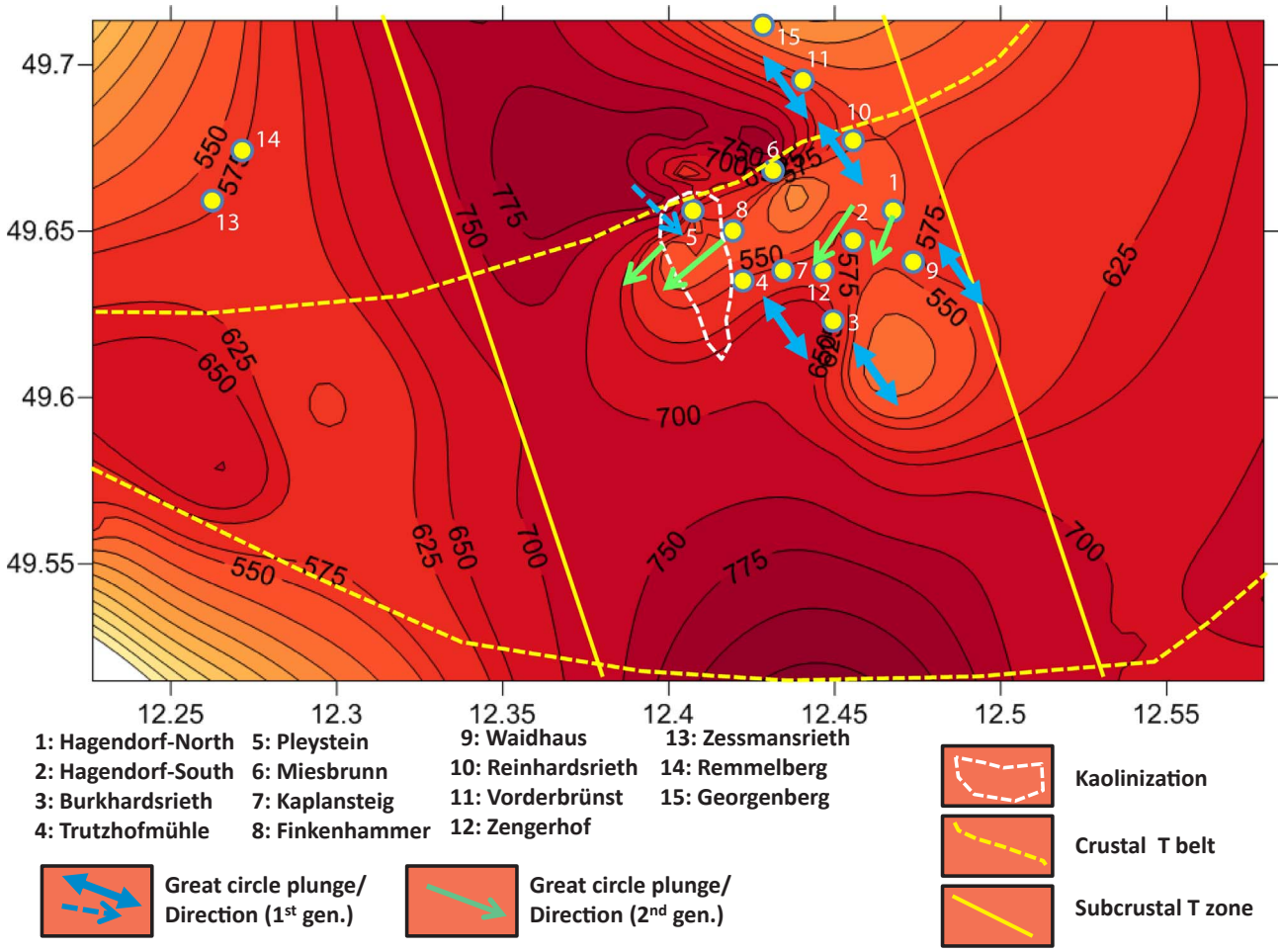

Fig. 12. Structures and temperature – The maximum temperature of formation based on silicate minerals (e.g. wollastonite, diopside, epidote, andalusite.....) and quartz thermometry in the Hagendorf-Pleystein Pegmatite Province and its surroundings (see also Fig. 1b, c). The major deposits of pegmatitic and aplitic rocks are indicated full-color circles, the argillic alteration (mainly kaolinization) is shown by the white stippled line. The structural trends are shown by arrowheads (for detailed information see also stereographic projections in Figs. 9 and 10).

The great circle azimuth of the main pegmatites at Hagendorf-North and South runs perpendicular to the afore-mentioned steeply-dipping pegmatite and aplite bodies similar to those of the footwall facies of the Kreuzberg Pegmatite, all of which are aligned parallel to the elongated temperature minimum in NE-SW direction: Hagendorf-North A3-A4: 286°/82°, Hagendorf-South A3-A4: 298°/81°, Kreuzberg A5-A6: 318°/78°, A5: 321°/60° (Figs. 10a–d, 12 – 2nd generation green pattern. Mimetic or facsimile crystallization did not only play a decisive role for the tabular pegmatites and aplites emplaced along the limbs of the host anticline but were also crucial for the emplacement of the stock-like analogues of type A. According to the field observations by Stein (1988), F3 generation of folding is accompanied by a retrograde metamorphism, and so does the pegmatitization in the low-T zone at the intersection of the cluster-belt and the high-T zone (Fig. 12). High heat flow with temperatures of close to 800 °C and overprinting (F3 ⇒ F4) in the host anticline are accountable for the emplacement, the asymmetric morphology and the zonation of the hinge-zone-related pegmatites of type A (Fig. 13a, b). Generation 1 – mobilization and differentiation started off around 680 °C leading to the barren and unzoned tabular pegmatites of type B along the limbs and stockwork-like hydrofracture veinlets of A7 and A8 responsible for the basic restite rim abundant in Fe, Mg, Ca. The onset of generation 2- mobilization can be established at temperature below 570 °C resulting in a rim of Na-K feldspar around a siliceous core (Fig. 13b). The classical papers on metamorphic differentiation trying to explain K- and Na-enriched layers of granitic gneiss interbedded with Fe- and Mg-enriched gneissic and schistose layers were published by O'Harra (1961) and Bowes et al. (1964). There are many pegmatoid deposits mined for their alkaline feldspar and/or quartz which never saw a granite as heat source close by. Numerous granite pegmatites worked for feldspar have been listed by Harben and Kužvart (1996). It may be a bit pre-emptive in this place, but keeping to the rules of economic geology it has to be stated explicitly, that the numerous pegmatitic rocks mentioned even in the study area and from the overall Bohemian Massif have been right on target for their feldspar and not for the wealth of exotic minerals accommodating fluxing agents such as F, Li, or Be.

To provide a realistic model of pegmatitic mineralization in accordance with nature is unfortunately often impeded by the refusal of alternative ideas for the formation of rare-element granites such as metamorphic processes, anatexis or fluid-induced overprinting of barren pegmatites (Černy, 1992; Černý et al., 2005). I did not found any reliable holistic approach, encompassing structural geology, petrography, mineralogy and geochemistry based upon which such alternative theories were discarded. The concept of regional metamorphism as a modifier of preexisting, mainly sulfidic and oxidic ore deposits by upgrading its ore grade is commonplace and does not cause much dispute. Moreover there are numerous papers addressing the formation of metamorphogenic ore deposits (Pohl, 1992; Barker and Foster, 1993; Yardley and Cleverley, 2013; Corriveau and Spry, 2014).

Table 4
The chronology from a barren pegmatitic to a rare-metal pegmatitic system. The types mentioned in column two refer to the classification scheme used in Fig. 2a and Tables 2a, 2b. Green bands mark metamorphic processes crucial for the formation of pegmatitic and granitic rocks, white bands denote magmatic processes of subcrustal origin. The remaining color codes are equivalent to those used in Tables 2a, 2b Breiter and Siebel, 1995; Dill et al., 2009; Siebel et al., 1995; 1997; Wemmer and Ahrendt, 1993.

Lithology (reference sites)	Type of rock	Whole rock Rb/Sr - zircon-monazite U/Pb	Biotite	Muscovite	Columbite	Reference for age data
Granitoid, granitoid-metagranite-orthogneiss / granitic gneiss (South of the Luhe Line Lineamentary Fault Zone)	H4	Neoproterozoic to early Paleozoic (radiometric data not available)				Voll (1960), Forster (1961, 1965), Bauberger (1967, 1993)
Granitoid magmatism	H5	480±3 Ma 523±12/-7 Ma				Dörr et al. (1995, 1996)
Metapegmatite (Menzelhof , Wildenreuth , Störnstein, Wendersreuth , Püllersreuth, Irchenrieth, Oedenthal)	G	480+7/-9 Ma		mega crystal 440±4 Ma 481±5 Ma small crystal 352±5 Ma 468±5 Ma	482±13 Ma (outside the working area from Domažlice Crystalline Complex (Czech Republic)	Glodny et al.(1998) Glodny et al. 1995
Pegmatoid, aploid, aplite (Oberkotzau Münchberg Gneiss Complex	F			372.5 Ma 377.0 Ma		Kreuzer et al. (1993)
Pegmatoid (KTB-Pilot hole 433m)	F		375 Ma			Kreuzer et al. (1993)
Pegmatoid (KTB-Pilot hole 3297 m)	F		370 Ma			Kreuzer et al. (1993)
Metamorphism (KTB-Pilot hole <3455 m)			319 Ma 316 Ma LP	372 Ma 363 Ma HP/MP		Wemmer and Ahrendt (1993)
Quartz dykes (e.g., Weißenstein, Burkhardsrieth)	E	Younger 321 Ma — 329 Ma				Siebel et al. (2006) (host granodiorites)
Aploid-pegmatoid (Georgenberg Brünst)	B2			316±3 Ma		Glodny et al. (1995)
Aploid-pegmatoid (Plössberg)	B2			315±3 Ma		Glodny et al. (1995)
Pegmatite (Hagendorf-South)	A2-A3			317±3 Ma		Glodny et al. (1995)
Pegmatite (Hagendorf-North)	A2-A3		314.0±5.5 Ma 266.9±10.6Ma	305.3±3.4 Ma		Dill et al. (2013)
Granodiorite (to diorite) “Redwitzite”	H1	322 Ma				Kováříková et al. (2007)
Monzogranite-granodiorite (Leuchtenberg)	H1-H2	326±2 Ma				Siebel et al. 1995, 1997,
Granite (Leuchtenberg)	H2	321±8 Ma				Köhler et al. (1974)
Lamprophyre (KTB-Pilot hole 2231 m)			306.0 ± 4 Ma 295.1± 3 Ma			Kreuzer et al. .(1993)
Granite (Falkenberg)	H2	311±4 Ma	300±1 Ma	307±1 Ma 310±1 Ma		Wendt et al. (1986)
Granite (Flossenbürg)	H2	304.0±11 Ma 311.9±2.7 Ma	292 Ma			Köhler et al. (1974) , Wendt et al. (1994)
Granite (Bärnau)	H2	313.2±2.0 Ma	297 Ma 289 Ma (Chlorite)	306 Ma		Wendt et al. (1994)
Aploid (Trutzhofmühle)	B2				302.1±3.3Ma 376±14Ma	Dill et al. (2008)
Aplite granite (Silbergrube)	A5				302.8±1.9 Ma	Dill et al. (2009)
Pegmatite (Hagendorf South)	A2-A3				299.6±1.9Ma	Dill et al. (2008)
Pegmatite (Křížový kámen / Kreuzstein)	A2-A3				297 ±2 Ma	Breiter and Siebel (1995)

5.3. Chemical patterns of barren and rare metal pegmatites vs. geodynamic setting

5.3.1. Mobilization of Si, Al, K, REE, Na, P and Fe at the crossing of metatectic metamorphic lithologies and mega shear zones

Even if O’Driscoll did not focus on the structural geology and exploration of pegmatites, its idea centered on some world class mineral deposits in Australia, his ideas of deep-seated lineaments and mega shear zones can also be used as an innovative solution in the exploration of pegmatitic deposits as demonstrated in the following paragraphs (Bourne and Twidale, 2007). They are not handled as a stand-alone tool but in context with the chemical patterns of the individual pegmatitic and granitic rocks and a trend analysis of elements.

Silica, aluminum, potassium and rare-earths elements are mobilized from the lithologies 6, 7, 13 south of the Luhe Line fault zone abundant in felsic mobilizates (Figs. 1c, d, 7a, Table 3). The “hot spot” lies at the intersections point of a NW-SE striking mega shear marked by the quartz veins and the turning point (W ⇒ NNE-ENE) of the afore-mentioned lithologies. It reflects the initial state of pegmatitization in a retrograde metamorphic regime which is gradually overprinted by an embryonic subcrustal magmatic impact (Fig. 6a). Coupled trace element mobilization and strain softening in quartz following high grade metamorphism at 750 °C, in the course of retrograde fluid infiltration has been recorded by Ellis and Obata (1992) and Sørensen and Larsen (2009). A similar scenario as described for the NW-NNW-striking shear zone was studied by Nouar et al. (2011) along the Raghane mega shear zone in Algeria. The circular patterns of types A1, A2, A4, A5, A8, B1, B3, D, F, and G of the anticlinal pegmatites originated through mobilization from metamorphic rocks (Fig. 6b, c, Tables 2a, 2b). These three elements Na, P and Fe follow as similar way as far as the mobilization is concerned with a stronger magmatic input and contrast with regard to the orientation of the venting structures (Table 3). Phosphorus is

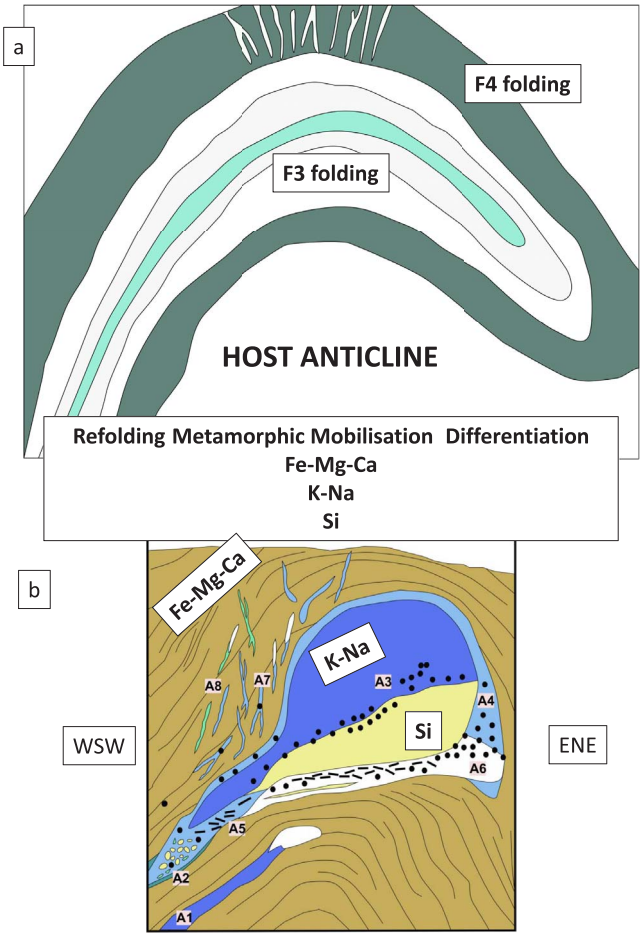

Fig. 13. Refolding, metamorphic mobilization and differentiation entail the formation of zoned pegmatite bodies in an antiform. a) Refolded fold F4 in the host anticline produced by folding F 3 (idealized model based on large-scale examples at outcrop reported by Forster (1965) and Stein (1986). See also Fig. 3. The fractures in the hinge zone of F4 correspond to type A 7 and A 8 aplite veins in Fig. 13b. b) Zooming in Fig. 2a and focusing on the anticlinal hinge-zone hosted pegmatites and aplites which evolved from metamorphic rocks through metamorphic differentiation in zones of high heat flow, mobilizing K, Na and Si and leaving behind a chemical residue enriched in Ca, Mg and Fe in the exocontact of the zone pegmatite.

ubiquitous in garnet and feldspar of the granitic mobilizates and their host paragneisses a fact also recorded from elsewhere by Broska et al. (2004) and Breiter et al. (2005). A double entry of elements in Table 3 attests to different stages of mobilization characterized by the orientation of the structure zones channelizing the fluid migration.

5.3.2. Mobilization of As, Fe, Ni, Ti, Nb, Bi and Cu along the E-W trending root zone of the nappe

The Early Variscan Luhe Line is the controlling lineamentary fault zone for these accessory elements in the pegmatite system (Table 3). Arsenic and bismuth are frequently found together with gold mineralization in the Bohemian Massif (Herzog et al., 1997; Morávek and Lehrberger, 1997). The most proximal stratiform Au-As-Bi mineralization is found immediately S of the Luhe Line in cordierite-sillimanite gneisses (Lehrberger et al., 1990). Arsenopyrite, loellingite, maldonite, native and native bismuth are concentrated in an isoclinals fold of a km-wide amplitude at a temperature of at least 630 °C and a pressure of 2.5 kbar during a polymetamorphic process. These mobilizates are correlative with the stratiform type B aploids and pegmatoids as to the P-T regime and the lens-shaped and stellate patterns emplaced under similar physical-chemical conditions (Figs. 2a, 6b). Although gold is not a common constituent of pegmatitic ore bodies, pegmatite veins, veinlets and quartz veins associated with gold and different styles of argillic alteration were reported by Bakke et al. (1998) from Fort Knox, Alaska-USA. The main minerals in question are native bismuth, maldonite, bismuthinite, and tellurobismutite.

Titanium stands out mostly by its negative anomalies in necking-down patterns and is accumulated in circular pattern. It is the element most characteristic of restites (e.g. A3, B3) left over after strong fractionation during pegmatite emplacement and an indicator element for a strong interaction with country rocks or metamorphic mobilization from the surrounding paragneisses (e.g. A2, A4). In granitic rocks it also stands for some kind of cumulus at the beginning of fractionation (e.g. H1). The afore-mentioned chemical signature finds its mineralogical expression in the “nigrine” aggregates disseminated in the metamorphic country rocks of the pegmatites and quartzose pegmatitic rocks e.g. A4 (Dill et al., 2007, 2014a).

Copper and nickel and are common marker elements for basic and ultrabasic rocks as underscored in many textbooks on economic geology (Evans, 1993; Robb, 2004; Laznicka, 2006; Gilbert and Park, 2007; Ridley, 2013; Dill, 2010; Pohl, 2011). Nickel experienced mainly depletion in many of the “necking-down pattern” indicative of strong differentiation. Only in the B-type rocks anomalous values of Ni may be recognized. It is an element of hydrothermal origin which occurs side-by-side with As and Cu in the wall zone of F-type pegmatoids in calc-silicate-amphibolites (Figs. 2a, 8). This holds true also for Cu as far as the proximity to F-type pegmatoids is concerned. The pegmatoids and mineralized structures run sub parallel to the Luhe Line. In some cases different from it with regard to the host rock such as A3, A7, A8, B2 and E this theory cannot be applied. The lineamentary structure zone marked by type E mobilizates are a strong argument that Cu in this pegmatite province has been supply along lineamentary fault zone by deep-seated fluid introduction which at the very end also stresses a (ultra)basic source rock (see also Zn, Mo).

Niobium is widely used for discrimination due to its refractory character and resistance of its host minerals against supergene and hypogene alteration. In combination with Cr, Nb can be used for the determination of the source rock lithology of rutile (Zack et al., 2004; Stendal et al., 2006; Triebold et al., 2007; Meinhold, 2010; Dill and Skoda, 2017). It occurs in metabasic, metapelitic and pegmatitic rocks (arranged in order of increasing Nb contents). The pegmatite-aplite-gneiss system is the most diversified one with regard to the Nb-Fe-Ti system and contains the most elevated amounts of niobium in Ti oxide or in minerals of the columbite-tantalite s.s.s. (Černy et al., 1989, 1999, 2000; Dill et al., 2007, 2014a). Niobium is taken as reference element for strong pegmatitic fractionation and encountered in lens-shaped, necking-down and stellate patterns. Pegmatitic rocks of little or almost no differentiation and restites are poor in Nb (Fig. 6b, A8, B3). Excluding A1 and A8, being emplaced at the margin of the anticlinal pegmatite system, all pegmatites and aplites are strongly fractionated (Tables 2a, 2b, Fig. 6).

5.3.3. Mobilization of Ba, Mo, Mn, Zn, Rb, Pb, Zr, Mg, Ca, and P along NW-SE and N-S- trending deep-seated lineamentary fault zones

The Late Variscan embryonic Franconian Line Lineament and the Lineament of Bad Elster-Bad Brambach Marienbad-Taus of the same age are of control on the elements mentioned in the header (Fig. 1c) (Teuscher and Weinelt, 1972). Barium is abnormally enriched in A2 where barite comes into existence as a rather rare mineral (e.g. Ploesberg) but still more widespread than some of the early-stage K–Ba–Sc–Zr phosphates spotted in the Trutzhofmühle Aploid (Fig. 6b) (Dill, 2015b). Elevated barium contents were found genetically associated with massive sulfide deposits and their Pb and S isotopes are well in accordance with those sediment-hosted deposits classified as Sullivan-type/Meggen-type deposits *sensu* Jiang et al. (1998) and Taylor and Beaudoin (2000), where they occur at the margin or were accumulated during early stages of mineralization. Another important barium concentration took place in vein-type deposits bound to deep-seated structure zone, equivalent to the Franconian Line Lineament

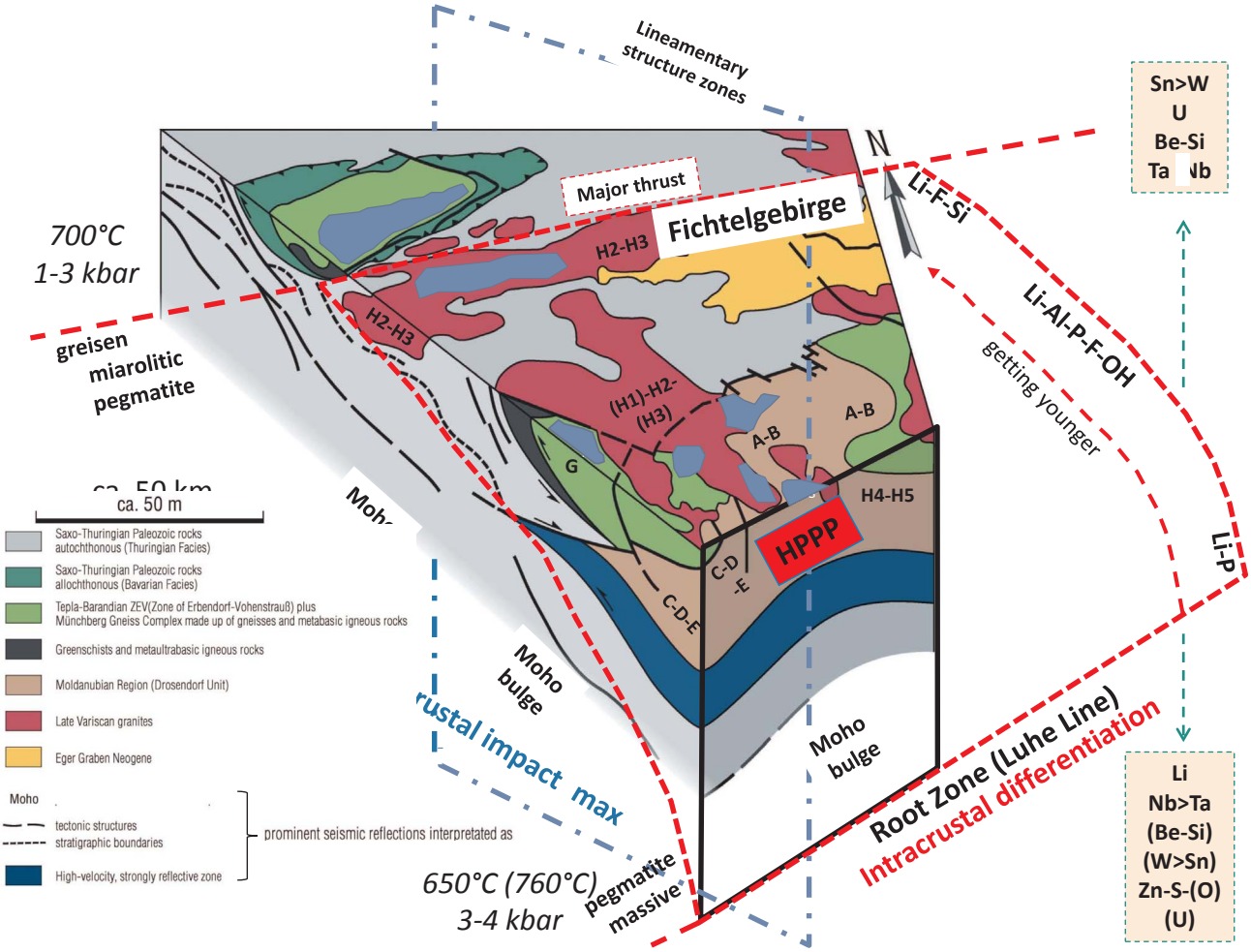

Fig. 14. The 3-D representation is to show the geological setting (modified from Dill, 2015b) and supplemented with those planar architectural elements from structural geology relevant to the explanation of the genesis of the pegmatites along the boundary between the Saxo-Thuringian and Moldanubian Zones and the contact between the allochthonous (root zone + major trust) and autochthonous units. The lineamentary structure zones striking around the N-S direction coincide with a bulge of the Moho. Element variation as a function of depth and geodynamic setting is given on the right-hand side. The various pegmatitic rocks are shown in blue, the Hagendorf-Pleystein Pegmatite Province (HPPP) marked by the red box. metap. = metapegmatite, peg = pegmatite. Li-F-Si = lithium mica (e.g. zinnwaldite), Li-Al-P-F-OH = lithium-bearing Al-phosphates (e.g. montebrasite-amblygonite), Li-P = lithium-bearing phosphate (e.g. triphylite). The subcrustal impact on the pegmatite system increases towards the S along with a steepening of the thrust plane. The categorization of felsic mobilizates is given with letters A–H as used in Tables 2a, 2b, Fig. 2a and referred to in the text. (For interpretation of the references to color in this figure legend, the reader is referred to the web version of this article.)

(Dillm 1989; Dill et al., 2008b). Anomalous Ba contents imply a strong subcrustal impact. Richter and Stettner (1979) found a steady decrease in Ba from the older towards the younger granites in the adjacent Fichtelgebirge Mts. Barium substitutes for K and Rb in many silicates such as feldspar and mica, many of which common to pegmatites. Unfractionated A2 pegmatoid-pegmatite has the lowest K/Ba ratio of 0.53, followed by A8 (K/Ba: 1.15) and A7 (K/Ba: 1.32) whereas A3 pegmatite scores the highest ratio (K/Ba: 27.75), followed by A6 (K/Ba: 6.94), A5 (K/Ba: 3.80) and A4 (K/Ba: 2.90). A1 is in the reaches of the halo of argillitization but as to the emplacement a separate entity (K/Ba: 11.29). The Ba-Rb couple is a marker for the degree of fractionation, with high Ba contents attesting to the initial moderately fractionated stages in the pegmatite system and Rb to the strongest degree of fractionation. Based upon these chemical parameters the anticlinal pegmatite system evolved in a way “outside ⇒ inside”. The most proximal granites H2 (K/Ba: 6.32) and their cogenetic pegmatites H3 (K/Ba: 2.28) do not fit into this regular pattern of A2–A8 pegmatite system. The hinge-zone pegmatite system differentiated in-situ from a metamorphic mobilizates unrelated to the nearest granites.

Manganese, calcium and magnesium have one thing in common the bivalent valence state. Manganese attracts the attention of exploration geologists as it frequently plays a similar role as Ba in many deposits mentioned above being indicative of a subcrustal source (Hein et al., 2006; Malahoff et al., 2006; Huang et al., 2011). In the current pegmatitic systems this idea may be ruled out in the majority of cases considering the lens-shaped chemical patterns, where Mn is always bound to P anomalies (Figs. 6b – A7, B2, 6c – C, E). Manganese is hotly contest by two host minerals in the pegmatite system, Mn-bearing apatite and Mn-enriched garnet (spessartine). Toward a deeper level of intrusion, as was the case in the Bayerischer Wald, S of the study area, garnet gradually got enriched in Mn, leading at the very end to a garnet s.s.s dominated by spessartine (Schaaf et al., 2008). At a shallower level, as it is the case in the study area, Mn apatite is the major host followed by various secondary Mn-bearing phosphates (Dill, 2015b). Manganese is thus indicative of the depth or pressure exerted on the pegmatitic system.

Magnesium contrasts with the overall major elements by its conspicuous negative anomalies giving rise to necking-down patterns. It forms a restite on strong fractionation or got preserved as a remnant in mica and chlorite during metamorphic mobilization.

While Mg plays only a passive role during pegmatite emplacement, Ca next of kin in chemical terms to Mg, plays in parts of the pegmatite system a leading role, e.g., A8, A2 and B, flagging the exocontact zone of it (Figs. 2a, 6).

Molybdenum, zinc and lead share the same sort of formation, having been derived from hydrothermal solutions at different distances from the pegmatoid/pegmatite (Fig. 8). They are frequently coupled with As and Cu and observed in the same structures along the walls of pegmatitic rocks. Molybdenum which is accommodated in molybdenite is associated with graphite and meta-bituminous substances and U oxides (Dill, 2010). It forms part of structure bound U mineralization in H4-type granitoids and along deep-seated quartz dykes (Fig. 2a).

Zinc follows suit to the afore-mentioned elements as long as structure bound mineral assemblages in and around pegmatites are concerned. In some pegmatites, e.g., A3, Zn appears, however, during the initial stages of pegmatite emplacement accommodated in Fe-enriched or marmatitic sphalerite in an intimate intergrowth with the matrix silicates. Zinc is also common to many limb- and faultbound pegmatitic rocks of type B, E, and F but never present in the granitic suite another fact which can be cited as evidence against a direct derivation of the pegmatitic rocks from the adjacent granitic intrusives of type H2 (Fig. 6). It is an element from a deep-seated subcrustal source added during an early stage of pegmatite emplacement to the felsic mobilizates.

Zirconium is another a member of the so-called restite elements which stand out by a “negative anomaly” in the necking-down patterns typical of strong differentiation (e.g. A3) or form a strong positive anomaly in pegmatitic residues such as denoted by B 3 (Fig. 6b).

5.4. Chemical patterns of primary and secondary kaolinization

The chemical patterns in section 5.3 are diagnostic for the primary emplacement of pegmatitic rocks. Out of them, A1 and A 6 are submitted to hypogene kaolinization (Figs. 2a, 6, Tables 2a, 2b). From the association of major elements little information can be obtained to discriminate between hypogene and supergene kaolinization, excluding MgO and CaO (Fig. 11a). Magnesium and to a lesser extent Ca are depleted in pegmatitic rocks and hydrothermal solutions provoking kaolinite-group phyllosilicates to form are poor in Mg. Meteoric fluids may, locally, wash Mg and Ca from outside into the regolith and account for a higher Mg and Ca content during supergene kaolinization. Trace elements, typical of hydrothermal (e.g., Zn, Bi, Cu) and pegmatitic (e.g. Rb, Nb) origin frequently appear in hypogene kaolin (Fig. 6a). Moreover, these elements are less variable in hypogene argillaceous zones. Even refractory elements such as Ti and Zr reveal a higher mobility in supergene aquatic regimes (Cornu et al., 1999; Kurtz et al., 2000; Hodson, 2002; Stiles et al., 2003).

5.5. The Variscan-type pegmatitic system and the geological setting

The evolution of Variscan-type pegmatitic systems may be deduced from the 3-D diagram which has been designed based on data from seismic, gravimetric and magnetic surveys (Dill, 2015b) (Tables 2a, 2b, 4, Figs. 2, 14). The pegmatitic system covers approx. 400 million years of formation of mobilizates composed of quartz, feldspar and mica endowed, in places, with rare metals accommodated in more than 275 minerals. They are different in composition but almost negligible in view of the amount of siliceous melt produced in this crust (Fig. 14).

5.5.1. From metatectic to diatectic gneisses

The cluster belt in Fig. 12 coincides with Neoproterozoic to early Paleozoic rocks running the gamut from the diatectic gneiss to granitoids undergoing diaphoresis from south of the Luhe-Line Lineamentary Fault Zone towards the north (Table 4, Fig. 2c, d). These lithologies are the start-up for the dynamo- and regional metamorphic evolution of the feldspar-quartz-mica mobilizates, or in other words of the numerous barren pegmatoids/pegmatites and their unmineralized analogues of the granitic suite (Table 4 – H4) (Voll, 1960; Forster, 1961, 1965; Bauberger, 1967, 1993). The intracrustal sialic mobilization S of the Luhe Line Lineamentary Fault Zone, the root zone of a crustal wedge complex, started off at temperatures around 650 to 760° C under a pressure regime of 3 to 4 kbar (Tables 2a, 2b, 4, Figs. 2a, 14). The chemical patterns testify that metamorphic mobilization and the ensuing differentiation were more intensive than the magmatic differentiation of the granites of type H2 (Fig. 6). The granitoids of type H5 are remnants of a Cambro-Ordovician felsic magmatism (Dörr et al., 1995, 1996). Until the late Cambrian there was strong differentiation on a chemical scale but with no mineralogical indication of rare-element mobilizates.

5.5.2. From metapegmatites, metamorphic pegmatoids to thrusting

From the Ordovician through the Devonian pegmatites or pegmatoids developed in the allochthonous complexes and brought about a small beryl-columbite mineralization, a manifesto of isolated rare-metal pegmatites (Glodny et al., 1995, 1998). The only age information of columbite in the metapegmatite of the allochthonous units has been derived from the Domažlice Crystalline Complex (Czech Republic) which is outside the working area. Caledonian rare-element pegmatites are known along the NE-SW East Carlow Deformation Zone in Ireland devoid of any late Paleozoic successor of rare-metal pegmatites like in SE Germany (Barros et al., 2015). It is an area which did not suffer from a Late Paleozoic orogenic rejuvenation. No direct genetic tie-line can be drawn from the Be-Nb mineralization in the metapegmatites to the late Paleozoic Be-Nb accumulation of type A3, either. The G-type Be-Nb mineralization is bound to host rocks in a klippen, whereas the A3-type Be-Nb mineralization is situated tectonically in a window position. One may draw the conclusion, that a pre- to syn-Ordovician Be-Nb concentration existed in the root zone from which the allochthonous units became disconnected when they were thrusted onto the Moldanubian autochthonous series. It is logical to assume the late Paleozoic A-type mineralization to have been sourced from the root zone, too (Fig. 14). During the late Devonian, the nappes underwent HP/MP regional metamorphism and were converted into metapegmatites (type G) (Kreuzer et al., 1993). The overthrusting of the allochthonous units, today present in two discrete klippen, the Münchberg Gneiss Complex (MGC) in the N and the Zone of Erbendorf-Vohenstrauβ (ZEV) in the S were accompanied by the emplacement of tectonically induced felsic mobilizates along their eastern boundaries derived from retrograde metamorphic processes (type F) during the waning stages of a MP-HP metamorphic regime (Figs. 2a, 14, Table 4). In the MGC lineamentary fault zones are absent and type-F pegmatoids show up as barren pegmatoids, whereas in the ZEV, HT and LT hydrothermal mineralization and postmagmatic/-granitic alteration linked to deep-seated crustal sources left their imprints on the felsic mobilizates (Figs. 1, 14, Tables 2a, 2b).

5.5.3. From the crust to the mantle – from barren to rare metal pegmatites

320 Ma ago a LP metamorphism overprinted the crystalline basement rocks, including the feldspar-quartz-mica systems. It provided the physical-chemical regime for a wide range of pegmatitic, aplitic and granitic rocks to appear (Figs. 2a, 14). The entire process is characterized by a bimodal magmatism with huge amounts of felsic rocks accompanied by a minor fraction of intermediate to ultrabasic rocks, both of which overlap each other in time and space (Fig. 1, Table 4). Felsic intrusive rocks make use of the same structures prevalently striking NW- to NNW as the quartz veins (type E). The same holds true for lamprophyric rocks, which, in some places, are older while in others younger than the aplitic, pegmatitic and granitic rocks whose significance for rare-element concentration has been discussed (Table 4) (Kováříková et al., 2007; Štemprok et al., 2014). In the Krušné hory/Erzgebirge the spatial association of greisens and lamprophyres suggests that the greisenizing fluids migrated along similar geological structures. Aplites, felsic porphyries, microgranites and mafic dykes belong to a bimodal magmatism with a strong mantle impact (Štemprok et al., 2014). Siebel et al. (2006) determined the age of the intrusive rocks parallel to the “Great Bavarian Quartz Lode” (Bayerischer Pfahl),

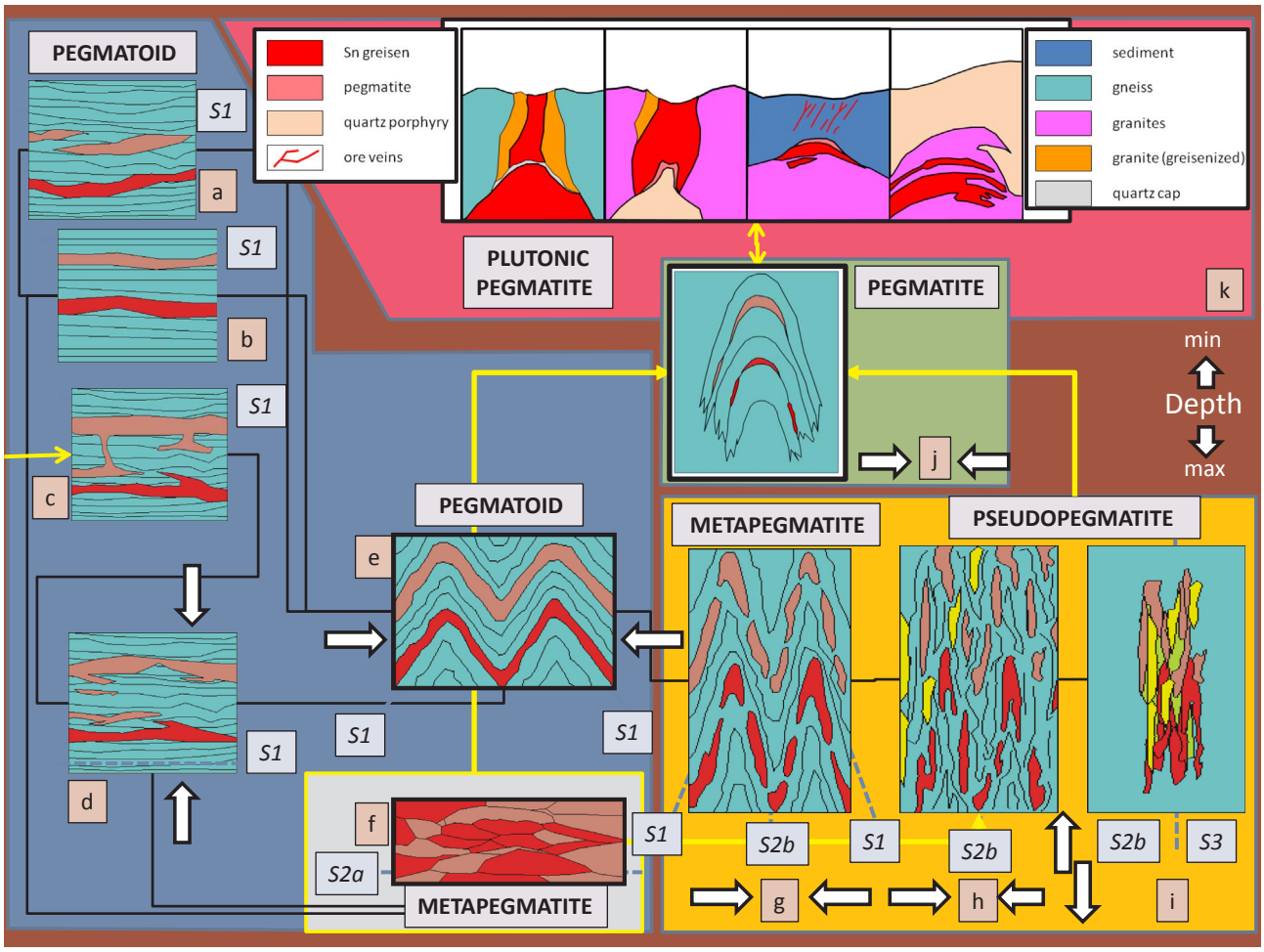

Fig. 15. Structural geology and the evolution of pegmatitic rocks in a crustal section S = layering and schistosity (stippled blue line), numbers = generations of planar architectural elements through evolution of morphological type of pegmatites s.l., depth max = morphological types of pegmatites and patterns found at greater depth, depth min = morphological types of pegmatites and patterns found at shallower depth, yellow line = conduit from source to host (modified from Dill, 2016a,b). *Blue pattern (structural element S 1):* a) Partial melting in high-grade metamorphic rocks. b) Metamorphic differentiation. c) Intrusion or injection of a felsic melt. d) Flattening of the metamorphic lithology and accentuating the layering in the metamorphic rocks. e) Folding of the pegmatitic mobilizates and their country rocks. *Grey pattern (structural element S 2a):* f) Formation of metapegmatites, compression and imposition of a new schistosity S 2a. *Yellow pattern* (structural elements S 1 ⇒ S 2b ⇒ S 3): g) Formation of metapegmatites, extension, transposition of S 1 and incipient stages of the S 2b foliation. h) Formation of pseudopegmatites, extension, metasomatism and advanced stages of the S 2b foliation. i) Formation of pseudopegmatites, extension, metasomatism, thrusting and shearing using the S 2b foliation as guidelines for orientation. *Green pattern:* i) Stock-like pegmatites developed in the hinge area of folds, while tabular pegmatites formed along the limbs as a result of accommodation space provided during the waning stages of orogeny. They form proximal to the root zones of nappes in ensialic orogens. *Red pattern:* k) Plutonic pegmatites transitional into pegmatite-greisens and eventually ending up in vein-type deposits came into being at the shallowest level of pegmatization. They form proximal to the frontal parts of nappes in ensialic orogens. The black bold faced frames denote the Variscan-type pegmatitic, aplitic and granitic rocks dealt with in the current study. (For interpretation of the references to color in this figure legend, the reader is referred to the web version of this article.)

the most prominent shear zone which cuts through the NE Bavarian Basement in NW-SE direction, as between 321 Ma and 329 Ma. Basic intrusive (redwitzites, lamprophyres) and felsic rocks bearing witness of syngenetic subcrustal and crustal processes paving the way to the build-up of rare-metal pegmatites from barren predecessors. The felsic mobilizates related to this high-T event is described by a tripartite scheme: (1) granitic rocks (H-type), (2) structure bound rocks (C-, D-, E type), (3) anticline- and limb-hosted rocks (B- and A-type) (Fig. 2a, Tables 2a, 2b).

Granitic rocks: Late Paleozoic postorogenic sill- or sheetlike granites (H2) (postorogenic magmatic mobilization ("Older Granites" S of the Luhe Line H2a/("Younger Granites" N of the Luhe Line H2b).) and their more basic predecessors (H1) (postorogenic magmatic mobilization from a subcrustal source (?) with fractionation leaving behind a basic cumulate) are encountered along zones of structural weakness but granitic pegmatites genetically related to them (H3) are scarce (Tables 2a, 4, Fig. 14). The granitic pegmatites *sensu stricto* are common to the northern granites of the Fichtelgebirge- Krušné hory/Erzgebirge-Anticline, albeit present they only attain mineralogical scale (Baumann et al., 2000; Thomas et al., 2009). Lithium is found mainly disseminated in micas (Rieder et al., 1970). Granitic pegmatites are eclipsed by alteration zones in granites called greisens, which are enriched in Sn and W and can be traced from Germany through Great Britain and France into the Iberian Peninsula (Alderton, 1993; LeBoutillier, 2002; Neiva, 2008; Lerouge et al., 2017).

Structurebound rocks: E-, D- and C mobilizates show different affiliation to the metamorphic country rocks and a varying subcrustal impact. Type C denotes metamorphic felsic mobilizates resultant from retrograde processes with moderate wall rock reaction and moderate fractionation devoid of any subcrustal impact. Type E rocks stand out by their rather strong subcrustal impact resultant in rare metal mineralization due to mixing of fluids from pegmatitic fractionation and deeply circulating fluids. Equivalent veins with specularite in granites were mined in the Fichtelgebirge Mts. (Dill et al., 2008b) (Fig. 14). Type D takes a position in between the two types (Tables 2a, 2b).

Anticline- and limb-hosted rocks: The primary feldspar-quartz-mica aggregates of B- and A-type pegmatitic and aplitic rocks formed through retrograde metamorphic processes and fractionated *in situ* from the rim

to the center in structural traps provided by the pre-existing fold structures (Tables 2a, 2b, Fig. 2a). Investigations of feldspar-quartz associations from the Proterozoic through the Late Paleozoic provide evidence that this mineral intergrowth is highly adaptable from the textural point of view and reflects the most recent P-T changes; relic mica and columbite prove the parent material and intermediate stages of, e.g., metamorphic overprinting (Table 4). This fact opens the door for a second generation of rare-metal pegmatites with Li, Nb, Ta, Be, Zn, U, Bi, As, Pb, Sn, W and Sc to evolve from A- and B-type barren pegmatites reaching their climax stage of rare metal accumulation in type A3 and B2, respectively (Table 4). Uebel (1975) has already shown in a cartoon the structural differentiation into an "Older Pegmatite" and a "Younger Pegmatite" at Hagendorf. It reflects a "chimney-like" thermal cell within the pegmatite system that controls the fluid migration and accumulation of the rare metals. In the zoned pegmatites, they are concentrated at the contact between the massive quartz underneath (2nd gen.) and the zone of quartz fragments (1st gen.) above. Mapping the distribution and the shape of the silicification front in a pegmatite *sensu stricto* guides us to the primary rare element concentration. The "chimney" has much in common with the Sn-bearing siliceous greisen deposits at Altenberg and Sadisdorf, in the Saxothuringian Zone and may be explained with the up-dip-effect of ascending hyperfusible-rich fluids *sensu* Černý (1991). Unless the subcrustal impact had not taken place between 300 and 290 Ma the barren pegmatite would not have been converted into rare-metal pegmatites (Table 4). A closer look at the U/Pb age of columbite in the Trutzhofmühle Aploid yields two values 302.1 ± 3.3 Ma and 376 ± 14 Ma (Table 4) (Dill et al., 2008a). The second data is reminiscent of the MP-HP metamorphism which affect the Ordovician columbite, or, in other words even in the B2 mobilizates relics of the G metapegmatites may still be recognized (Table 4). The conversion of a barren pegmatite into a rare-metal pegmatite is hallmarks the climax of primary emplacement of pegmatitic rocks (Tables 2a, 2b, 4, Fig. 14). By contrast the part of the HT and the LT hydrothermal alteration reflects the secondary processes of pegmatite mineralization which gradually passes into the supergene alteration of pegmatites (Dill, 2015a,b).

6. Conclusions

The Variscan orogeny *sensu* Suess (1888) which overlaps with the Alleghanian one (Carboniferous-Permian) is limited to the interval Devonian-Triassic, but the primary emplacement of Variscan-type felsic mobilizates (pegmatitic, aplitic, and granitic rocks) covers a much wider period of time from the Neoproterozoic (H5, H4) through the Permian (A3, A4) (Figs. 1a–d, 15). The Caledonides, in particular during Ordovician through the Devonian, play a role as some kind of a protore stage (Caledonides (rare metal pegmatites) ⇒ Variscides (metapegmatites with minor rare elements (G)) ⇒ Alpides (barren metapegmatites).

The term Variscan-type refers to the style of formation which is linked to the ensialic orogens but it is also an expression for a time-bound mineralization which differs from those of the Cenozoic age in the Himalaya or Alpine Mts. Range as well as those of Precambrian age in the ancient cratons, all of which are strikingly distinct from each as to the geodynamic setting that impacts on the "physiognomy of pegmatites" (Göd, 1989; Partington et al., 1995; Sweetapple and Collins, 2002; Bastos Neto et al., 2009; Dewaele et al., 2013; Dill, 2015a) (Fig. 15):

- The emplacement of Variscan-type felsic rocks resulted from a multistage process with two principal rock types the "barren" and the "rare-metal pegmatites" (Table 4, Figs. 2a, 5).
- Late syn-to postorogenic barren pegmatoids, aploids and granitoids evolved along a retrograde pathway from HP/MP to LP regional metamorphism (Table 4, Figs. 2a, 3, 12, 13). Reaching the climax of the LP heat event triggered the B- and A-type rocks to develop, as *in-situ* mobilization gave rise to a melt which gradually became self-intrusive and strongly fractionated in the hinge zone and along the limbs of anticlines (mimetic or facsimile crystallization in pre-existing structural traps).
- From the structural point of view the most effective traps for these mobilizates are encountered where the directions of the 1st generation great circle plunge and 2nd generation great circle plunge cut each other at an almost right angle (Figs. 9, 10, 12). Using stereonet diagrams is a meaningful way to account for the structural relation between felsic mobilizates and the regional fold and fault tectonics.
- A prominent subhorizontal planar architectural element dipping towards the S which coincides with the metamorphic lithologies 7, 6, 5, and 4 characterizes the zone of the most intensive mobilization along the E-W trending Luhe Line (Figs. 2c, 14). It is cut across by deep-seated lineaments at different directions from NW through NE (Table 3). In the "temperature depression" of the retrograde system, the Hagendorf-Pleystein Pegmatite Province is located and the rare-metal pegmatites were spawned from the barren felsic intrusive rocks (Figs. 7, 12, 14). Based on geophysical data, this subhorizontal plane is correlated with the Moho gentling dipping southward and with bulges of the Moho sparking fluids to ascend along (sub) vertical lineamentary fault zones (Fig. 14).
- Chemical contour maps illustrate the regional trends and cluster belts of elements that are interpreted as vent systems and source rock lithologies, respectively (Figs. 1b–d, 7, 14).
- Chemical profiling unravels the accumulation of elements in the exo- and endocontact zones of felsic mobilizates and their accumulation in the course of fractionation (Fig. 8a, b).
- In places, felsic mobilizates act as structural traps only without any chemical interaction between ore-forming fluids and granitoids (Fig. 8a).
- The spider diagrams of elements relevant for the primary emplacement of felsic mobilizates may be categorized into four chemical patterns: (1) circular patterns with or without shift (= metamorphic mobilizates, magmatic mobilization), (2) necking-down patterns (= different degrees of fractionation), (3) lens-shaped patterns (= wall rock alteration), (4) stellate pattern (= different degrees of fractionation and mixing of fluids).
- The major elements in spider diagrams interpreted as marker: Si-Fe-P: metamorphic to magmatic (sub)crustal mobilizates, K-Na-Al: metamorphic mobilizates, Ti-Mg: restites of metamorphic and magmatic mobilizates, Ca: restite in the exocontact of pegmatitic systems, Mn: marker of depth + pressure (in context with P + Si).
- The minor elements in spider diagrams interpreted as marker: As-Bi: HT hydrothermal-metamorphic fluids, Cu-Ni-Mo: hydrothermal-deep-seated + (ultra)basic sources, U-Zn: hydrothermal-deep-seated sources, Pb: LT hydrothermal, Nb-Ba-Rb: pegmatitic fractionation-Ba (early)-Rb (late), Zr: restites of metamorphic mobilization + fractionation, REE: metamorphic mobilizate.
- X–y plots are used to discriminate hypogene and supergene kaolinization: Hypogene: depletion in Ca, Mg, enrichment in Zn, Cu, Bi, Rb, Nb), supergene: enrichment in Zr, Ti.
- The current study is part of a trilogy that is aimed at a holistic approach, encompassing geology, mineralogy, petrography, chemistry, geomorphology, sedimentology and geophysics to account for the evolution of pegmatitic and aplitic rocks within the framework of global geodynamics and regional lithogenesis: (1) hypogene processes leading to the emplacement of these felsic mobilizates (current study), (2) supergene alteration of the felsic mobilizates (Dill, 2017a,b), (3) applied and genetic economic geology of pegmatitic and aplitic rocks (Dill, 2015a). The trilogy is based upon the CMS classification scheme (**C**hemical composition-**M**ineral assemblage-**S**tructural geology) – linking geology to mineralogy of pegmatitic and aplitic rocks (Dill, 2016a) and supplemented by a monographic study or case history centered on the Hagendorf-Pleystein Province

as an integral part of the metallogenesis in an ensialic orogen (Dill, 2015b).

- The quintessence of this tripartite study is as follows: Pegmatitic and aplitic rocks are members of a lithological clan of its own besides the granite clan. They may derive from metamorphic and from magmatic rocks as a separate lithological entity depending on their geodynamic position, the degree of mobilization, and fractionation as a function of the budget of common and rare elements. The impact of the crust and the mantle is crucial in a pegmatite field or province and the key as to the presence or absence of barren or rare-element pegmatites. The way of emplacement of these felsic mobile components in the crust closely resembles the I- and S-type concept applied to the granitic clan.
- From the technical point of view, there is no other way to disentangle the enigma of the origin of pegmatite bodies than combining mineralogy and chemistry with field geology and geophysics unless there is only interest in nice and new minerals for which the pegmatites are outstanding host rocks.

Acknowledgements

I thank very much two anonymous reviewers for their valuable comments made to a first draft of my paper. I also extend my gratitude to Franco Pirajno, editor-in-chief of *Ore Geology Reviews,* for his editorial handling of the paper and some valuable comments helping to clarify the terminology. I dedicate this trilogy of pegmatite studies to my late good friend Berthold Weber (1959-2013).

References

Ackerman, L., Zachariáš, J., Pudilová, M., 2007. P-T and fluid evolution of barren and lithium pegmatites from Vlastějovice, Bohemian Massif, Czech Republic. Int. J. Earth Sci. 96, 623–638.

Alderton, D.H.M., 1993. Mineralization associated with the Cornubian granite batholith. In: Pattrick, R.A.D., Ploya, D.A. (Eds.), Mineralization in the British. Chapman & Hall, Isles, pp. 270–354.

Alfonso, P., Melgarejo, J.C., 2000. Boron vs. phosphorus in granitic pegmatites: the Cap de Creus case (Catalonia, Spain). J. Czech Geol. Soc. 45, 131–141.

Alves, P., Mills, S., 2013. Nuevos datos sobre los fosfatos de Bendada, Sabugal (Portugal). Acopios 4, 349–377.

Aryal, R.K., 2001. Current Status of Precious and Semi-Precious Stones of Nepal. Unpublished Report. Ministry of Industry, Department of Mines and Geology, Kathmandu.

Bakke, A.A., Morrell, R.P., Odden, J.C., 1998. The Fort Knox Porphyry Gold Deposit, Eastern-Central Alaska: An overview and update. In: Porter, T.M. (ed.), 1998 Porphyry and Hydrothermal Copper and Gold Deposits – A Global Perspective PGC Publishing, Adelaide, pp. 89–98.

Baljinnyam, V., Lkamsuren, J., Ivanov A.N., 1993. Pegmatite-substantial composition and previous estimation for the natural economic demand. Unpublished report, Fond, Ulaanbaatar, 94 pp (in Mongolian).

Barker, A.J., Foster, R.P., 1993. Metamorphic fluids and mineral deposits. Mineral. Mag. 57, 363–364.

Barros, R., Menuge, J.F., Costanzo, Feely, M. 2015. The LCT pegmatite belt along the eastern margin of the Leinster Granite. 7th International Symposium on Granitic Pegmatites, PEG 2015, 1–3, Książ, Poland.

Bartholomew, M.J., Whitaker, A.E., 2010. The Alleghanian deformational sequence at the foreland junction of the Central and Southern Appalachians. In: In: Tollo, R.P., Bartholomew, M.J., Hibbard, J.P., Karabinos, P.M. (Eds.), From Rodinia to Pangea: The Lithotectonic Record of the Appalachian Region 206. GSA Memoir, pp. 431–454.

Bassot, J.-P., Morio, M., 1989. Morphologie et mise en place de la pegmatite kibarienne a Sn, Nb, Ta, Li de Monono (Zaire). Chron. Reche Min. 496, 41–56.

Bastos Neto, A.C., Pereira, V.P., Ronchi, L.H., de Lima, E.F., Frantz, J.C., 2009. The world-class Sn, Nb, Ta, F (Y, REE, Li) deposit and the massive cryolite associated with the albite-enriched facies of the Madeira A-Type Granite, Pitinga Mining District, Amazonas State, Brazil. Can. Mineral. 47, 1329–1357.

Bates, R.L, Jackson, J.A., 1987. Glossary of Geology. American Geological Institute, Alexandria, 3th ed., p. 788.

Bauberger, W., 1957. Über die “Albit-Pegmatite” der Münchberger Gneismasse und ihre Nebengesteine. Geol. Bavaria 36, 1–77.

Bauberger, W., 1967. Erläuterungen zur Geologischen Karte von Bayern 1:25000 Blatt Nabburg. GLA München, p. 151.

Bauberger, W., 1993. Erläuterungen zur Geologischen Karte von Bayern 1:25000 Blatt Tännesberg. GLA München, p. 104.

Baumann, L., Kuschka, E., Seifert, T.H., 2000. Lagerstätten des Erzgebirges, Enke im Thieme Verlag, 1-300, Stuttgart.

Bavarian Environment Agency, 2009 Erdgeschichte des Oberpfälzer Waldes – Geologische Karte 1.150000, Augsburg.

Bettenay, L.F., Partington, G.A., Groves, D.I., Paterson, C., 1988. Nature and emplacement of the Giant rare-metal pegmatite at Greenbushes, Western Australia. Proc. Seventh Quadrennial IAGOD Symp., pp. 401–408.

Best, M.G., 2002. Igneous and Metamorphic Petrology. Blackwell Publishing, Oxford, pp. 729.

Beurlen, H., Da Silva, M.R.R., De Castro, C., 2001. Fluid inclusion microthermometry in Be-Ta-(Li-Sn)-bearing pegmatites from the Boroborema Province, northeast Brazil. Chem. Geol. 173, 107–123.

Beurlen, H., Barreto, S., Martin, R., Melgarejo, J., Da Silva, M.R.R., Souza Neto, J.A., 2009. The Borborema Pegmatite province, NE-Brazil revisited. Estudos Geológicos 19, 62–66.

Bucher, K., Grapes, R., 2011. Petrogenesis of Metamorphic Rocks. Springer, Heidelberg, pp. 428.

Bourne, J.A., Twidale, C.R. 2007. Crustal structures and mineral deposits: E.S.T. O’Driscoll’s contribution to mineral exploration. Rosenberg, p. 208.

Bowes, D.R., Wright, A.E., Park, R.G., 1964. Layered intrusive rocks in the Lewisian of the North-West Highlands of Scotland. Q. J. Geol. Soc. London 120, 153–184.

Bradley, D.C., McCauley, A., Buchwaldt, R., Shea, E., Bowring, S., Benowitz, J., O’Sullivan, P., 2015. Geochronology and orogenic context of lithium-cesium-tantalum pegmatites in the Appalachians. 7th International Symposium on Granitic Pegmatites, PEG 2015, 5-6, Książ, Poland.

Breiter, K., Novák, M., Koller, F., Cempírek, J., 2005. Phosphorus a omnipresent minor element in garnet of diverse textural types of leucocratic granitic rocks. Mineral. Petrol. 85, 205–221.

Breiter, K., Siebel, W., 1995. Granitoids in the Rozvadov pluton. Geol. Rundsch. 84, 506–519.

Breiter, K., Müller, A., 2009. Evolution of rare metal-specialised granite magmas documented by quartz trace-element chemistry. Eur. J. Mineral. 21, 335–346.

Bristow, C.M., Exley, C.S., 1994. Historical and geological aspects of the China-clay industry of Southwest England. Trans. R. Geol. Soc. Cornwall 21, 247–314.

Broska, I., Williams, C.T., Uher, P., Konečný, P., Leichmann, J., 2004. The geochemistry of phosphorus in different granite suites of the Western Carpathians, Slovakia: the role of apatite and P-bearing feldspar. Chem. Geol. 205, 1–15.

Burĺánek, D., Hanžl, P., Hrdličková, K., 2011. Pegmatite dykes and quartz veins with tourmaline: an example of partial melting in the contact aureole of the Chandman Massif intrusion, SW Mongolia. J. Geosci. 56, 201–213.

Bynoe, L., 2014. Shear zone influence on the emplacement of a giant pegmatite: The Whabouchi Lithium Pegmatite, Quebec, Canada. University of Western Ontario – Electronic Thesis and Dissertation Repository. Paper 1987. http://ir.lib.uwo.ca/etd/1987.

Černý, P., 1991. Rare-element granitic pegmatites. Part I: Anatomy and internal evolution of pegmatite deposits. Part II: Regional and global environments and petrogenesis. Geosci. Can. 18, 49–81.

Černy, P., 1992. Geochemical and petrogenetic features of mineralization in rare-element granitic pegmatites in the light of current research. Appl. Geochem. 7, 393–416.

Černy, P., Chapman, R., Göd, R., Niedermayr, G., Wise, M.A., 1989. Exsolution intergrowths of titanian ferrocolumbite and niobian rutile from the Weinebene spodumene pegmatites, Carinthia, Austria. Mineral. Petrol. 40, 197–206.

Černy, P., Chapman, R., Simmons, W.B., Chackowsky, E., 1999. Niobian rutile from the McGuire granitic pegmatite, Park County, Colorado: solid solution, exsolution, and oxidation. Am. Mineral. 84, 754–763.

Černy, P., Novák, M., Chapman, R., Masau, M., 2000. Two-stage exsolution of a titanium (Sc, Fe3+)(Nb, Ta)O4 phase in Norwegian niobian rutile. Can. Mineral. 38, 907–913.

Černý, P., Blevin, P.L., Cuney, M., London, D., 2005. Granite-related ore deposits. Econ. Geol. 337–370 100th Anniversary Volume.

Černý, P., London, D., Novák, M., 2012. Granitic pegmatites as reflections of their sources. Elements 8, 289–294.

Cornu, S., Lucas, Y., Lebon, E., Ambrosi, J.P., Luizao, F., Rouiller, J., Bonnay, M., Neal, C., 1999. Evidence of titanium mobility in soil profiles, Manaus, central Amazonia. Geoderma 91, 281–295.

Corriveau, L., Spry, P., 2014. Metamorphosed hydrothermal ore deposits. In: Scott, S.D., Treatise on Geochemistry: Edition: 2nd, Chapter: metamorphosed Hydrothermal Ore Deposits, Elsevier, pp. 175–194.

Cox, K.G., Bell, J.D., Pankhurst, R.J., 1979. The Interpretation of Igneous Rocks. Allen and Unwin, London.

Dallmeyer, R.D., Franke, W., Weber, K., 1995. Pre-Permian Geology of Central and Eastern Europe. Springer, Berlin, Heidelberg, pp. 604.

Davis, H., Reynolds, S.J., 1996. The Structural Geology of Rocks and Regions, second ed. Wiley.

Derré, C., Lecolle, M., Roger, G., de Freitas, Tavares, Carvalho, J., 1986. Tectonics, magmatism, hydrothermalism and sets of flat joints locally filled by Sn-W, aplite-pegmatite and quartz veins, southeastern border of the Serra de Estrela granitic massif (Beira Baixa, Portugal). Ore Geol. Rev. 1, 43–56.

De Vos, W., Tarvainen, T., Salminen, R., Reeder, S., De Vivo, B., Demetriades, A., Pirc, S., Batista, M.J., Marsina, K., Ottesen, R.T., O’Connor, P.J., Bidovec, M., Lima, A., Siewers, U., Smith, B., Taylor, H., Shaw, R., Salpeteur, I., Gregorauskiene, V., Halamic, J., Slaninka, I., Lax, K., Gravesen, P., Birke, M., Breward, N., Ander, E.L., Jordan, G., Duris, M., Klein, P., Locutura, J., Bel-lan, A., Pasieczna, A., Lis, J., Mazreku, A., Gilucis, A., Heitzmann, P., Klaver, G., Petersell, V., 2005. FOREGS Geochemical Atlas of Europe, Part 1: Background Information, Methodology and Maps, Geological Survey of Finland, p. 526.

Dewaele, S., Goethals, H., Thys, T., 2013. Mineralogical characterization of cassiterite concentrates from quartz vein and pegmatite mineralization of the Karagwe-Ankole and Kibara Belts, Central Africa. Geol. Belgica 16, 66–75.

Dill, H.G., 1983. Plutonic mobilization, sodium metasomatism, propylitic, wall rock

alteration and element partitioning from Höhensteinweg uranium occurrence (Northeast Bavaria). Uranium 1, 139–166.
Dill, H.G., 1989. Metallogenetic and geodynamic evolution in the central european variscides. A pre-well site study for the german continental deep drilling programme. Ore Geol. Rev. 4, 279–304.
Dill, H.G., 2010. The "chessboard" classification scheme of mineral deposits: mineralogy and geology from aluminum to zirconium. Earth-Sci. Rev. 100, 1–420.
Dill, H.G., 2015a. Pegmatites and aplites: their genetic and applied ore geology. Ore Geol. Rev. 69, 417–561.
Dill, H.G., 2015b. The Hagendorf-Pleystein Province: the center of pegmatites in an ensialic orogen. Modern Approaches in Solid Earth Sciences, Springer, Dortrecht, Heidelberg, London, New York, p. 475.
Dill, H.G., 2016a. The CMS classification scheme (Chemical composition-Mineral assemblage-Structural geology) – linking geology to mineralogy of pegmatitic and aplitic rocks. Neues Jahrbuch für Mineral. Abhandlungen 193, 231–263.
Dill, H.G., 2016b. Kaolin: soil, rock and ore from the mineral to the magmatic, sedimentary, and metamorphic environments. Earth Sci. Rev. 161, 16–129.
Dill, H.G., 2017a. Residual clay deposits on basement rocks: the impact of climate and the geological setting on supergene argillitization in the Bohemian Massif (Central Europe) and across the globe. Earth Sci. Rev. 165, 1–58.
Dill, H.G., 2017b. An overview of the pegmatitic landscape from the pole to the equator – applied geomorphology and ore guides. Ore Geol. Rev (in print).
Dill, H.G., Klosa, D., 2011. Heavy-mineral-based provenance analysis of Mesozoic continental-marine sediments at the western edge of the Bohemian Massif, SE Germany: with special reference to Fe-Ti minerals and the crystal morphology of heavy minerals. Int. J. Earth Sci. 100, 1497–1513.
Dill, H.G., Melcher, F., Fuessl, M., Weber, B., 2007. The origin of rutile-ilmenite aggregates ("nigrine") in alluvial-fluvial placers of the Hagendorf pegmatite province, NE Bavaria, Germany. Mineral. Petrol. 89, 133–158.
Dill, H.G., Melcher, F., Gerdes, A., Weber, B., 2008a. The origin and zoning of hypogene and supergene Fe-Mn-Mg-Sc-U-REE-Zn phosphate mineralization from the newly discovered Trutzhofmühle aplite (Hagendorf pegmatite province, Germany). Can. Mineral. 46, 1131–1157.
Dill, H.G., Sachsenhofer, R.F., Grecula, P., Sasvári, T., Palinkaš, L.A., Borojević-Šoštarić, S., Strmić-Palinkaš, S., Prochaska, W., Garuti, G., Zaccarini, F., Arbouille, D., Schulz, H.-M., 2008b. Fossil fuels, ore – and industrial minerals. In: In: McCann, T. (Ed.), Geology of Central Europe, Geological Society of London Special Publication, London, pp. 1341–1449.
Dill, H.G., Weber, B., Gerdes, A., Melcher, F., 2009. The Fe-Mn phosphate aplite "Silbergrube" near Waidhaus, Germany: epithermal phosphate mineralization in the Hagendorf-Pleystein pegmatite province. Mineral. Mag. 72, 1143–1168.
Dill, H.G., Skoda, R., Weber, B., Berner, Z., Müller, A., Bakker, R.J., 2012. A newly-discovered swarm of shearzone-hosted Bi-As-Fe-Mg-P aplites and pegmatites in the Hagendorf-Pleystein Pegmatite Province, SE Germany: a step closer to the metamorphic root of pegmatites. Can. Mineral. Special Volume dedicated to Petr Černý 50, 943–947.
Dill, H.G., Skoda, R., Weber, B., Müller, A., Berner, Z.A., Wemmer, K., Balaban, S.-I., 2013. Mineralogical and chemical composition of the Hagendorf-North Pegmatite, SE Germany – a monographic study. Neues Jahrbuch für Mineral. Abhandlungen 190, 281–318.
Dill, H.G., Weber, B., Melcher, F., Wiesner, W., Müller, A., 2014a. Titaniferous heavy mineral aggregates as a tool in exploration for pegmatitic and aplitic rare-metal deposits (SE Germany). Ore Geol. Rev. 57, 29–52.
Dill, H.G., Balaban, S.-I., Witt, B., Wershofen, H., 2014b. Capturing digital data of rock magnetic, gamma-ray and IR spectrometry for in-situ quality control and for the study of the physical-chemical regime of residual kaolin deposits, SE Germany. Ore Geol. Rev. 57, 172–190.
Dill, H.G., Dohrmann, R., Kaufhold, S., Balaban, S.-I., 2015. Kaolinization – a tool to unravel the formation and unroofing of the Pleystein pegmatite-aplite system (SE Germany). Ore Geol. Rev. 69, 33–56.
Dill, H.G., Skoda, R., 2017. Provenance analysis of heavy minerals in beach sands (Falkland Islands/Islas Malvinas) – a view to mineral deposits and the geodynamics of the South Atlantic Ocean. J. South Am. Earth Sci. 78, 17–37.
Dill, H.G., Buzatu, A., Maftei, A.E., 2017. Capturing digital data with handheld devices to determine the redox regime, lithology and provenance of siliciclastic sediments and residual deposits – A review and field manual. Arab. J. Geosci. 10, 188–217 (plus supplementary data).
Dörr, W., Fiala, J., Phillippe, S., Vejnar, Z., Zulauf, G., 1995. Cadomian versus imprints in the Teplá-Barrandian unit. Terra Nostra 95, 91.
Dörr, W., Fiala, J., Phillippe, S., Vejnar, Z., Zulauf, G., 1996. Evidence for a pervasive Cambrian magmatism in the Teplá-Barrandian: continental break up? Terra Nostra 96, 39–43.
Dudoignon, P., Beaufort, D., Meunier, A., 1988. Hydrothermal and supergene alterations in the granitic cupola of Montebras, Creuse, France. Clays Clay Miner. 36, 505–520.
Ellis, D.J., Obata, M., 1992. Migmatite and melt segregation at Cooma, New South Wales. Trans. R. Soc. Edinburgh, Earth Sci. 83, 95–106.
Evans, A.M., 1993. Ore Geology and Industrial Minerals – An Introduction. Blackwell, Oxford, pp. 358.
Finger, F., Roberts, M.P., Haunschmid, B., Schermaier, A., Steyrer, H.P., 1997. Variscan granitoids of central Europe: their typology, potential sources and tectonothermal relations. Mineral. Petrol. 61, 67–96.
Fossen H., 2010. Structural Geology. Cambridge University Press, p. 480.
Forster A., 1961. Erläuterungen zur Geologischen Karte von Bayern 1:25000 Blatt Eslarn. GLA München, p. 90.
Forster A., 1965. Erläuterungen zur Geologischen Karte von Bayern 1:25,000 Blatt Vohenstrauss/Frankenreuth. GLA München, p. 174.
Forster, A., Kummer, R., 1974. The pegmatites in the area of Pleystein-Hagendorf/North Eastern Bavaria. Fortschritte Mineral. 52, 89–99.
Franke, W., Kreuzer, H., Okrusch, M., Schüssler, U., Seidel, E., 1995. Saxothuringian Basin: exotic metamorphic nappes, stratigraphy, structure and igneous activity. In: Dallmeyer, D., Franke, W., Weber, K. (Eds.), Pre-Permian Geology of Central and Western Europe. Springer, Berlin, pp. 277–294.
Fry, N., 1991. The field description of metamorphic rocks. Geological Society of London Handbook Series, Book 14, Wiley, London, p. 112.
Garate-Olave, I., Roda-Robles, E., Gil-Crespo, P.P., Pesquera, A., Torres-Ruiz, J., 2015, Micas as recorders of the evolution of the pegmatite-granite systems: A case study from the Tres Arroyos pegmatite field (Badajoz, Spain). 7th International Symposium on Granitic Pegmatites, PEG 2015, 31–32, Książ, Poland.
Gerdes, A., Finger, F., Parrish, R.R., 2006. South-westward progression of a late-orogenic heat front in the Moldanubian zone of the Bohemian Massif and formation of the Austro-Bavarian anatexite belt. Geophysical Research Abstract 8, 10698, EGU, Wien.
Gilbert, J.M., Park Jr., C.F., 2007. The Geology of Ore Deposits. Waveband Press, Long Grove, IL, pp. 985.
Glodny, J., Grauert, B., Krohe, A., 1995. Ordovizische Pegmatite in variszischen HAT Metamoprhite des KTB-Umfeldes: Hinweis auf hohe Stabilität des Rb-Sr-Systems in Muskowiten. Terra Nostra 4. Kolloquium, Jena, 98.
Glodny, J., Grauert, B., Fiala, J., Vejnar, Z., Krohe, A., 1998. Metapegmatites in the western Bohemian massif: ages of crystallization and metamorphic overprint, as constrained by U-Pb zircon, monazite, garnet, columbite and Rb–Sr muscovite data. Geol. Rund. Int. J. Earth Sci. 87, 124–134.
Glover, A.S., Rogers, W.Z., Barton, J.E., 2012. Granitic pegmatites: storehouses of industrial minerals. Elements 4, 269–273.
Göd, R., 1989. The spodumene deposit at "Weinebene" Koralpe, Austria. Miner. Deposita 24, 270–278.
Hansen, B.T., Teufel, S., Ahrendt, H., 1989. Geochronology of the Moldanubian-Saxothuringian Transition Zone, Northeast Bavaria. In: Emmermann, R., Wohlenberg, J. (Eds.), The German Continental Deep Drilling Program (KTB). Springer, Berlin, pp. 55–66.
Harben, P.W., Kužvart, M., 1996. Industrial Minerals. A Global Geology. London Industrial Minerals Information Ltd., pp. 462.
Hein, J. R., Staudigel, H., Koppers, A., Hart, S. R., Dunham, R., 2006. Hydrothermal manganese mineralization near the Samoan Hotspot. American Geophysical Union, Fall Meeting 2006, abstract, V13A–0637.
Herzog, T., Lehrberger, G., Stettner, G., 1997. Goldvererzungen bei Neualbenreuth im Saxothuringikum des Waldsassener Schiefergebirge, Oberpfalz. Geol. Bavarica 102, 173–206.
Hodson, M.E., 2002. Experimental evidence for mobility of Zr and other trace elements in soils. Geochim. Cosmochim. Acta 66, 819–828.
Huang, J., Chu, X., Jiang, G., Feng, L., Chang, H., 2011. HYdrothermal origin of elevated iron, manganese and redox-sensitive trace elements in the c. 635 Ma Doushantuo cap carbonate. J. Geol. Soc. 168, 805–816.
Jahns, R.H., 1955. The study of pegmatites. Econ. Geol. 1955, 1025–1130.
Jiang, S.-Y., Palmer, M.R., Slack, J.F., Shaw, D.R., 1998. Paragenesis and chemistry of multistage tourmaline formation in the Sullivan Pb–Zn–Ag deposit, British Columbia. Econ. Geol. 93, 47–67.
Kalt, A., Corfu, F., Wijbrams, J.R., 2000. Time calibration of a P-T- path from a Variscan high-temperature low-pressure metamorphic complex (Bayerischer Wald, Germany), and the detection of inherited monazite. Contrib. Mineral. Petrol. 138, 143–163.
Kitagawa, R., Köster, H.M., 1991. Genesis of the Tirschenreuth kaolin deposit in Germany compared with the Kohdachi kaolin deposit in Japan. Clay Miner. 26, 61–79.
Köhler, H., Müller-Sohnius, D., Cammann, K.C., 1974. Rb/Sr-Altersbestimmungen an Mineral- und Gesamtgesteinsproben des Leuchtenberger und Flossenbürger Granits, NE-Bayern. Neues Jahrbuch Mineral. Abhandlungen 123, 63–85.
Konzett, J., Schneider, T., Hauzenberger, C., Krenn, K., Melcher, F., Gerdes, A., 2015. Staurolite-rare metal-bearing pegmatites from the Eastern Alps, Northern Italy: variable rare-metal enrichment during regional metamorphic anatexis? 7th International Symposium on Granitic Pegmatites, PEG 2015 Książ, Poland, 38–39.
Kováříková, P., Siebel, W., Jelínek, E., Štemprok, M., Kachlík, V., Holub, F.V., Blecha, V., 2007. Petrology, geochemistry and zircon age for redwitzite at Abertamy, NW Bohemian Massif (Czech Republic): tracing the mantle component in Late Variscan intrusions. Chemie der Erde/Geochem. 67, 151–174.
Kramer, W., Seifert, W., 1994. Mica-lamprophyres and related volcanics of the Erzgebirge and metallogenetic aspects. In: Seltmann, R. (Ed.), Metallogeny of Collisional Orogens. Czech Geological Survey, Prague, pp. 159–165.
Kremer, P.D., Lin, S., 2006. Structural geology of the Bernic Lake area, Bird River greenstone belt, southeastern Manitoba (NTS 52L6): implications for rare element pegmatite emplacement; in Report of Activities 2006, Manitoba Science, Technology, Energy and Mines, Manitoba Geological Survey, pp. 206–213
Kreuzer, H., Henjes-Kunst, F., Seidel, E., Schüßler, U., Bühn, B., 1993. Ar–Ar spectra on minerals from KTB and related medium pressure units. KTB-Report 93–2, 133–136, Hannover.
Kurtz, A.C., Derry, L.A., Chadwick, O.A., Alfano, M.J., 2000. Refractory element mobility in volcanic soils. Geology 28, 683–686.
Lahti, S.I.. (editor) with contributions by Alviola R. and Nironen M., 1989. Late orogenic and synorogenic Svecofennian granitoids and associated pegmatites of Southern Finland Symposium IGCP Project 247 Precambrian Ore Deposits Related to Tectonic Styles Precambrian Granitoids Petrogenesis, geochemistry and metallogeny, University of Helsinki, Finland, p. 50.
Laznicka, P., 1985. Empirical Metallogeny. Elsevier, Amsterdam, pp. 1794.
Le Bas, M.J., Le Maitre, R.W., Streckeisen, A., Zanettin, B., 1986. A chemical classification of volcanic rocks based on the total alkali-silica diagram. J. Petrol. 27, 745–750.
LeBoutillier, N.G., 2002 The tectonics of Variscan Magmatism and Mineralization in

South West England, Ph.D. Thesis, University of Exeter, 639 pp + appendix.
Lehrberger, G., Preinfalk, C., Morteani, G., Lahusen, L., 1990. Stratiform Au-As-Bi-Vererzung in Cordierit-Sillimanit-Gneisen des Moldanubikums bei Oberviechtach-Unterlangau, Oberpfälzer Wald (NE-Bayern). Geol. Bavarica 95, 133–176.
Lerouge, C., Gloaguen, E., Wille, G., Bailly, L., 2017. Distribution of In and other rare metals in cassiterite and associated minerals in Sn ± W ore deposits of the western Variscan Belt. Eur. J. Mineral. http://dx.doi.org/10.1127/ejm/2017/0029-2673.
Linhardt, E., 2000. Der Beryllpegmatit der Feldspatgrube Maier, Püllersreuth. Lapis 25, 13–23.
Linnemann, U., Nance, R. D., Kraft, P., Zulauf, G., 2007. The Evolution of the Rheic Ocean: From Avalonian-Cadomian Active Margin to Alleghanian-Variscan collision. The Geological Society of America Special Paper, 423, 1–630, Boulder, Colorado.
Linnen, R.L., Van Lichervelde, M., Černý, P., 2012. Granitic pegmatites: as sources of strategic metals. Elements 8, 275–280.
Lisle, R. J., Brabham, P., Barnes, J.W., 2011. Basic Geological Mapping (Geological Field Guide), paperback John Wiley & Sons; 5th ed., p. 230.
London, D., 2008. Pegmatites. The Canadian Mineralogist. Special Publication, pp. 347.
Malahoff, A., Kolotyrkina, I.Ya., Midson, B.P., Massoth, G.J., 2006. A decade of exploring a submarine intraplate volcano: Hydrothermal manganese and iron at Lo 'ihi volcano, Hawai'i. Geochem. Geophys. Geosyst. 7, 1–26.
Malkovský, M., 1979. Tektogenese der Plattformbedeckung des Böhmischen Massivs. Knihovna Ústř Úst Geol Praha 53, 1–176.
Matte, P., 2001. The Variscan collage and orogeny (480 ± 290 Ma) and the tectonic definition of the Armorica microplate: a review. Terra Nova 13, 122–128.
Martins, T., Lima, A., Simmons, W.B., Falster, A.U., Noronha, F., 2011. Geochemical fractionation of Nb-Ta oxides in Li-bearing pegmatites from the Barroso-Alvão pegmatite field, Northern Portugal. Can. Mineral. 49, 777–791.
Mehnert, K.R., 1968. Migmatites and the origin of granitic rocks. Elsevier, Amsterdam, pp. 391.
Meinhold, G., 2010. Rutile and its applications in earth sciences. Earth Sci. Rev. 102, 1–28.
Moon, C., Whateley, M., Evans, A., 2006. Introduction to Mineral Exploration, second ed. John Wiley & Sons Ltd, pp. 496.
Morávek, P., Lehrberger, G., 1997. Die genetische und geotektonische Klassifikation der Goldvererzungen in der Böhmischen Masse. Geol. Bavarica 102, 7–31.
Neiva, A.M.R., 2008. Geochemistry of cassiterite and wolframite from tin and tungsten quartz veins in Portugal. Ore Geol. Rev. 33, 221–238.
Neiva, A.M.R., Gomes, M.E.P., Ramos, J.M.F., Silva, P.B., 2008. Geochemistry of granitic aplite–pegmatite sills and their minerals from Arcozelo da Serra area (Gouveia, central Portugal). Eur. J. Mineral. 20, 465–485.
Neiva, A.M.R., Silva, P.B., Ramos, J.M.F., 2012. Geochemistry of granitic aplite-pegmatite veins and sills and their minerals from the Sabugal area, central Portugal. Neues Jahrbuch für Mineralogie 189, 49–74.
Norton, J.J., 1964. Geology and mineral deposits of some pegmatites in the southern Black Hills South Dakota. Geological Survey Professional Paper 297-E, pp. 1–55.
Nouar, O., Henry, B., Liégeois, J.P., Derder, M.E.M., Bayou, B., Bruguier, O., Ouabadi, A., Amenna, M., Hemmi, A., Ayache, M., 2011. Eburnean and Pan-African granitoids and the Raghane mega-shear zone evolution: Image analysis, U-Pb zircon age and AMS study in the Arokam Ténéré (Tuareg shield, Algeria). J. Afr. Earth Sc. 60, 133–152.
O'Hara, M.J., 1961. Zoned ultrabasic and basic gneiss masses in the Early Lewisian Complex at Scourie, Sutherland. J. Petrol. 2, 248–276.
Okrusch, M., Matthes, S., Klemd, R., O'Brien, P.J., Schmidt, K., 1991. Eclogites at the northwestern margin of the Bohemian Massif: a review. Eur. J. Mineral. 3, 707–730.
Paxton, S.T., Aufill, M., Kamann, P., Krstyniak, A., 2016. Spectral gamma-ray response of Oklahoma Shales in outcrop. http://www.ogs.ou.edu/pdf/GSPaxtonFinalS.pdf.
Partington, G.A., Mc Naughton, N.J., Williams, I.S., 1995. A review of the geology, mineralization, and geochronology of the Greenbushes Pegmatite, Western Australia. Econ. Geol. 90, 616–635.
Passchier, C.W., Trouw, R.A.J., 2005. Microtectonics. Springer, Heidelberg, Berlin, pp. 366.
Paz-Ferreiro, J., Vázquez, E., Vieira, S., 2010. Geostatistical Analysis of a Geochemical Dataset. Bragantia, Campinas, 69, Suplemento, 121–129.
Pivec, E., Holub, F.V., Lang, M., Novák, J., Štemprok, M., 2002. Rock-forming minerals of lamprophyres and associated mafic dykes from the Krušné hory/ Erzgebirge (Czech Republic). J. Czech Geol. Soc. 47, 23–32.
Pohl, W., 1992. Defining metamorphogenic mineral deposits —an introduction. Mineral. Petrol. 45, 145–152.
Pohl, W., 2011. Economic Geology. Wiley-Blackwell, Oxford, pp. 663.
Psyrillos, A., Manning, D.A.C., Burley, S.D., 1998. Geochemical constraints on kaolinization in the St. Austell granite, Cornwall, England. J. Geol. Soc. London 155, 829–840.
Reimann, C., Birke, M., Demetriades, A., Filzmoser, P., O'Connor, P., 2014. Chemistry of Europe's Agricultural Soils, Part B general background information and further analysis of the GEMAS DATA SET. Geol. Jahrb. B103, 1–352.
Richter, P., Stettner, G., 1979. Geochemische und petrographische Untersuchungen der Fichtelgebirgsgranite. Geol. Bavarica 78, 1–144.
Richter, P., Stettner, G., 1986. Untersuchungen zur Form und räumlichen Lage der Granitplutone Im Projektgebiet der Lokation Oberpfalz. Final report, German Science Foundation, Würzburg, p. 20.
Ridley, J., 2013. Ore Deposit Geology. Cambridge University Press, pp. 409.
Rieder, M., Huka, M., Kucerova, D., Minarik, L., Obermajer, J., Povondra, P., 1970. Chemical composition and physical properties of lithium-iron-micas from the Krusne Hory Mts. (Erzgebirge)-Part A, Chemical composition. Contrib. Mineral. Petrol. 27, 131–158.
Robb, L.J., 2004. Introduction to Ore-forming Processes. Blackwell Publ., pp. 416.
Roda-Robles, E., Pesquera, A., Gil-Crespo, P.P., Vieiera, R., Lima, A., Garate-Olave, I., Martins, T. Torres-Ruiz, J., 2015. Lithium mineralizations in the central Iberian Zone (Spain-Portugal): Occurrence, typology and origin. 7th International Symposium on Granitic Pegmatites, PEG 2015, 81–82, Książ, Poland.
Saarberg-Interplan Uran, 1982. CEA-Excursion June 21–22-Project Oberpfalz. Unpublished report. Saarberg-Interplan Uran GmbH, Saarbrücken, pp. 44.
Saffarini, G., Lahawani, Y., 1992. Multivariate statistical techniques in geochemical exploration applied to Wadi sediments' data from an arid region: Wadi Dana, SW-Jordan. J. Afr. Earth Sci. 14, 417–427 Pergamon Press, Oxford.
Schaaf, P., Sperling, T., Müller-Sohnius, D., 2008. Pegmatites from the Bavarian Forest, SE Germany: geochronology, geochemistry and mineralogy. Geol. Bavarica 108, 204–303.
Schmidt, C., Dandar, S., 1995. Information of fluid inclusion study of Zakhiin tsokhio area.- Mongolian University Science and Technology. Mineral. Museum Sci. Trans. 12, 57–63.
Schneiderhöhn, H., 1961. Die Pegmatite [The pegmatites]. Gustav Fischer Verlag, Stuttgart, p. 720. (in German).
Scott, P.W., Bristow, C.M., 2002. Field excursion to study aspects of the St Austell Granite and its related kaolinization and other mineralization. Geosci. Southwest Engl. 10, 370–372.
Seifert, Th., 2008. Metallogeny and Petrogenesis of Lamprophyres in the Mid-European Variscides – Postcollisional Magmatism and Its Relationship to Late Variscan Ore-Forming Processes in the Erzgebirge (Bohemian Massif). IOS Press BV, Amsterdam.
Siebel, W., Breiter, K., Höhndorf, A., Wendt, I., Henjes-Kunst, F., 1995 Preliminary note on age relationships and Nd isotope composition of granitoids from the Bärnau-Rozvadov pluton, Western Bohemia. 8th Conference of the German Continental Deep Drilling Programme (KTB) Giessen, May 25–26, 1995.
Siebel, W., Trzebski, R., Stettner, G., Hecht, L., Casten, U., Höhndorf, A., Müller, P., 1997. Granitoid magmatism of the NW Bohemian Massif related: gravity data composition, age relations and phase concept. Geol. Rundsch. 86, 45–63.
Siebel, W., Thiel, M., Chen, F., 2006. Zircon geochronology and compositional record of late- to post-kinematic granitoids associated with the Bavarian Pfahl zone (Bavarian Forest). Mineral. Petrol. 86, 45–62.
Siebel, W., Shang, C.K., Reitter, E., Rohrmüller, J., Breiter, K., 2008. Two distinctive granite suites in the SW Bohemian massif and their record of the emplacement: constraints from geochemistry and zircon 207Pb/206Pb chronology. J. Petrol. 49, 1853–1872.
Silva, D., Lima, A., Gloaguen E., F. Noronha, Gumiaux, C., Guillou-Frottier, L., 2015. What's new on the Pegmatite Field Barroso-Alvão? 7th International Symposium on Granitic Pegmatites, PEG 2015 Książ, Poland, 93–94.
Simmons, W.B., 2005. A look at pegmatite classifications. http://www.minsocam.org/msa/special/pig/PIG_articles/Elba%20Abstracts%2018%20Simmons.pdf.
Simmons, W.B., Pezzotta, F., Shigley, J.E., Beuerlen, H., 2012. Granitic pegmatites as source colored gemstones. Elements 8, 281–287.
Sørensen, B.E., Larsen, R.B., 2009. Coupled trace element mobilization and strain softening in quartz during retrograde fluid infiltration in dry granulite protoliths. Contrib. Miner. Petrol. 157, 147.
Stein, E., 1988. Die strukturgeologische Entwicklung im Übergangsbereich Saxothuringikum/Moldanubikum in NE-Bayern. Geol. Bavarica 92, 5–131.
Steiner, L., 1986. Die Granitoide Des Oberpfälzer Waldes-Voruntersuchungen Zum Kontinentalen Tiefbohr-Programm (KTB). German Science Foundation, Hannover, pp. 109.
Štemprok, M., Dolejš, D., Holub, F.V., 2014. Late Variscan calc-alkaline lamprophyres in the Krupka ore district, Eastern Krušné hory/Erzgebirge: their relationship to Sn–W mineralization. J. Geosci. 59 (41–6), 8.
Stendal, H., Toteu, S.F., Frei, R., Penaye, J., Njel, U.O., Bassahak, J., Nni, J., Kankeu, B., Ngako, V., Hell, J.V., 2006. Derivation of detrital rutile in the Yaoundé region from the Neoproterozoic Pan-African belt in southern Cameroon (Central Africa). J. Afr. Earth Sc. 44, 443–458.
Stettner, G., 1992. Geologie Im Umfeld Der Kontinentalen Tiefbohrung Oberpfalz-Einführung Und Exkursionen. Bayerisches Geologisches Landesamt, München, pp. 240.
Stiles, C.A., Mora, C.I., Driese, S.G., 2003. Pedogenic processes and domain boundaries in a Vertisol climosequence: evidence from titanium and zirconium distribution and morphology. Geoderma 116, 279–299.
Storm, L.C., Spear, F.S., 2007. Application of the titanium-in-quartz thermometer to peliticmigmatites from the Adirondack Highlands, New York. J. Metamorph. Geol. 27, 479–494.
Streckeisen, A.L., 1976. To each plutonic rock its proper name. Earth Sci. Rev. 12, 1–33.
Streckeisen, A., 1980. Classification and nomenclature of volcanic rocks, lamprophyres, carbonatites and melilitic rocks IUGS Subcommission on the Systematics of Igneous Rocks Recommendations and suggestions. Int. J. Earth Sci. 69, 194–207.
Suess, E., 1888. Das Antlitz der Erde. vol. 2, Temsky, Prag & Wien, Freytag, Leipzig, p. 703.
Sweetapple, M.T., Collins, P.L.F., 2002. Genetic framework for the classification and distribution of Achaean rare metal pegmatites in the North Pilbara craton, Western Australia. Econ. Geol. 97, 873–895.
Taylor, B.E., Beaudoin, G., 2000. Sulphur stratigraphy of the Sullivan Pb–Zn–Ag deposit, B.C: evidence for hydrothermal sulphur, and bacterial and thermochemical sulphate reduction. In: Lydon, J.W., Höy, T., Slack, J.F., Knapp, M. (eds.), The Sullivan Deposit and its Geological Environment Special Publication, 1, Mineral Deposits Division of the Geological Association of Canada, St. John's, Newfoundland, pp. 696–719.
Teuscher, E.O., Weinelt, W., 1972. Die Metallogenese im Raum Spessart-Fichtelgebirge-Oberpfälzer Wald-Bayerischer Wald. Geol. Bavarica 65, 5–73.
Thomas, H., 2005. Metamorphism and Crustal Evolution. Atlantic Publishers & Dist, New Delhi, pp. 389.
Thomas, R., Davidson, P., Rhede, D., Leh, M., 2009. The miarolitic pegmatites from the

Königshain: a contribution to understanding the genesis of pegmatites. Contrib. Miner. Petrol. 157 (4), 505–523.
Triebold, S., von Eynatten, H., Luvizotto, G.L., Zack, T., 2007. Deducing source rock lithology from detrital rutile geochemistry: an example from the Erzgebirge, Germany. Chem. Geol. 244, 421–436.
Uebel, P.-J., 1975. Platznahme und Genese des Pegmatit von Hagendorf-Süd. Neues Jahrbuch Mineral. Monatshefte 1975, 318–322.
Ulrych, J., Pivec, E., Lang, M., Balogh, K., Kropácek, V., 1999. Cenozoic intraplate volcanic rock series of the Bohemian Massif: a review. Geolines 9, 123–129.
Van der Pluijm, B.A., Marshak, S., 2004. Earth Structure – An Introduction to Structural Geology and Tectonics, second ed. W.W. Norton, New York, pp. 656.
Vasyukova, E.A., Izokh, A.E., Borisenko, A.S., Pavlova, G.G., Sukhorukov, V.P., Anh, Tran Tuan., 2011. Early Mesozoic lamprophyres in Gorny Altai: petrology and age boundaries. Russ. Geol. Geophys. 52, 1574–1591.
Voll, G., 1960. Stoff, Bau und Alter in der Grenzzone Moldanubikum/Saxothuringikum in Bayern unter besondere Berücksichtigung gabbroider, amphibolitischer und kalksilikatführender Gesteine. Beiheft Geol. Jahrbuch 42, 1–382.
Von Raumer, J.F., Stampfli, G.M., Bussy, F., 2003. Gondwana-derived microcontinents – the constituents of the Variscan and Alpine collision orogens. Tectonophysics 365, 7–22.
Wark, D.A., Watson, E.B., 2006. TitaniQ: a titanium-in-quartz geothermometer. Contrib. Miner. Petrol. 152, 743–754.
Weber, K., Behr, J.H., 1983. Geodynamic interpretation of the Mid-European Variscides. In: Martin, H., Eder, F.W. (Eds.), Intercontinental Fold Belts. Springer, Berlin/Heidelberg/New York, pp. 427–469.
Wemmer, K., Ahrendt, H., 1993. Age determination on retrograde processes in rocks of the KTB and the surrounding area. KTB-Report 93–2, 129–131.
Wendt, I., Kreuzer, H., Müller, P., Schmidt, H., 1986. Gesamtgesteins- und Mineraldatierungen des Falkenberg Granite. Geol. Jahrbuch E 34, 5–56.
Wendt, I., Carl, C., Kreuzer, H., Müller, P., Stettner, G., 1992. Ergänzende Messungen zum Friedenfelser Granite Steinwald und radiometrische Datierung des Ganggranite im Falkenberger Granit. Geol. Jahrbuch A 137, 3–24.
Wendt, I., Ackermann, H., Carl, C., Kreuzer, H., Müller, P., Stettner, G., 1994. Rb/Sr-Gesamtgesteins und K/Ar-Glimmerdatierungen der Granite von Flossenbürg und Bärnau. Geol. Jahrbuch E 51, 3–29.
Wimmenauer, W., Bryhni, I. 2007. Migmatites and related rocks. Web version of 01.02.07 https://www.bgs.ac.uk/scmr/docs/papers/paper_6.pdf.
Winkler, H.G.F., 1976. Petrogenesis of Metamorphic Rocks. Springer, pp. 348.
Yardley, B.W.D., Cleverley, J.S., 2013. The role of metamorphic fluids in the formation of ore deposits. In: Jenkin, G.R.T., Lusty, P.A.J., McDonald, I., Smith, M.P., Boyce, A.J., Wilkinson, J.J., (eds.), Ore Deposits in an Evolving Earth, Geological Society, London, Special Publications, first published online October 7, 2013, doi: 10.1144/SP393.5, 393.
Zack, T., von Eynatten, H., Kronz, A., 2004. Rutile geochemistry and its potential use in quantitative provenance studies. Sed. Geol. 171, 37–58.